National Environmental Satellite, Data, and Information Service

# Microwave Instruments & Products

**Dr. Fuzhong Weng, Chief**
**Sensor Physics Branch**
**Satellite Meteorology and Climatology Division**
**Center for Satellite Applications and Research**
**National Environmental, Satellites, Data and Information Service**
**National Oceanic and Atmospheric Administration**

**Presented at the Workshop on Applications of Remotely Sensed Observations in Data Assimilation, University of Maryland, August 6, 2007**
**University of Maryland**

**For questions and comments: please send email to Fuzhong.Weng@noaa.gov**

National Environmental Satellite, Data, and Information Service

# NESDIS SSM/I Climate Data Records Started Since 1987

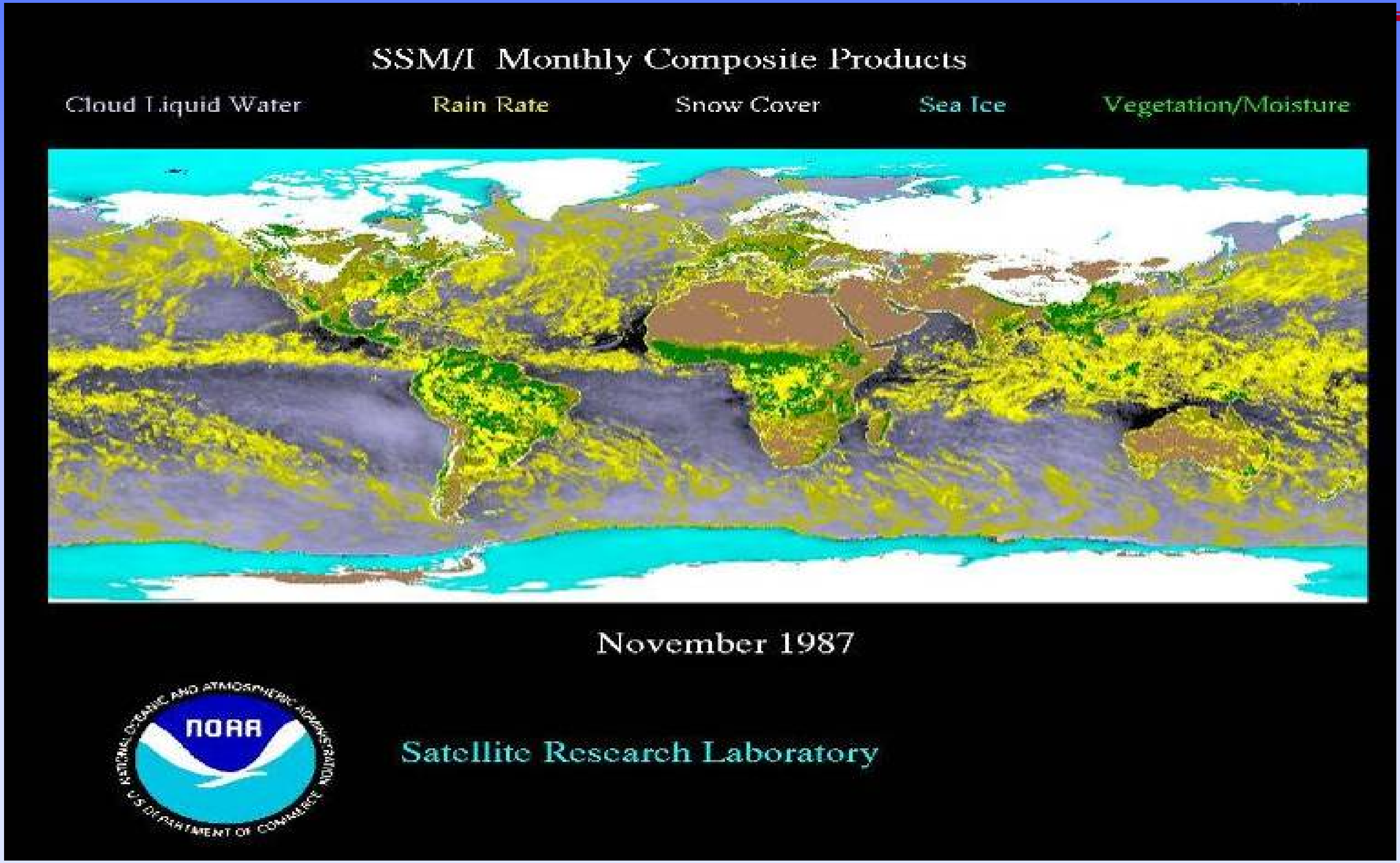

# Global Forecast Score Improvements

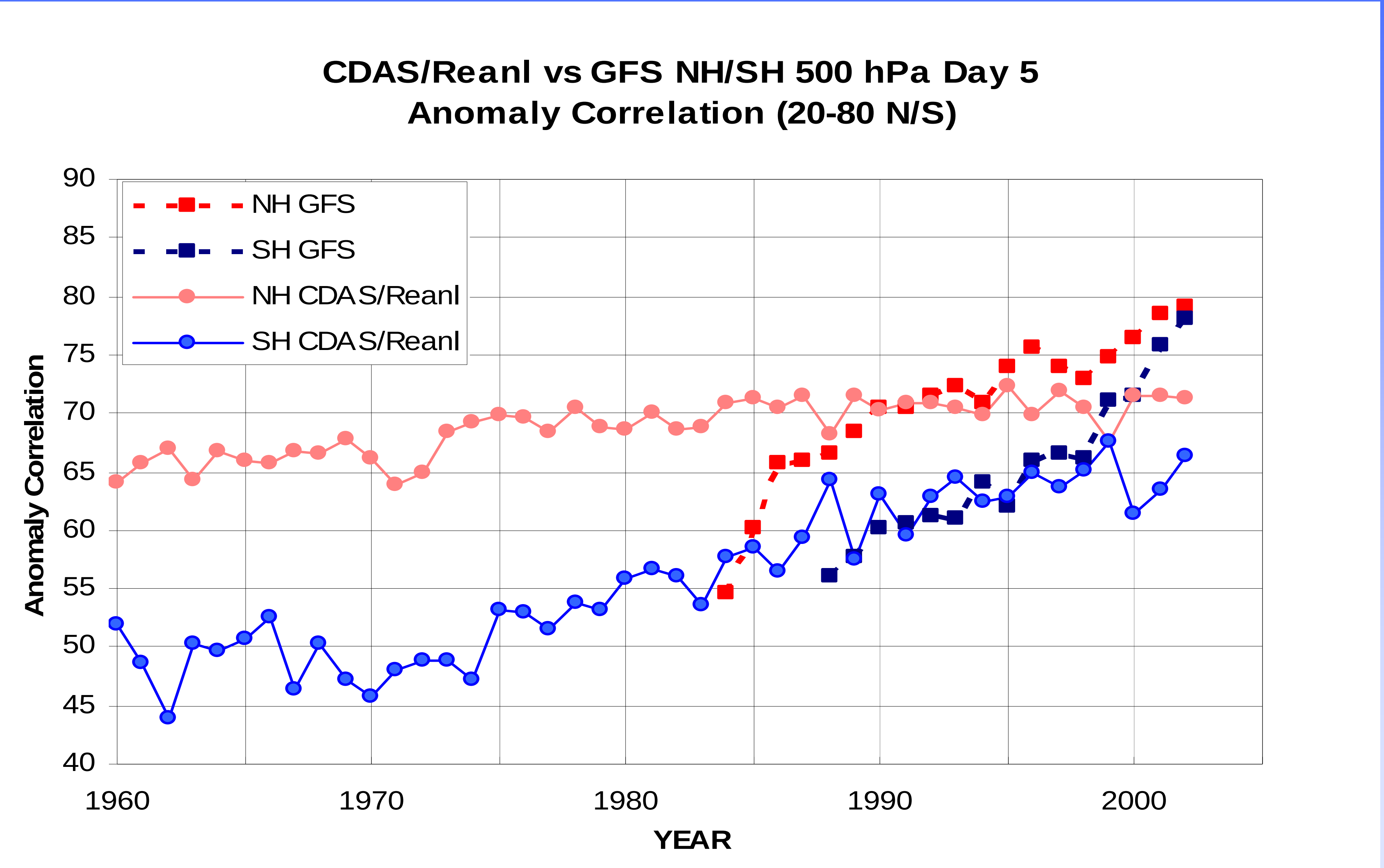

# Content

- **Introduction**
  - Impact of satellite microwave data on weather forecasts
  - MW gas spectrum
  - Sensor history
  - Radiometry system
  - Data format
- **Radiative Transfer Approximation**
  - Emission-based
  - Two-stream scattering model
- **Retrieval Algorithms**
  - Cloud liquid water
  - Cloud ice water
  - Atmospheric temperature and water vapor
- **Product Applications**
  - Intercomparison
  - NWP model validations
  - Climate monitoring

# Our Vision

**In 2015, Nation's monitoring and predictions of severe storms will be empowered by uses of *advanced instrument data from geostationary and polar-orbiting satellites***

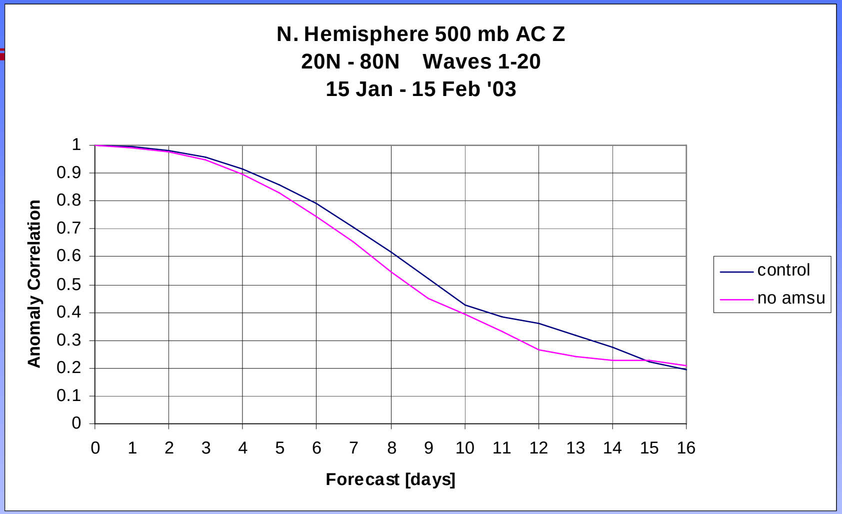


## ORA's Role in Satellite Program Developments

- Definition of scientific and operational requirements for new instruments
- Observation system simulation experiments
- Instruments calibration
- Algorithm developments and data analysis
- Forward model development
- Quality assurance and product validation
- Data assimilation and numerical modeling testing
- Analysis of impacts on forecast applications
- Implementation and delivery of improved forecasts and products to user communities

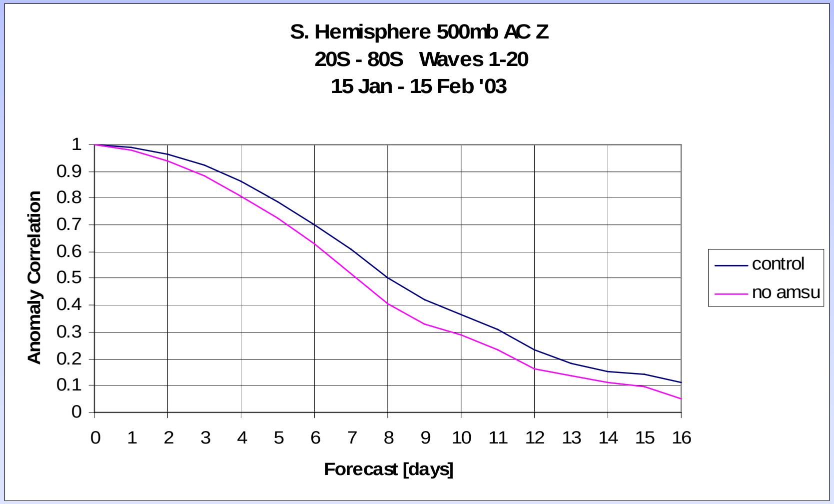

# Microwave Absorption Spectrum

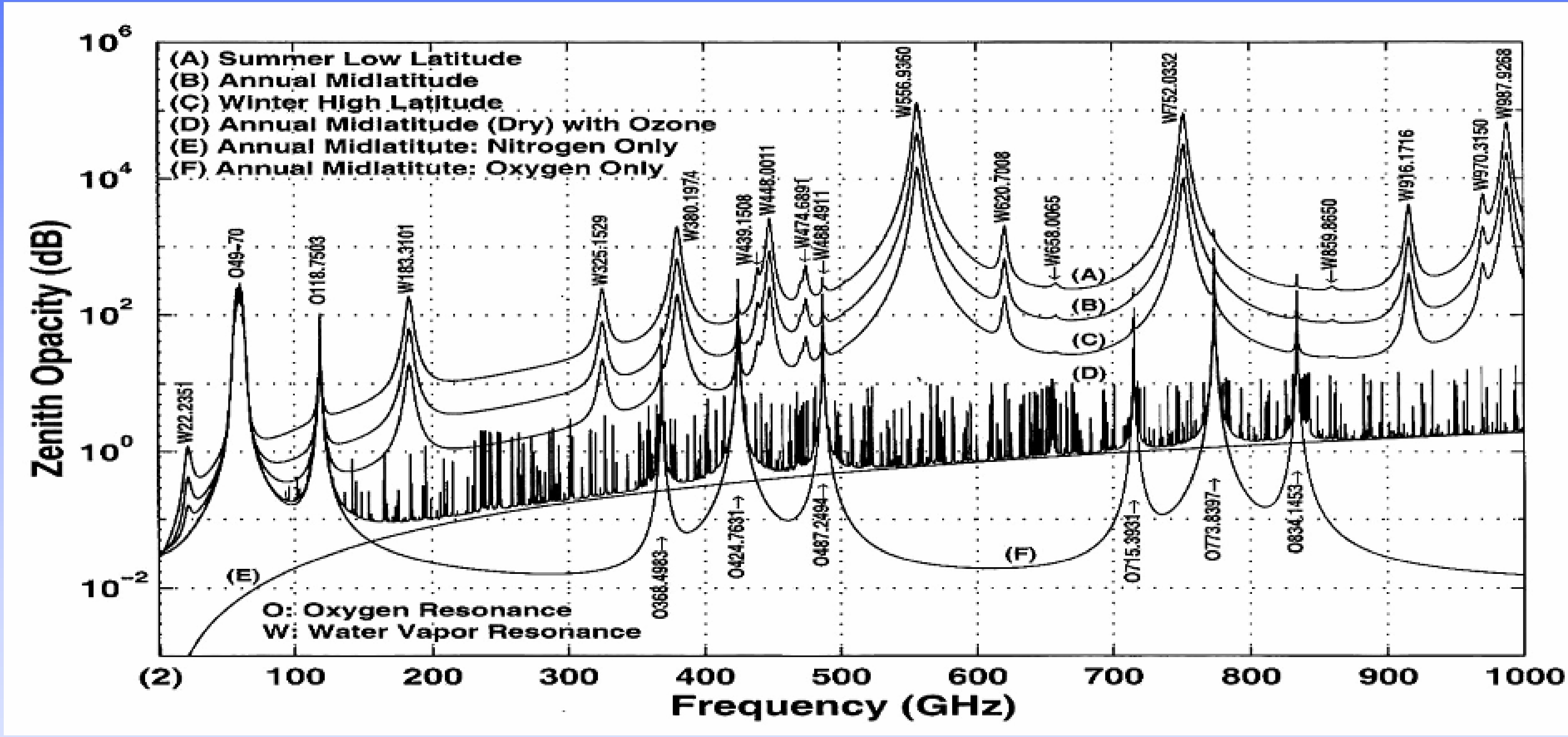


*Janssen M. A., 1993: Atmospheric remote sensing by microwave radiometry, Chapter 2, John Wiley &Son inc*

1. Rotational transition line: $O_3$,$H_2O$,CO,ClO, $N_2O$…
2. Spin-rotational transition: $O_2$ and zeeman splitting in upper atmosphere where geomagnetic field is important
3. Doppler and pressure broading

# Microwave Penetration Depth

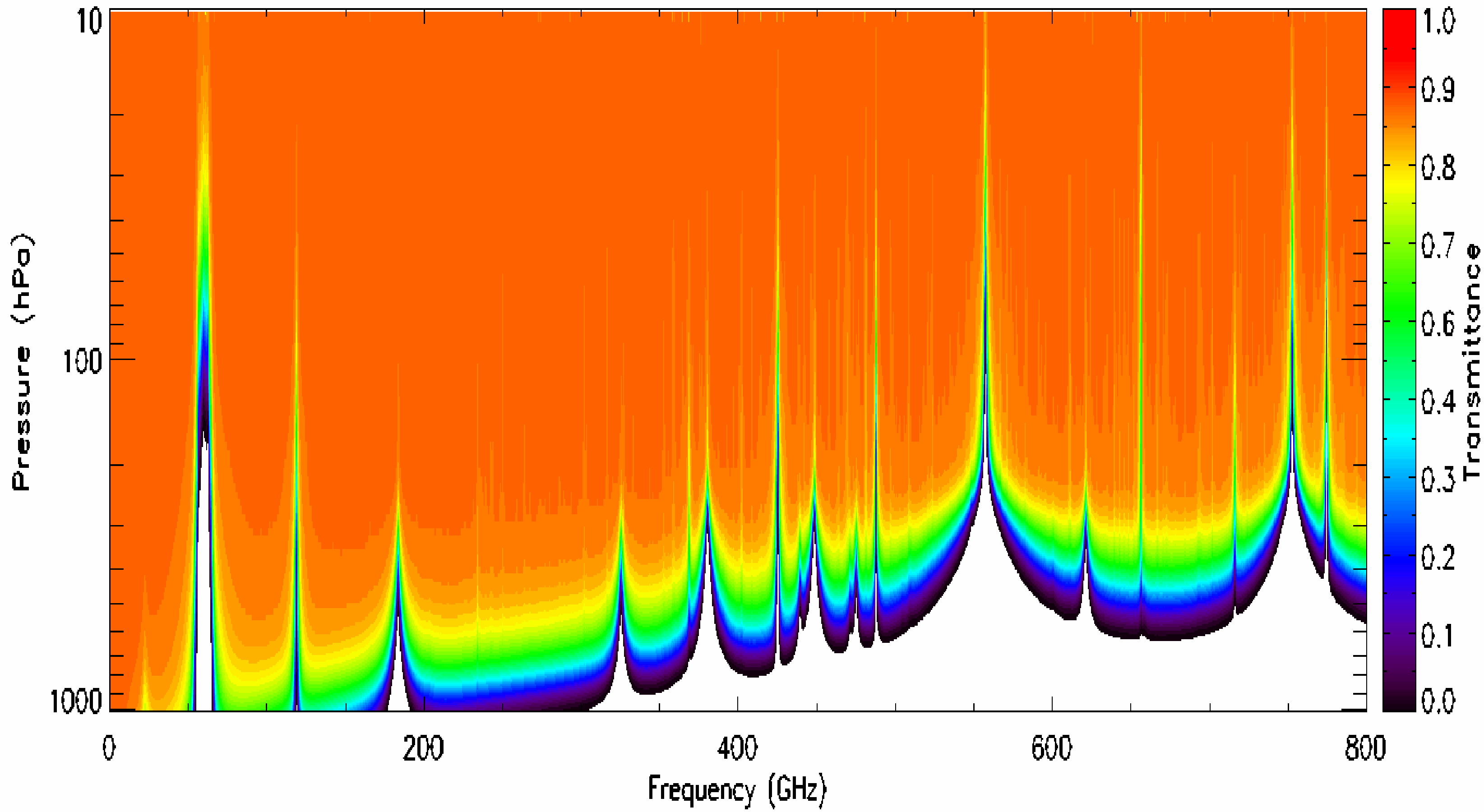

National Environmental Satellite, Data, and Information Service

# Instrument Spectrum Allocations

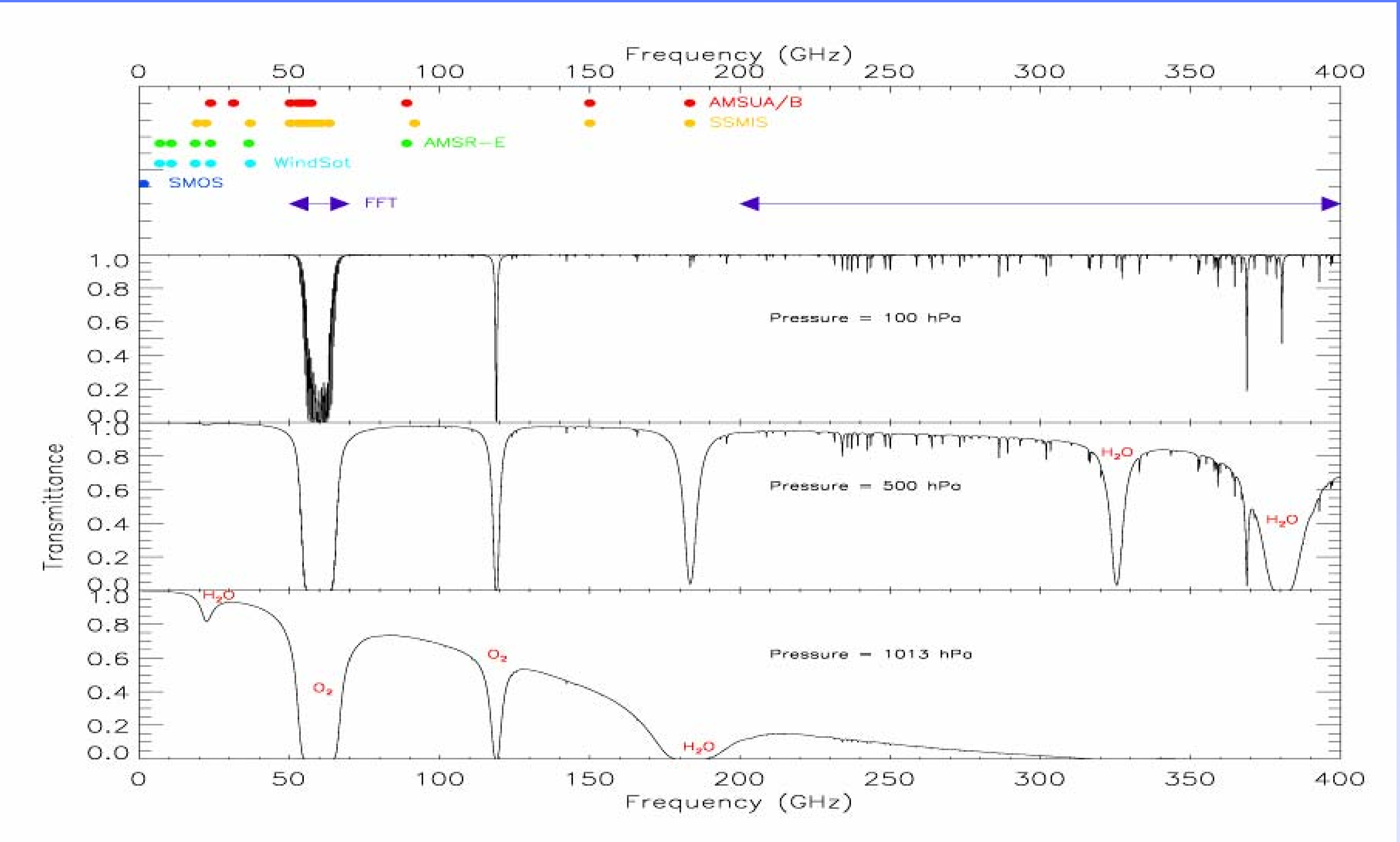

# MW Stratosphere and Mesosphere Sounding

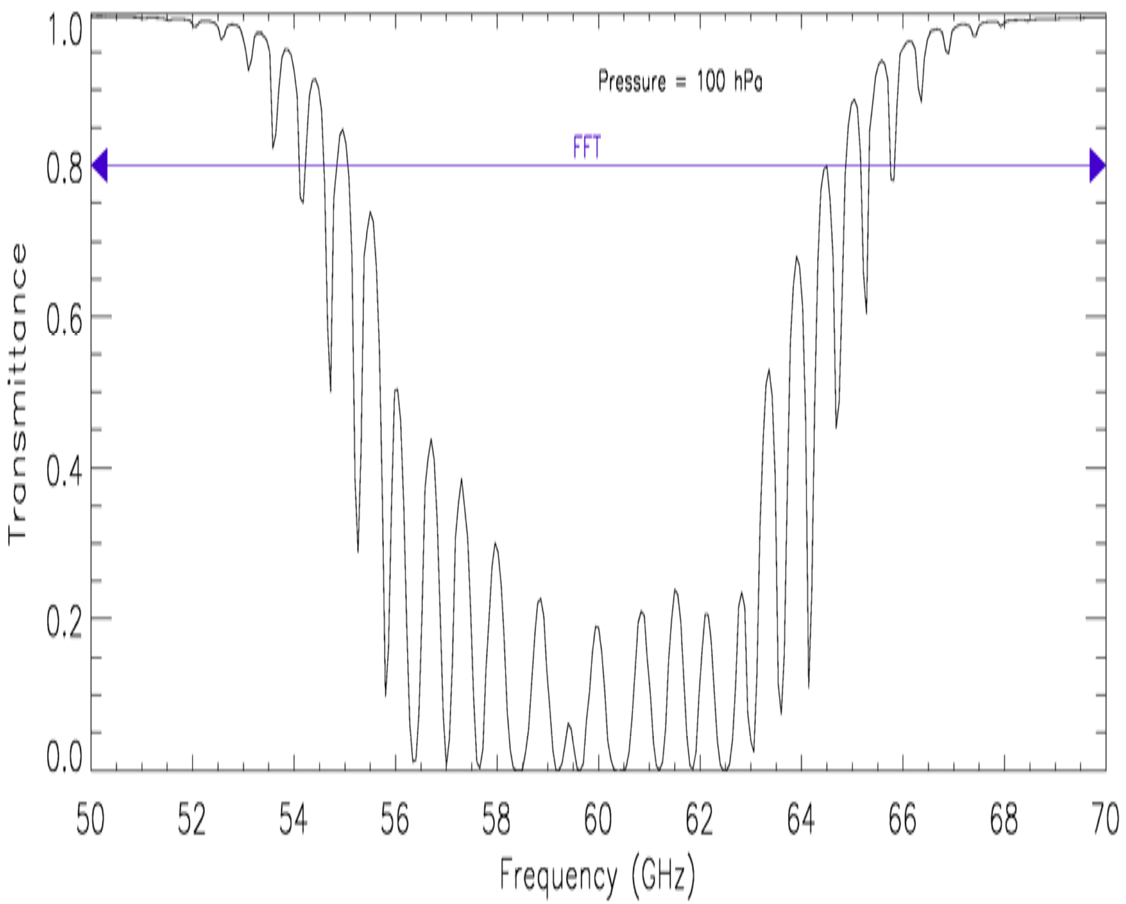


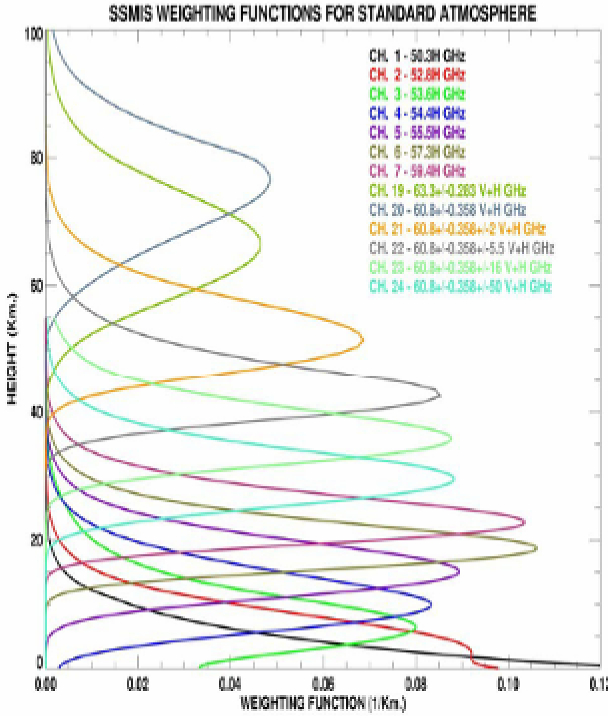


Figure 7.2: SSMIS Weighting function

# Millimeter Wavelength Spectroscopy

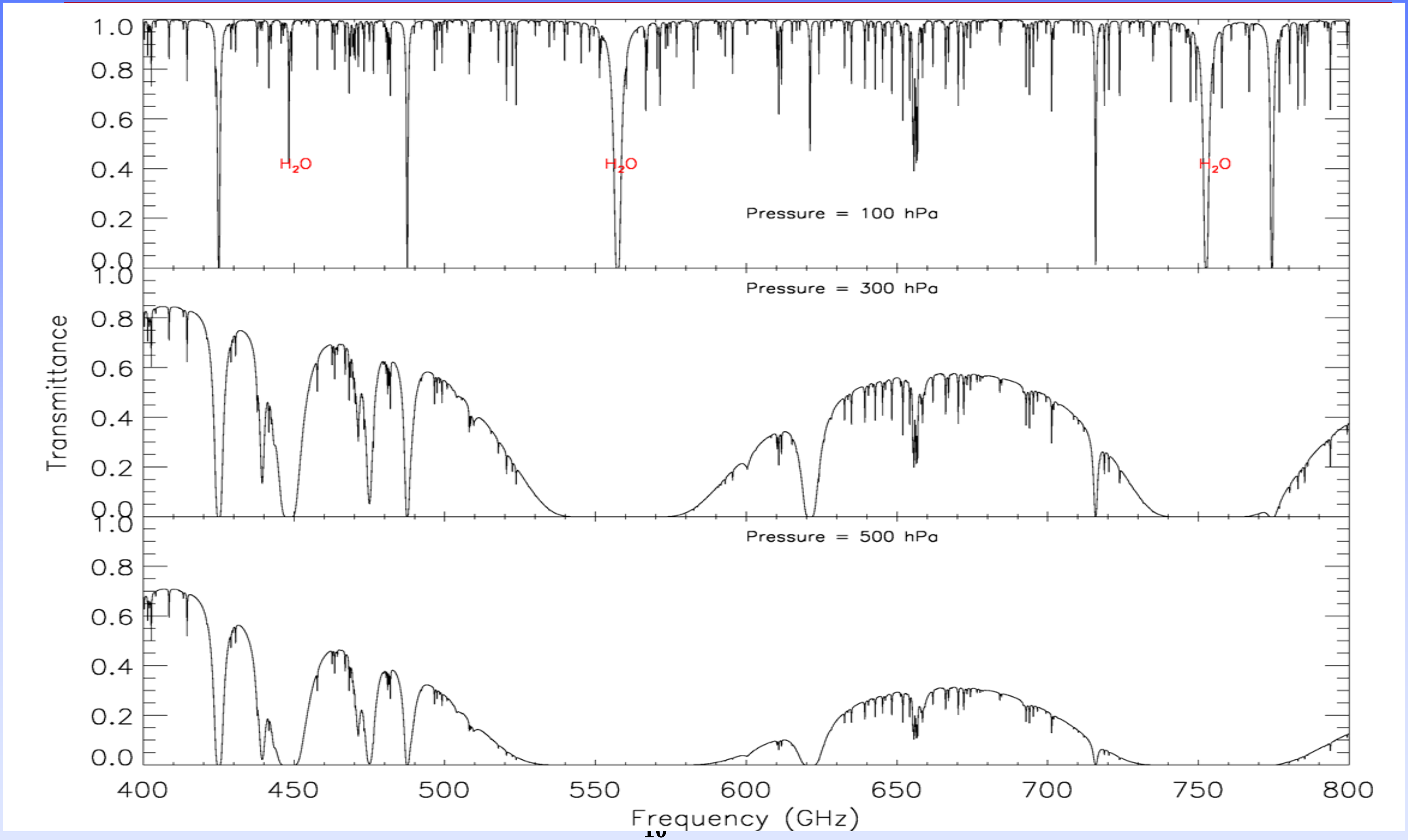

# Evolution of Passive Microwave Sensors

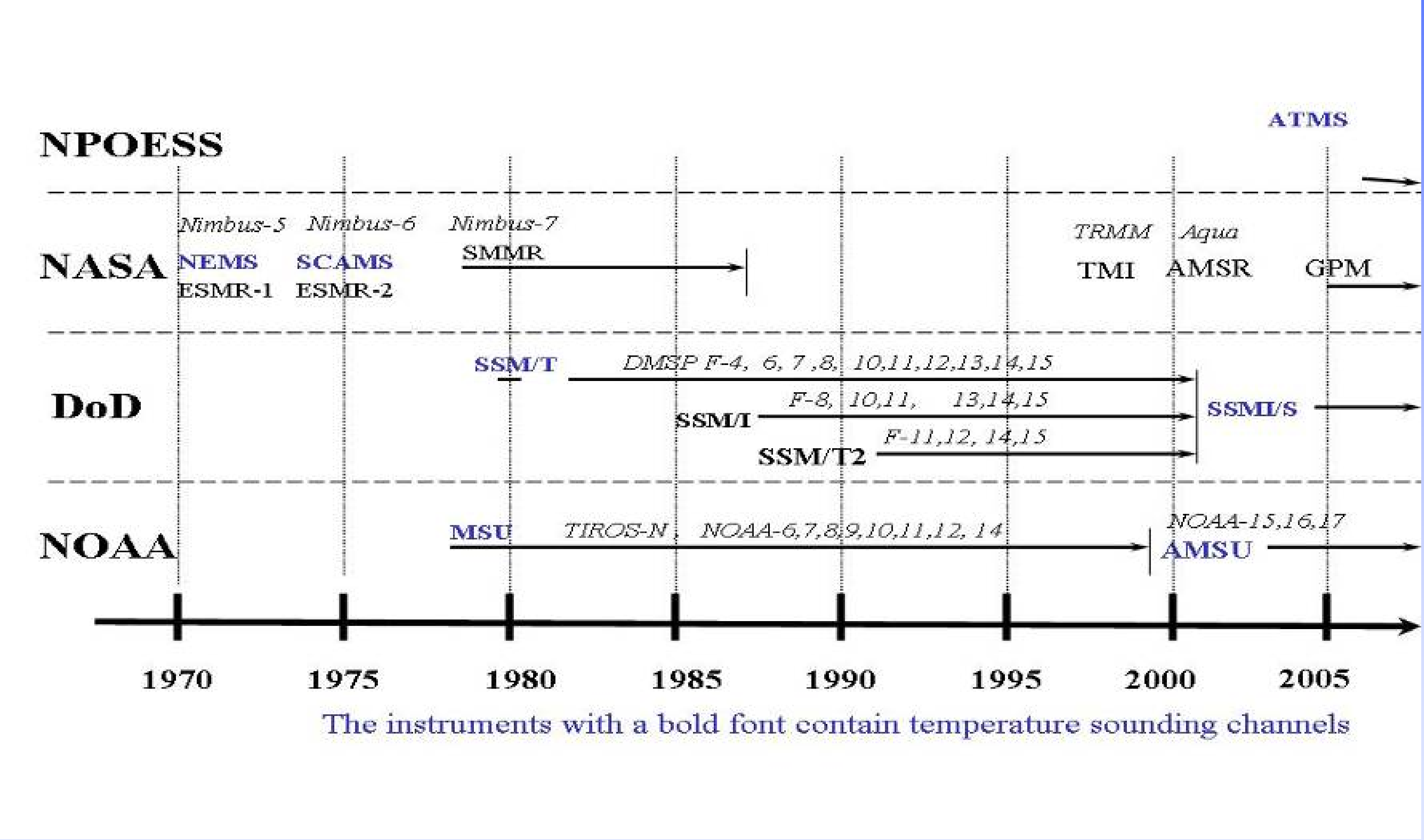

# Microwave Products Developed for Weather and Climate Studies

| SDR/EDR | POES AMSU-A/B MHS | DMSP SSMIS | NPOESS CMIS ATMS | Geo-STAR | DMSP SSM/I |
|---|---|---|---|---|---|
| **Radiances** | ✓ | ✓ | ✓ | ✓ | ✓ |
| **Temp. profile** | ✓ | ✓ | ✓ | ✓ | |
| **Moist. Profile** | ✓ | ✓ | ✓ | ✓ | |
| **Hydr. profile** | ✓ | ✓ | ✓ | ✓ | |
| ***Precip rate**** | ✓ | ✓ | ✓ | ✓ | ✓ |
| ***Snow cover**** | ✓ | ✓ | ✓ | | ✓ |
| ***Sea ice **** | ✓ | ✓ | ✓ | | ✓ |
| ***Cloud water**** | ✓ | ✓ | ✓ | | ✓ |
| ***Ice water**** | ✓ | ✓ | ✓ | ✓ | |
| ***Surface temp**** | ✓ | ✓ | ✓ | | ✓ |
| ***Surface wind*** | | ✓ | ✓ | | ✓ |
| ***Land emis**** | ✓ | ✓ | ✓ | | ✓ |
| **Soil moisture** | | | ✓ | | ✓ |

***  Currently produced through NOAA Advanced Microwave Sounding Unit (AMSU/MHS).  Many of EDRS were not planned when the sensor  was developed.***

# Microwave Radiometry System

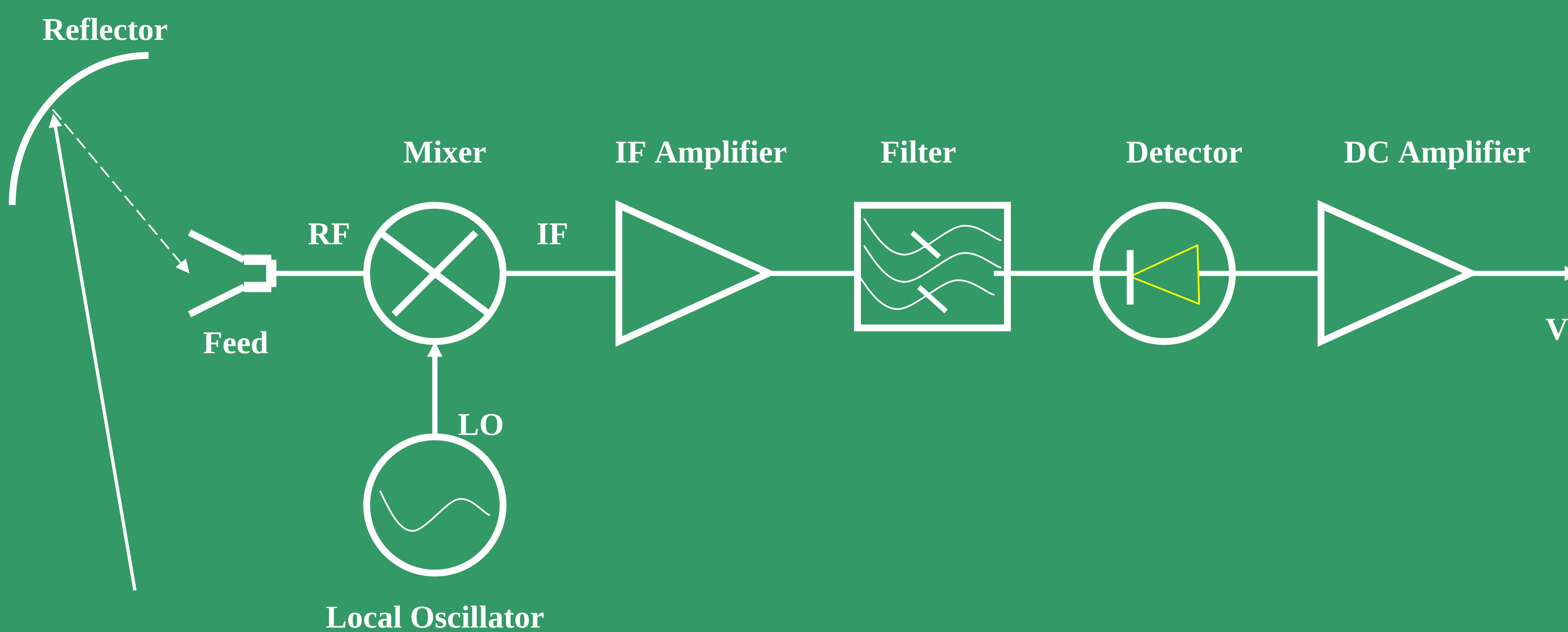

# Microwave Radiometry Calibration

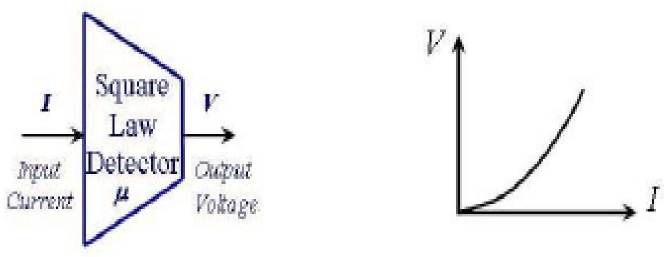


Figure 1.4: Microwave square law detector

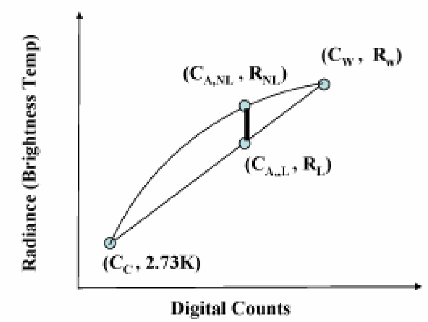


Figure 1.3: Two-point calibration algorithm used for microwave instrument calibration

The calibration error can be also introduced by neglecting the non-linearity effects. This is mainly because the microwave total power radiomeneter is not a perfect square law detector in which its output voltage, $V$, is a polynomial function of input current, $I$, as shown in Fig. (1.2.1).

$$V = a_1 I + a_2 I^2 + a_3 I^3 + a_4 I^4. \tag{1.1}$$

After the integration in time, its average voltage is a function of current square in that

$$\langle V \rangle = (a_2 + 3a_4 \langle I^2 \rangle) \langle I^2 \rangle. \tag{1.2}$$

# Calibration including non-Linearity Effect

Using Nyquist theorem, this current square is related to the total power input to the IF system which is the radiance from either calibration targets or earth scenes such that

$$\langle I^2 \rangle \;=\; KBG[R(T_A) + R(T)], \tag{1.3}$$

where $G$, $B$ and $T$ is the amplifier gain, bandwidth and temperature, respectively, and $K$ is the Baltzman constant. Combining 1.13and 1.15 results in

$$\langle V \rangle \;=\; b_0 + b_1 R(T_A)[1 + \mu R(T_A)], \tag{1.4}$$

where $\mu$ is the non-linear parameter and $b_0$ and $b_1$ are linear term parameters that can be determined from two-point calibration directly. They are expressed as

$$\begin{aligned} b_0 &= [a_2 + 3a_4 KBR(T)]KBGR(T), \\ b_1 &= [a_2 + 6a_4 KBR(T)]BG, \\ \mu &= 3a_4 \frac{KBG}{a_2}, \end{aligned}$$

Two-point calibration will eliminate $b_0$ and $b_1$ from Eq.(1.4) and result in

$$R_A = R_C + S(C_A - C_C) + \mu S^2 (C_A - C_C)(C_A - C_W), \tag{1.5}$$

where $S$ is a parameter and its inverse is often referred as the radiance gain.

$$S = \frac{R_W - R_C)}{C_W - C_C}. \tag{1.6}$$

For microwave application, we often write

$$T_A = T_C + S(C_A - C_C) + \mu S^2 (C_A - C_C)(C_A - C_W), \tag{1.7}$$

and

$$S \;=\; \frac{T_W - T_C}{C_W - C_C}. \tag{1.8}$$

# Other Factors Affecting Microwave Calibration

- Main-reflector conically scans the earth scene
- Sub-reflector views cold space to provide one of two-point calibration measurements
- Warm loads are directly viewed by feedhorn to provide other measurements in two-point calibration system
- Warm load calibration may be contaminated
- Occasional lunar contamination on space view

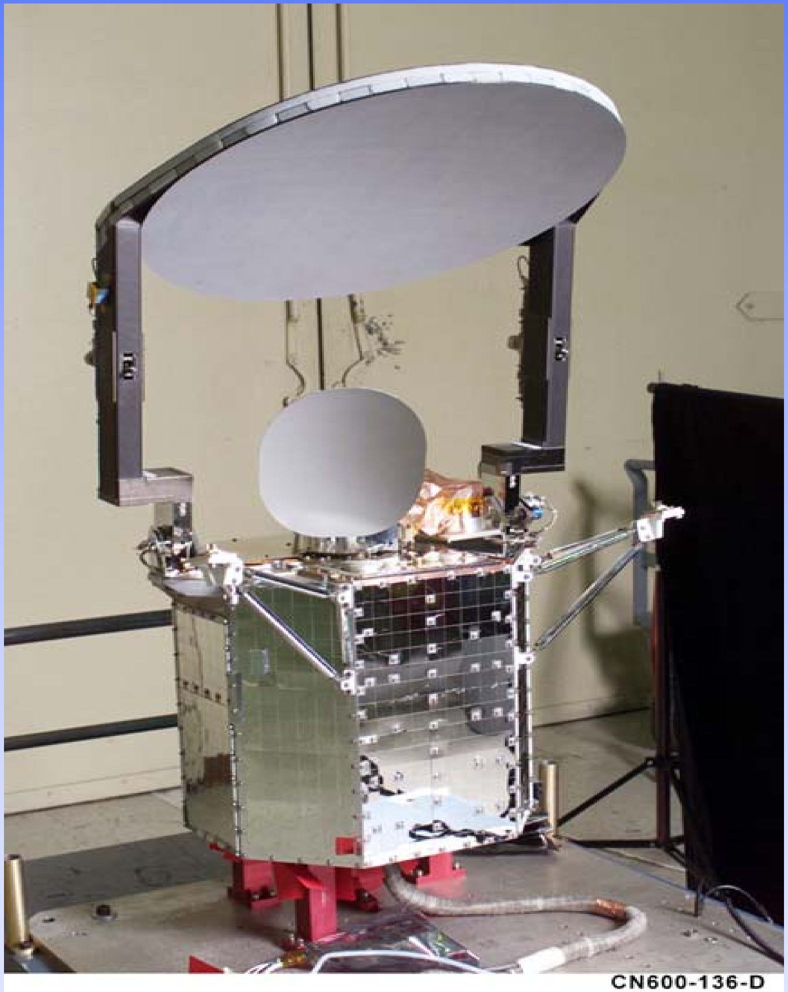

# Microwave Measurement Data Records

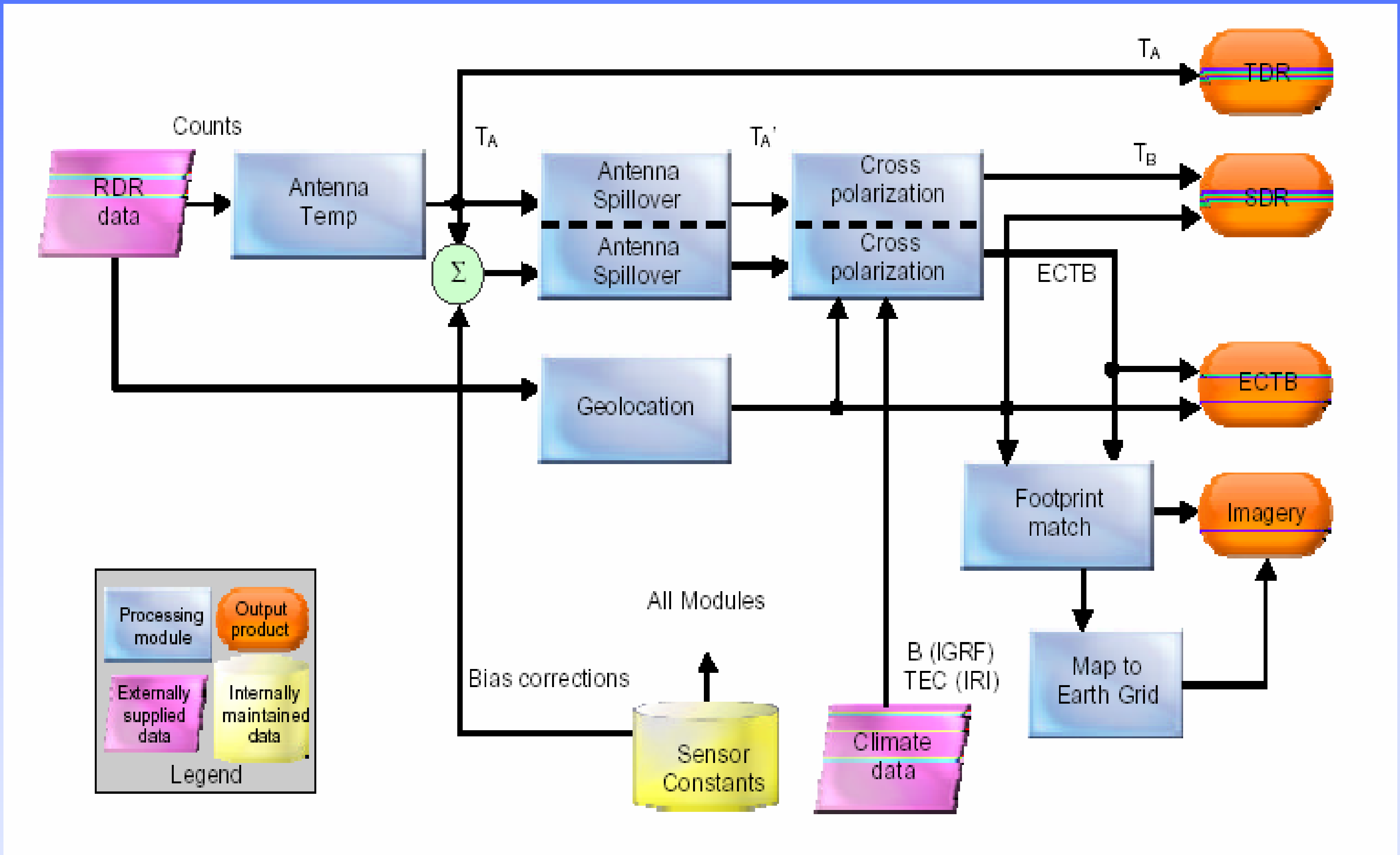

# Microwave Surface Emissivity Spectra

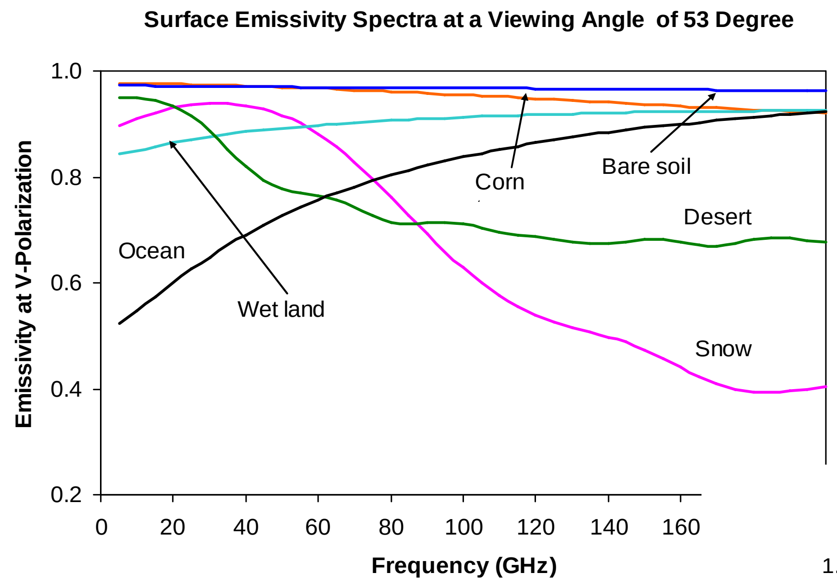


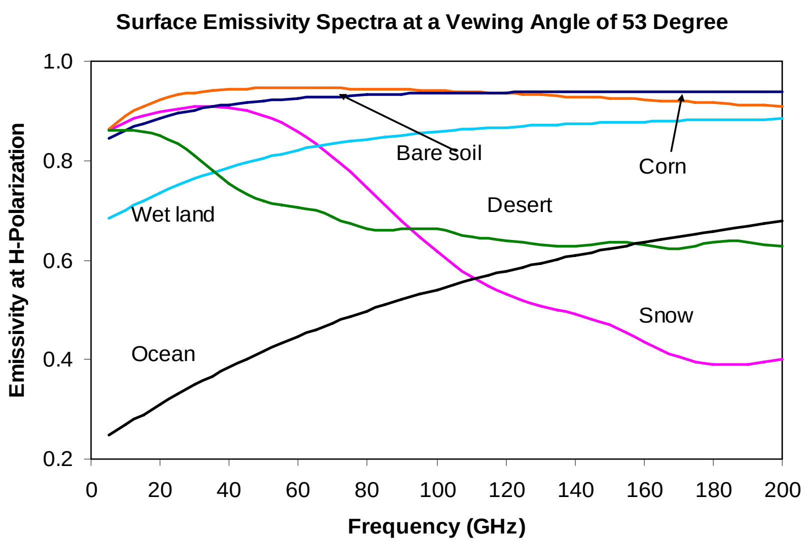

# Advanced Microwave Sounding Unit

## Imaging and Temperature Sounding Channels

23.8 GHz

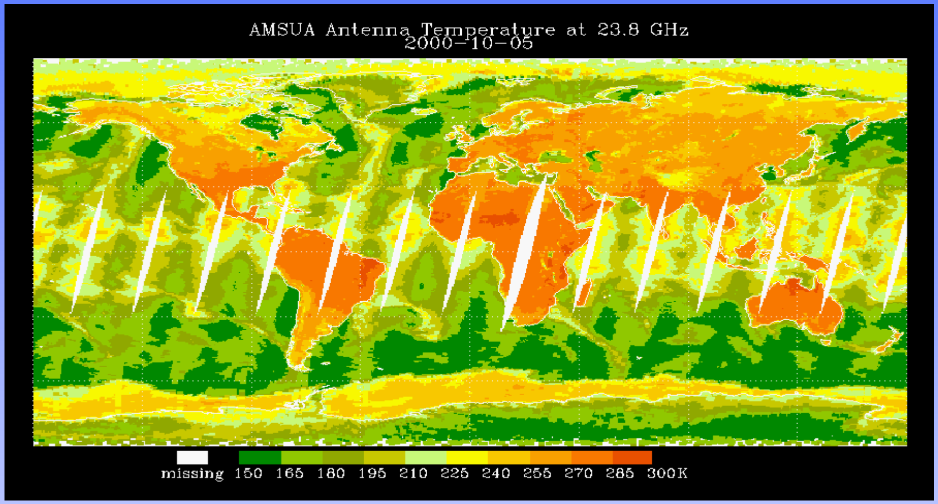


31.4 GHz

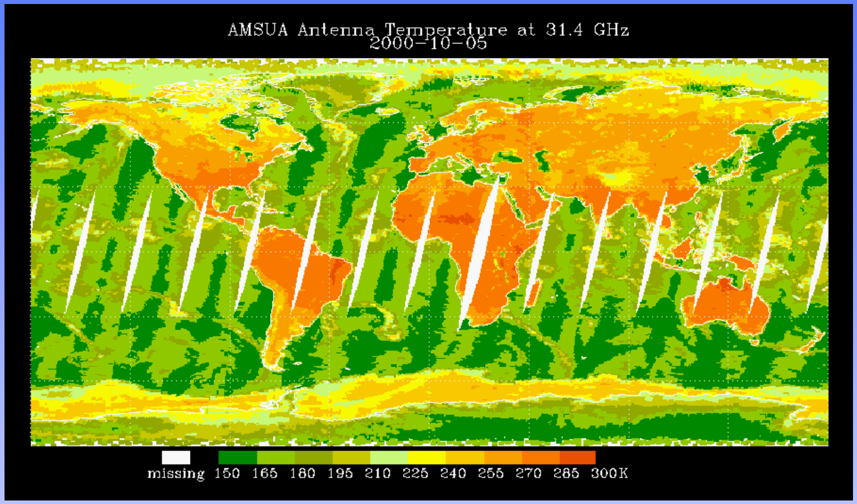


52.8 GHz

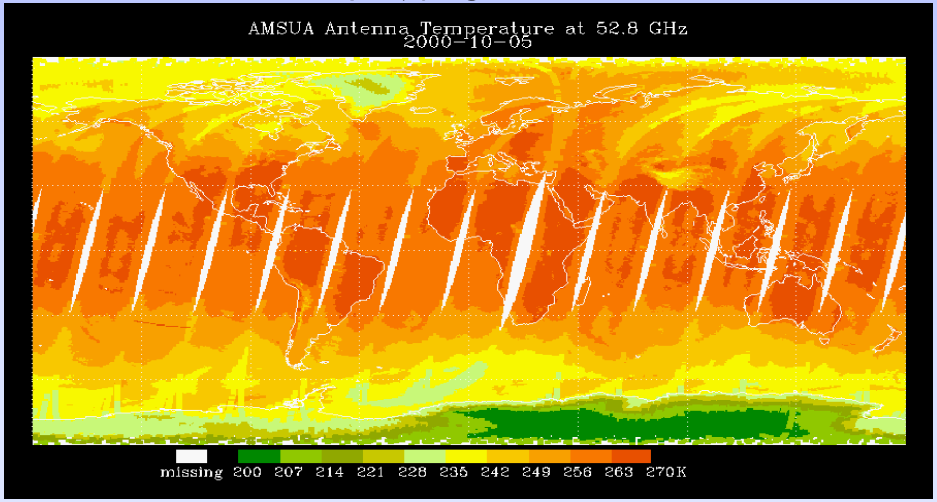


53.7 GHz

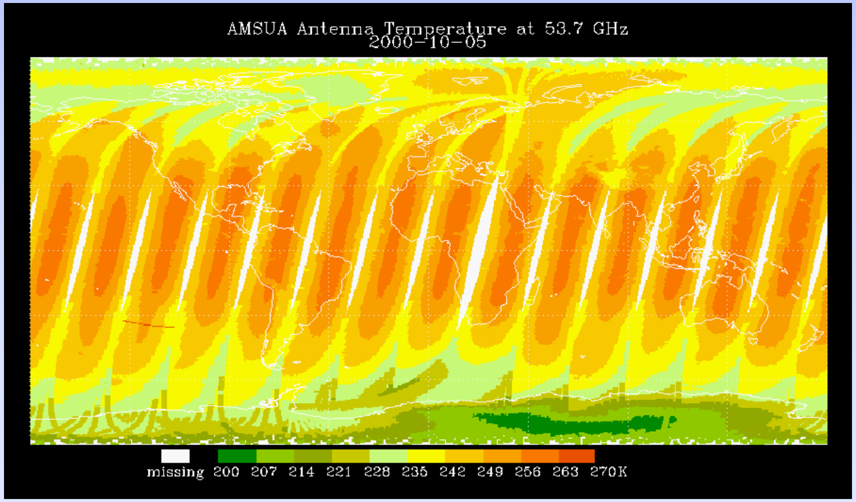

# Advanced Microwave Sounding Unit

## Imaging and Moisture Sounding Channels

89 GHz

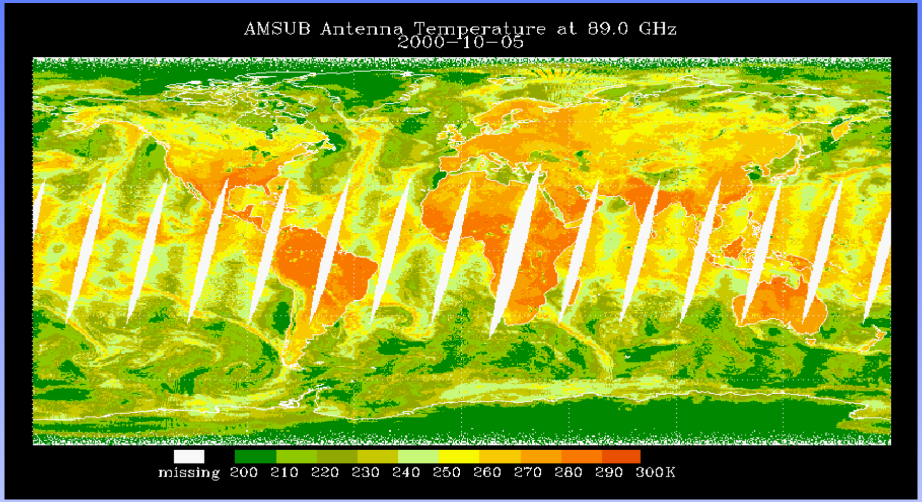


183±3 GHz

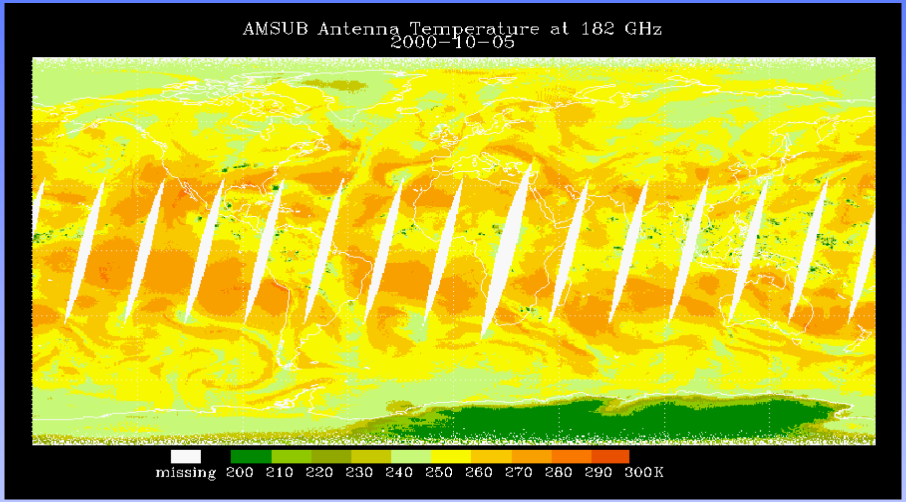


150 GHz

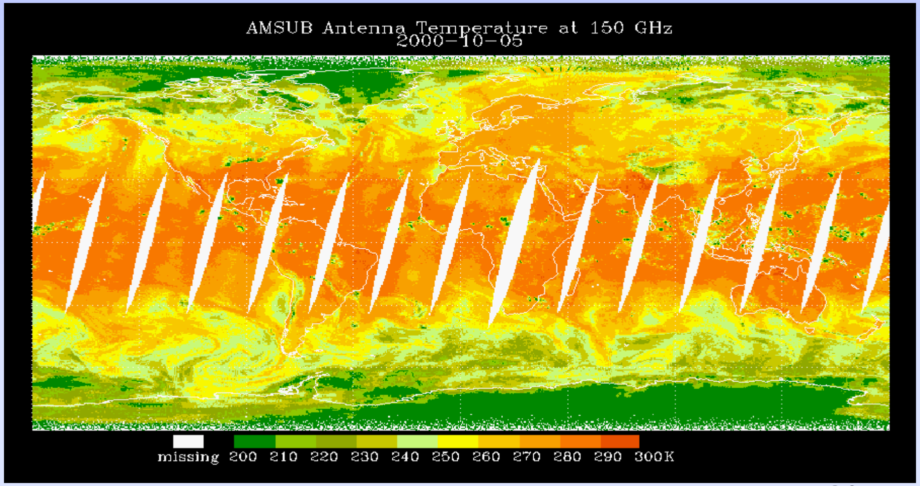


183± 1 GHz

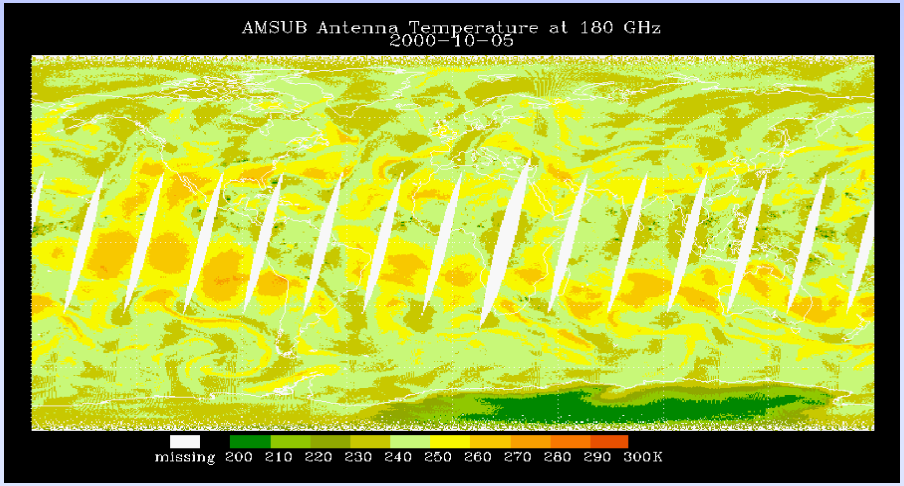

# Content

- Introduction
  - Impact of satellite microwave data
  - MW gas spectrum
  - Sensor history
  - Radiometry system
  - Data format
- Radiative Transfer Approximation
  - Emission-based
  - Scattering based
- Retrieval Algorithms
  - Cloud liquid water
  - Cloud ice water
  - Atmospheric temperature and water vapor
- Product Applications
  - Intercomparison
  - NWP model validations
  - Climate monitoring

# Microwave Remote Sensing of Clouds

- A large contrast exists between cloudy and “clear” conditions, thanks to low ocean emissivity.
- Brightness temp increases exponentially with liquid water, thus requiring a logarithmic function for linearization
- “The linear regime” is dependent on frequency. We can meet more customer’s needs (e.g. rain water..) if the measurements at each frequency are optimally utilized in the retrievals

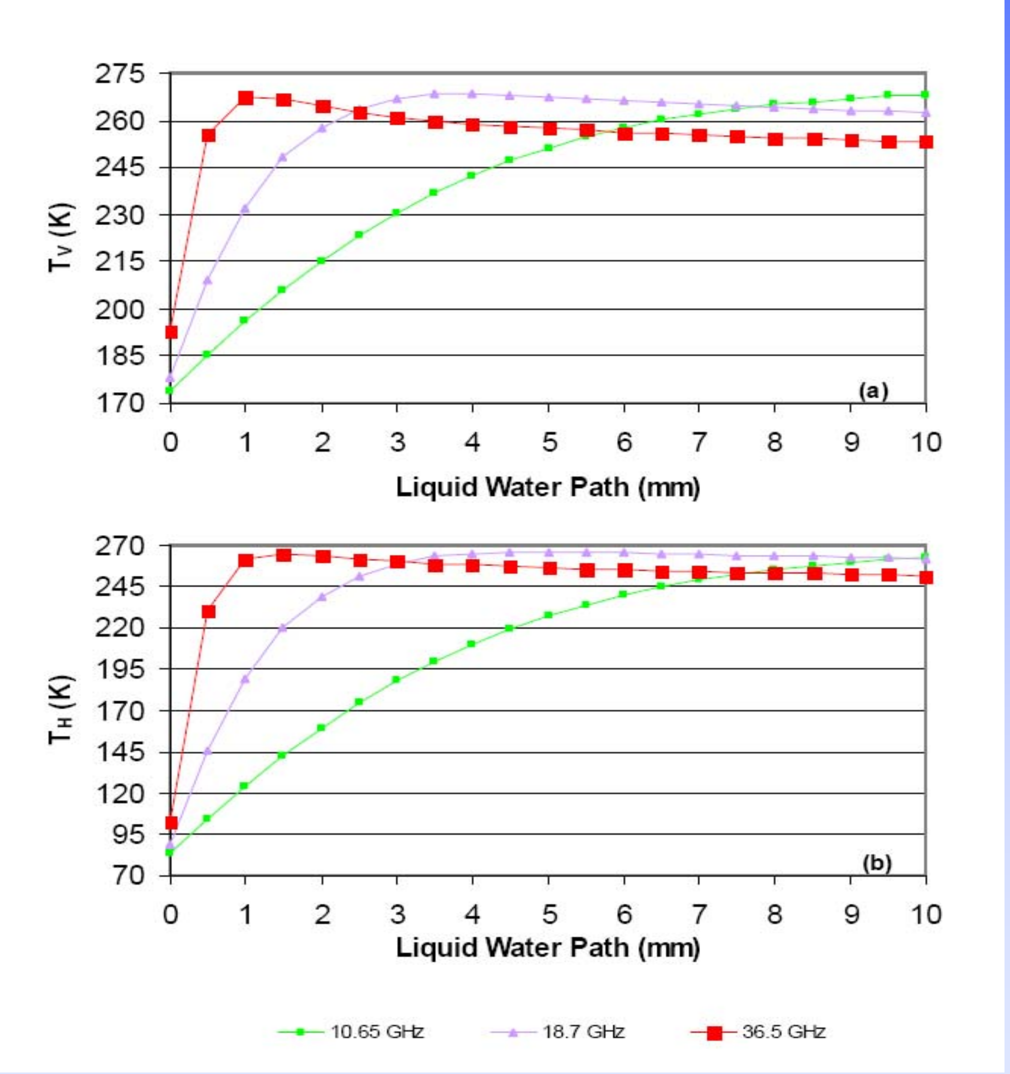

# Emission Approach

## 3.3 Radiative Transfer Approximation

### 3.3.1 Emission-Based Model

Microwave radiative transfer can be simplified if single and multiple scattering terms are neglected and there is no azimuthally dependent terms are included. Thus, in Eq. 3.17, we can derive

$$\mu \frac{d\mathbf{I}(\tau,\mu)}{d\tau} = \mathbf{I}(\tau,\mu) - \mathbf{B}(\tau), \tag{3.21}$$

where $\mathbf{I}$ is the zeroth order term of radiance in the cosine mode in Eq.3.17. For convenience, we neglect the subscript of Fourier zeroth component. when the terms from single and multiple scattering are neglected and scattering. After the integration term disappears, the solution of radiance vector can be expressed in a form (Liou, 1980)

$$\begin{aligned} \mathbf{I}(\tau_0,\mu) &= \mathbf{I}(\tau_s,\mu)\exp(-\tau_s/\mu) + \\ &\int_0^1 \mathbf{r_s}(\mu,\mu')d\mu' \int_{\tau_0}^{\tau_s} \mathbf{B}(\tau,T)\exp[-\frac{(\tau-\tau_0)}{\mu'}]d\tau/\mu + \\ &\int_{\tau_s}^{\tau_0} \mathbf{B}(\tau,T)\exp[-\frac{(\tau_s-\tau)}{\mu}]d\tau/\mu, \end{aligned} \tag{3.22}$$

or

$$\begin{aligned} \mathbf{I}(\tau_0,\mu) &= \mathbf{I}(\tau_s,\mu)\exp(-\tau_s/\mu) + \mathbf{I_u} + \mathbf{I_d}, \qquad (3.23) \\ \mathbf{I_u} &= \int_{\tau_s}^{\tau_0} \mathbf{B}(\tau,T)\exp[-\frac{(\tau_s-\tau)}{\mu}]d\tau,/\mu \\ \mathbf{I_d} &= \int_0^1 \mathbf{r_s}(\mu,\mu')d\mu' \int_{\tau_0}^{\tau_s} \mathbf{B}(\tau,T)\exp[-\frac{(\tau-\tau_0)}{\mu'}]d\tau/\mu \end{aligned}$$

(3.24)

# Emission-Based RT Model (1/3)

At the microwave frequencies, radiance is related to brightness temperature under Rayleigh-Jean approximation. Also, we only consider the first Stokes component (i.e. intensity), which is the brightness temperature. After some manipulation, we can derive

$$T_b = \epsilon T_s \exp(-\tau_s/\mu) + T_u + (1-\epsilon)(1+\Omega)(T_d + T_c)\exp(-\tau_s/\mu), \quad (3.25)$$

$$\begin{aligned} T_d &= \int_{\tau_0}^{\tau_s} B(\tau, T)\exp\left(-\frac{(\tau-\tau_0)}{\mu}\right) d\tau/\mu, \\ T_u &= \int_{\tau_s}^{\tau_0} B(\tau, T)\exp\left(-\frac{(\tau_s-\tau)}{\mu}\right) d\tau/\mu, \end{aligned} \quad (3.26)$$

where $\epsilon$ is the surface emissivity and $T_s$ is the surface temperature, and $T_c$ is the cosmic background brightness temperature. The parameter, $\Omega$, is introduced for non-specular effect of surface reflection and varies with surface roughness, sea surface wind speed, frequency, and atmospheric transmittance (Wentz, 1998). Eq. 5.1 has been so far widely used for retrieving surface emissivity assume other components such as $T_s$, upwelling and downwelling brightness temperatures are estimated from other means (Weng et al., 2000; Prigent, 2004).

# Emission-Based RT Model (2/3)

For an isothermal atmosphere, upwelling and downwelling components in terms of brightness temperatures can be approximated as

$$T_u \approx T_d \equiv (1 - \Upsilon) T_m, \quad (3.27)$$

where $\Upsilon = \exp(-\frac{(\tau_s - \tau_0)}{\mu})$ and $T_m$ is the atmospheric temperature. Thus,

$$T_b = T_s[1 - (1 - \epsilon)\Upsilon^2] - \Delta T (1 - \Upsilon)[1 + (1 - \epsilon)\Upsilon], \quad (3.28)$$

where $\Delta T = T_s - T_m$. It is apparent that brightness temperatures under these approximation is directly related by the layer mean temperature and atmospheric transmittance. When emissivity is low (0.9), brightness temperature increases as atmospheric transmittance (more cloud and water vapor) decreases (see Fig. 3.3.1. This is why over oceans clouds having liquid water increases brightness temperature and are easily detected from lower microwave measurements. Eq. 5.4 can be analytically used to retrieve cloud liquid water path when $\Delta T$ is very small.

# Emission-Based RT Model (3/3)

In an absence of scattering, brightness temperatures can be linearly a function of cloud liquid water path ($L$) and precipitable water path ($V$) (Weng et al. 2003) by further assuming an isothermal atmosphere in Eq. 5.4 and a Rayleigh scattering for liquid-phase droplets Eq. 3.44, i.e.,

$$T_b = T_s[1 - (1 - \epsilon)\Upsilon^2], \tag{6.1}$$

where $\epsilon$ and $T_s$ are surface emissivity and temperature, respectively, and

$$\Upsilon = \exp[-(\tau_O + \tau_V + \tau_L)/\mu)] \tag{6.2}$$

where $\tau_O$, $\tau_V$ and $\tau_L$ are the optical thicknesses of oxygen, water vapor and liquid respectively.

$$\tau_L = \int_{\Delta Z} \kappa^{Ray} LWC dz \tag{6.3}$$

where

$$\kappa^{Ray} = \frac{6\pi}{\lambda\rho_w} Im\left\{\frac{m^2 - 1}{m^2 + 2}\right\} \tag{6.4}$$

and

$$\tau_V = \int_0^\infty \kappa^{H_2O} \rho_V dz \tag{6.5}$$

where $\kappa_{H_2O}$ is the mass absorption coefficient of water vapor having a unit of $m^2/kg$, and $\rho_v$ is the water vapor density in atmosphere. Lets assume $\kappa^{Ray}$ and $\kappa^{H_2O}$ are independent of height. Then, we have

$$\tau_L = \kappa_L L \tag{6.6}$$

# Liquid Water Absorption

where $\kappa_L$ is the mass absorption coefficient of liquid-phase cloud, viz,

$$\kappa_L = \frac{6\pi}{\lambda\rho_w} Im\left\{\frac{m^2-1}{m^2+2}\right\}, \tag{6.7}$$

Here, we use a different notation to indicate there is a further approximation being made for cloud absorption coefficient which can be derived from a mean cloud temperature in the complex dielectric constant. And, we also have

$$\tau_V = \kappa_V V \tag{6.8}$$

where

$$V = \int_0^\infty \rho_V \, dz \tag{6.9}$$

and

$$L = \int_{\Delta Z} LWC dz \tag{6.10}$$

are the vertically integrated water vapor and liquid water, respectively. Thus, atmospheric transmittance becomes

$$\Upsilon = \exp[-(\tau_O + \kappa_V V + \kappa_L L)/\mu) \tag{6.11}$$

# Scattering Approach: 2 Streams Approximation

### 3.3.2 Scattering-Based Model

For a scattering and absorbing atmosphere, the radiance may be considered azimuthally independent so that the radiative transfer equation is given as

$$\mu\frac{dI(\tau,\mu)}{d\tau} = I(\tau,\mu) - \frac{\omega(\tau)}{2}\int_{-1}^{1} P(\mu,\mu')I(\tau,\mu')d\mu' - (1-\omega(\tau))B(T)\qquad(3.29)$$

where $I$ is the radiance; $\omega(\tau)$ the single-scattering albedo; $P(\mu,\mu')$ the phase function; $B(T)$ the Planck function; $T$ the thermal temperature; $\tau$ the optical thickness; $\mu$ the cosine of incident zenith angle and $\mu'$ the cosine of scattering zenith angle.

A solution for Eq. (??) was derived at arbitrary viewing angles using a two-stream approximation (Weng and Grody, 2000),

$$\mu\frac{dI(\tau,\mu)}{d\tau} = [1-\omega(1-b)]I(\tau,\mu) - \omega b I(\tau,-\mu) - (1-\omega)B,\qquad(3.30)$$

$$-\mu\frac{dI(\tau,-\mu)}{d\tau} = [1-\omega(1-b)]I(\tau,-\mu) - \omega b I(\tau,\mu) - (1-\omega)B,\qquad(3.31)$$

where $b$ and $1-b$ is the ratio of the integrated scattering energy in the backward and forward directions, respectively. For an isotropic scattering, $b = 1/2$ so that the scattered energy is the same in both directions. Since $b$ is generally less than 1/2, forward scattering is much stronger than backward scattering and the resulting upwelling radiation is reduced.

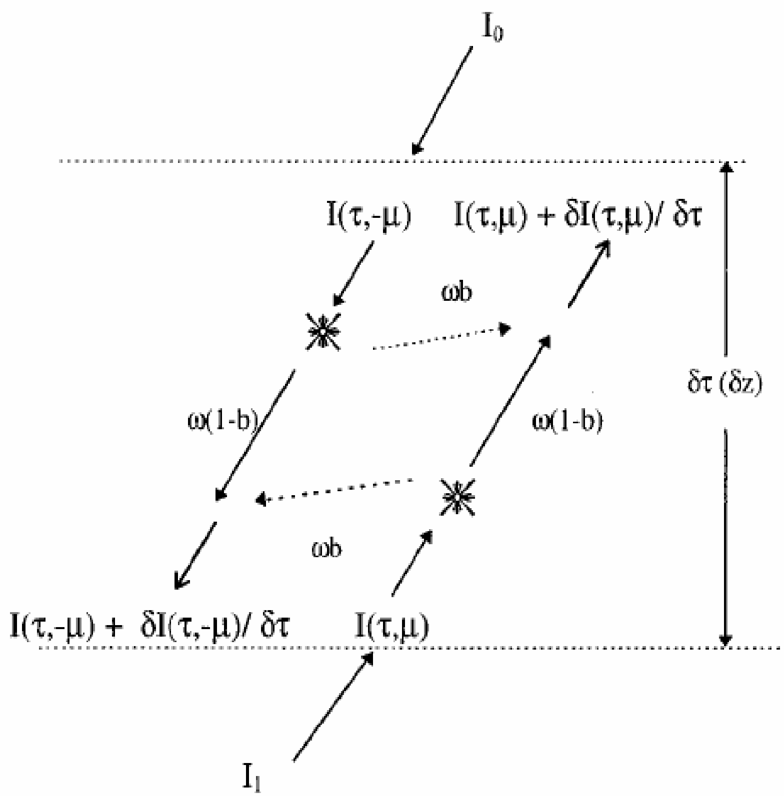


FIG. 1. A schematic diagram of the two-stream radiative transfer in an ice cloud layer.

# Two-Stream Model Solution

Equations (3.30) and (3.31) can be combined into two decoupled second order differential equations with constant coefficients, assuming that $\omega$, $b$ and $B$ are independent of $\tau$. These equations can be used to analyze the scattering from the atmosphere or surface. The upwelling radiance observed from satellites for an ice cloud layer is derived by neglecting reflections at the cloud top and bottom (Weng and Grody, 2000). However, for surfaces such as snow, the upwelling radiance is modified by the reflectivity and transmissivity at the upper boundary where a discontinuity in the dielectric constant occurs (see Fig. 1). As a result, the solutions for the upwelling and downwelling radiance are

$$I(\tau,\mu) = \frac{I_0'[\gamma_1 e^{\kappa(\tau-\tau_1)} - \gamma_2 e^{-\kappa(\tau-\tau_1)}] - I_1'[\beta_3 e^{\kappa(\tau-\tau_0)} - \beta_4 e^{-\kappa(\tau-\tau_0)}]}{\beta_1\gamma_4 e^{-\kappa(\tau_1-\tau_0)} - \beta_2\gamma_3 e^{\kappa(\tau_1-\tau_0)}} + B \tag{3.32}$$

$$I(\tau,-\mu) = \frac{I_0'[\gamma_4 e^{\kappa(\tau-\tau_1)} - \gamma_3 e^{-\kappa(\tau-\tau_1)}] - I_1'[\beta_2 e^{\kappa(\tau-\tau_0)} - \beta_1 e^{-\kappa(\tau-\tau_0)}]}{\beta_1\gamma_4 e^{-\kappa(\tau_1-\tau_0)} - \beta_2\gamma_3 e^{\kappa(\tau_1-\tau_0)}} + B \tag{3.33}$$

where $\kappa$ is the eigenvalue in solving the differential equations and related to particle optical parameters. Also, $I_1' = I_1 - B(1-R_{23})$; $I_0' = I_0(1-R_{12}) - B(1-R_{21})$, where $I_1$ is the upwelling radiance at $\tau = \tau_1$ from the bottom layer and $I_0$ is the downwelling radiance at $\tau = \tau_0$ from the top layer. The

# Content

- Introduction
  - Impact of satellite microwave data
  - MW gas spectrum
  - Sensor history
  - Radiometry system
  - Data format
- Radiative Transfer Approximation
  - Emission-based
  - Scattering based
- Retrieval Algorithms
  - Cloud liquid water
  - Cloud ice water
  - Atmospheric temperature and water vapor
- Product Applications
  - Intercomparison
  - NWP model validations
  - Climate monitoring

# Algorithms of Cloud (Rain) Liquid Water Path: Vertically Integrated Liquid Water over Unit Area

# Cloud Liquid Water Algorithm

$$\kappa_V V + \kappa_L L = -\frac{\mu}{2}\left\{\ln(T_s - T_b) - \ln[T_s(1-\epsilon)] + \frac{2\tau_{O_2}}{\mu}\right\} \quad (6$$

Using two channel measurements, we can derive

$$L = a_0\mu[\ln(T_s - T_{b,1}) - a_1\ln(T_s - T_{b,2}) - a_2], \quad (6$$

and

$$V = b_0\mu[\ln(T_s - T_{b,1}) - b_1\ln(T_s - T_{b,2}) - b_2], \quad (6.14)$$

respectively. $T_{b,1}$ is the channel sensitive to liquid and $T_{b,2}$ is the channel sensitive to water vapor. The coefficients, $a_{0,1,2}$ and $b_{0,1,2}$ are related to water vapoı and liquid water mass absorption coefficients as

$$a_0 = -0.5\kappa_{V2}/(\kappa_{V2}\kappa_{L1} - \kappa_{V1}\kappa_{L2}) \quad (6.15)$$
$$b_0 = 0.5\kappa_{L2}/(\kappa_{V2}\kappa_{L1} - \kappa_{V1}\kappa_{L2}) \quad (6.16)$$
$$a_1 = \kappa_{V1}/\kappa_{V2} \quad (6.17)$$
$$b_1 = \kappa_{L1}/\kappa_{L2} \quad (6.18)$$
$$a_2 = -2(\tau_{O,1} - a_1\tau_{O,2})/\mu + (1-a_1)\ln[T_s(1-\epsilon_1)] - a_1\ln(1-\epsilon_2) \quad (6.19)$$
$$b_2 = -2(\tau_{O,1} - b_1\tau_{O,2})/\mu + (1-b_1)\ln[T_s(1-\epsilon_1)] - b_1\ln(1-\epsilon_2) \quad (6.20)$$

From Rayleigh's approximation, $\kappa_L$ can be parameterized as a function of cloud layer temperature, $T_L$ in Celsius as

$$\kappa_L = a_L + b_L T_L + C_L T_L^2, \quad (6.21)$$

Oxygen optical thickness is parameterized as a function of sea surface temperature through

$$\tau_O = a_o + b_o T_s, \quad (6.22)$$

Table 6.1: The parameters calculated at four AMSU-A channels and used in liquid water and water vapor path algorithms

| | 23.8 GHz | 31.4 GHz | 50.3 GHz | 89 GHz |
|---|---|---|---|---|
| $\kappa_V$ | 4.80423E-3 | 1.93241E-3 | 3.76950E-3 | 1.15839E-2 |
| $\kappa_L$ - $a_L$ | 1.18201E-1 | 1.98774E-1 | 4.53967E-3 | 1.03486E00 |
| $\kappa_L$ - $b_L$ | -3.48761E-3 | -5.45692E-3 | -9.68548E-3 | -9.71510E-3 |
| $\kappa_L$ - $c_L$ | 5.01301E-5 | 7.18339E-5 | 8.57815E-5 | -6.59140E-5 |
| $\tau_O$-$a_o$ | 3.21410E-2 | 5.34214E-2 | 6.26545E-1 | 1.08333E-1 |
| $\tau_O$-$b_o$ | -6.31860E-5 | -1.04835E-4 | -1.09961E-3 | -2.21042E-4 |

Sometime, satellite measurements under clear condition can be used to derive some coefficients. From Eq. 6.13, set L=0

# Cloud Liquid Water Algorithm Evolution

$$\mathrm{LWP} = a_0\left[\ln(T_s - TB_1) - a_1 - a_2 \ln(T_s - TB_2)\right]$$
$$\mathrm{TPW} = b_0\left[\ln(T_s - TB_1) - b_1 - b_2 \ln(T_s - TB_2)\right]$$

**Statistical: all coefficients are from simulated data sets & Ts=290**

$$\ln(290 - TB_1) = a_1 + a_2 \ln(290 - TB_2)$$

**Semi–Physical: a0 is derived from simulated data set, a1 and a2 are from microwave measurements under clear conditions**

$a0 = -0.5\kappa v23 / (\kappa v23 \kappa l31 - \kappa v31 \kappa l23)$

$b0 = 0.5\kappa l23 / (\kappa v23 \kappa l31 - \kappa v31 \kappa l23)$

$a1 = \kappa v31 / \kappa v23;\ \ b1 = \kappa l31 / \kappa l23$

$a2 = -2.0(\tau o31 - a1\ \tau o23) / \mu + (1.0 - a1) \ln(Ts) + \ln(1.0 - \varepsilon 31) - a1 \ln(1.0 - \varepsilon 23)$

$b2 = -2.0(\tau o31 - b1\ \tau o23) / \mu + (1.0 - b1)\ln(Ts) + \ln(1.0 - \varepsilon 31) - b1 \ln(1.0 - \varepsilon 23)$

**Physical: all coefficients are derived as function of cloud layer temp, surface wind speed, & surface temp**

Emission-Based

$$TB = B[1-(1-\varepsilon)e^{-2\tau_1/\mu}] - [B(T_s) - B(T)](1-e^{-\tau_1/\mu})[1+(1-\varepsilon)e^{-\tau_1/\mu}]$$

**Physical: Microwave integrated Retrieval system, 1dvarwith scattering RT, all hydrometeors profiles**

Scattering Based

$$J = \frac{1}{2}\left(\mathbf{x}-\mathbf{x}^b\right)^T \mathbf{B}^{-1}\left(\mathbf{x}-\mathbf{x}^b\right) + \frac{1}{2}\left[\mathbf{I}(\mathbf{x})-\mathbf{I}^o\right]^T (\mathbf{E}+\mathbf{F})^{-1}\left[\mathbf{I}(\mathbf{x})-\mathbf{I}^o\right]$$

$$\mu\frac{d\mathbf{I}(\tau,\mu,\phi)}{d\tau} = -\mathbf{I}(\tau,\mu,\phi) + \frac{\varpi}{4\pi}\int_0^{2\pi}\int_{-1}^{1}\mathbf{M}(\tau;\mu,\phi;\mu',\phi')\mathbf{I}(\tau,\mu',\phi')d\mu' d\phi' + \mathbf{S}(\tau,\mu,\phi;\mu_0,\phi_0)$$

National Environmental Satellite, Data, and Information Service

# SSM/I Cloud Liquid Water Algorithm: Operational at FNMOC and NESDIS

**Pros:**

- *Semi-Physical with easy understanding*
- *Large dynamic range (rain and non-rain)*
- *Clean background due to uses of real measurements*
- *Validated with ASTEX data for non-raining clouds*

**Cons:**

- *Difficult to accommodate information from new channels and ancillary data*
- *Cloud layer temp is implicit*

$$\mathrm{LWP} = \begin{cases} \mathrm{LWP}_{19V} & \text{if} \quad \mathrm{LWP}_{19V} \geq 0.70 \text{ mm} \\ \mathrm{LWP}_{37V} & \text{if} \quad \mathrm{LWP}_{37V} \geq 0.28 \text{ mm} \quad \text{or} \quad \mathrm{WVP} \geq 30 \text{ mm}, \\ \mathrm{LWP}_{85H} & \text{otherwise} \end{cases}$$

TABLE 1. The coefficients for LWP algorithms.

| $\mathrm{LWP}_{chan}$ | $\mathrm{TB}_1$, $\mathrm{TB}_2$ | $a_0$ | $a_1$[a] | $a_2$[a] |
|---|---|---|---|---|
| $\mathrm{LWP}_{19V}$ | TV19, TV22 | −3.20[b] | 2.80 | 0.42 |
| $\mathrm{LWP}_{37V}$ | TV37, TV22 | −1.66[c] | 2.90 | 0.35 |
| $\mathrm{LWP}_{85H}$ | TH85, TV22 | −0.44[c] | −1.60 | 1.35 |

[a] Based on global clear sky measurements.
[b] Based on simulated "measurements" calculated from radiative transfer model.
[c] Based on collocated ground-based and satellite measurements for $\mathrm{LWP}_{37V}$ and $\mathrm{LWP}_{85H}$.

$$\mathrm{LWP}_{chan} = a_0[\ln(290 - \mathrm{TB}_1) - a_1 - a_2\ln(290 - \mathrm{TB}_2)],$$

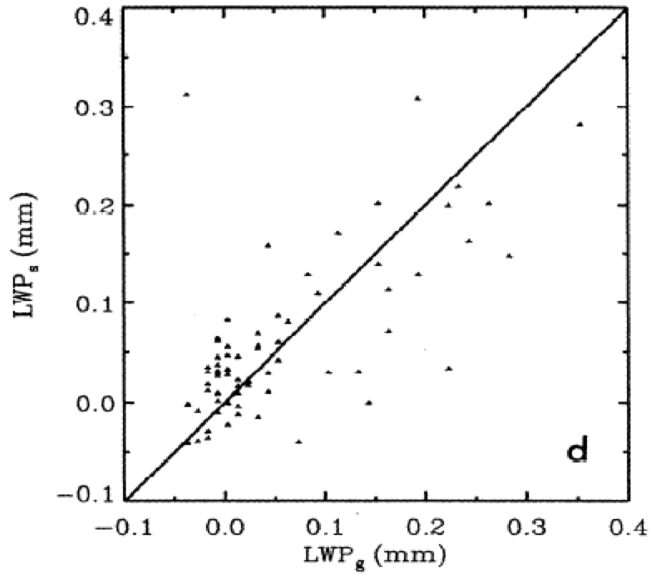

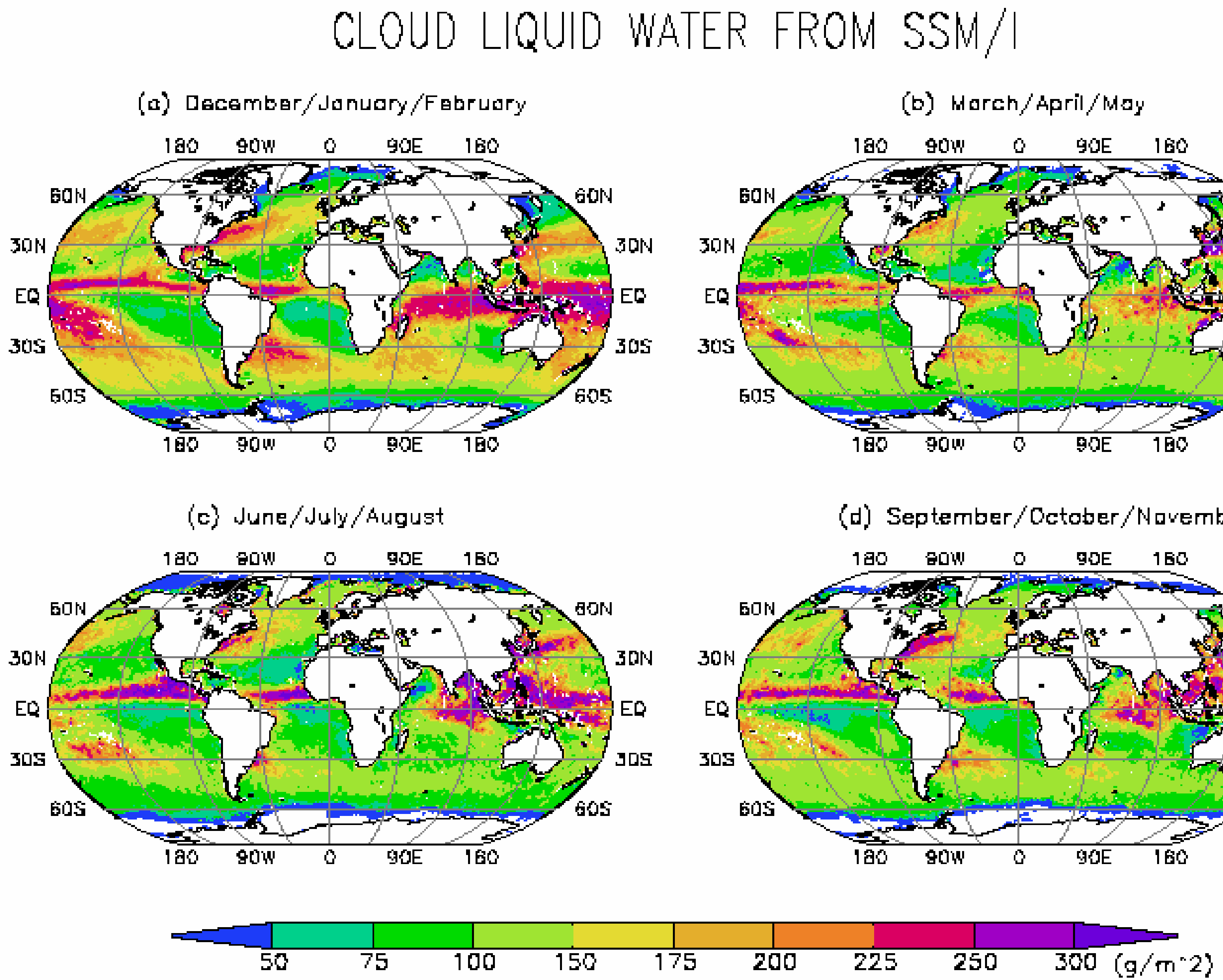
CLOUD LIQUID WATER FROM SSM/I
(a) December/January/February
(b) March/April/May
(c) June/July/August
(d) September/October/November
180
90W
0
90E
180
60N
30N
EQ
30S
60S
50
75
100
150
175
200
225
250
300
(g/m^2)

# NOAA POES AMSU


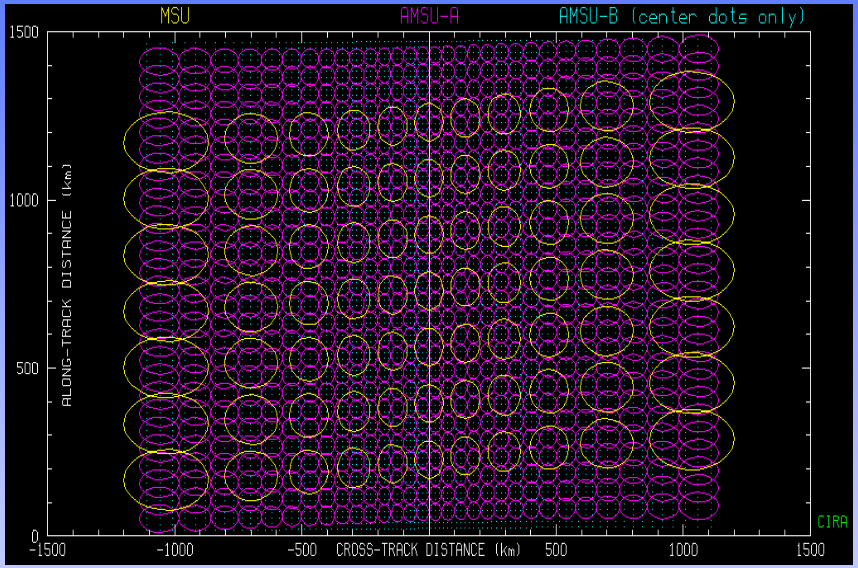


- AMSU are on board NOAA POES since 1998
- There are 20 channels divided into three sub-modules:
  - A1 – 13 channels located near the 60 GHZ oxygen absorption band
  - A2 – 2 window channels at 23.8 and 31.4 GHz
  - B – 2 high frequency channels at 89 and 150 GHz, and 3 channels near 183 GHz water vapor absorption line
- The field-of-view size varies as the instruments scan crossing track

# AMSU Weighting Functions

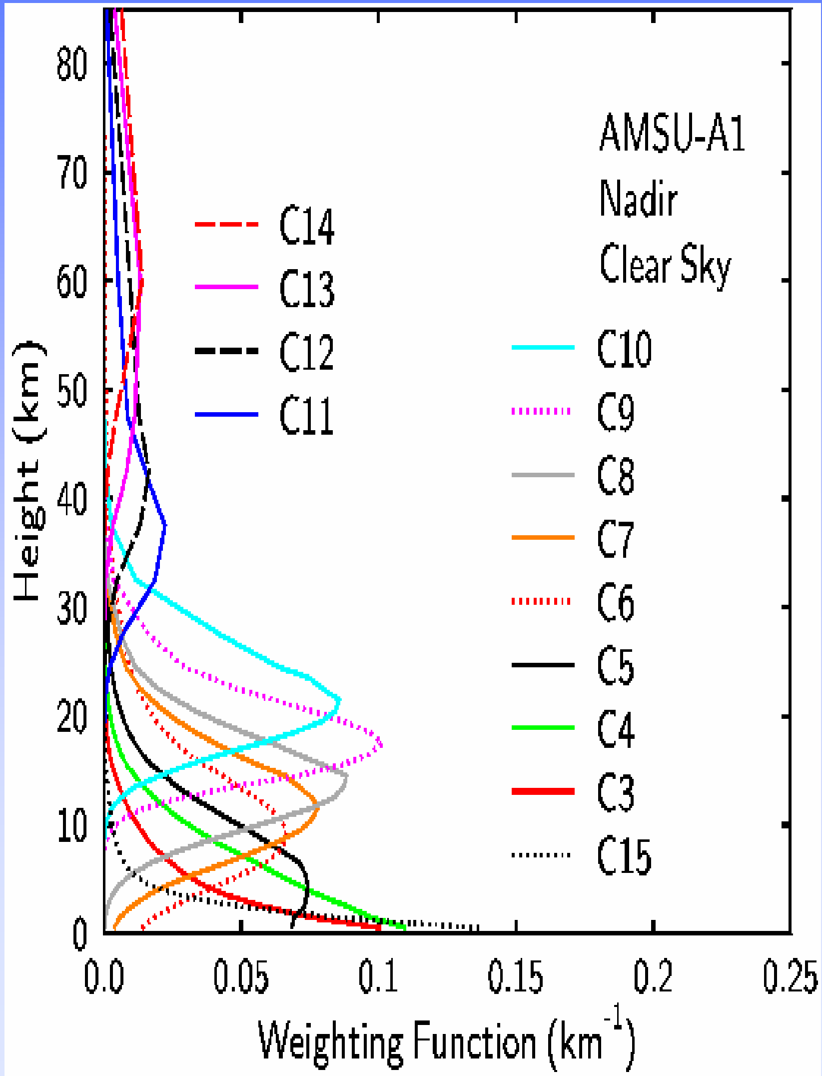


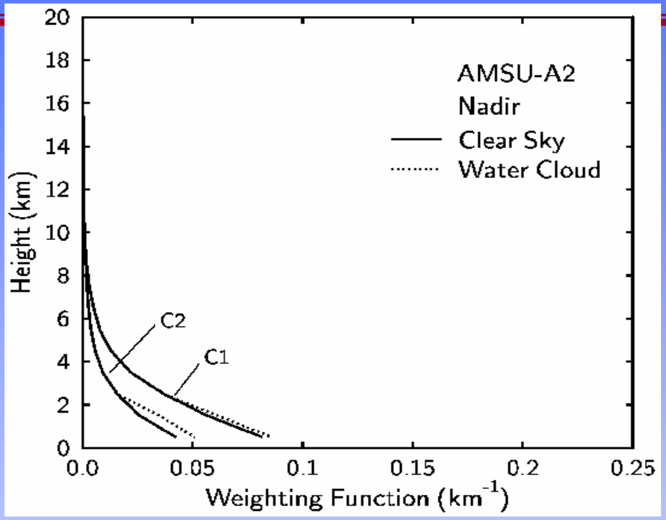


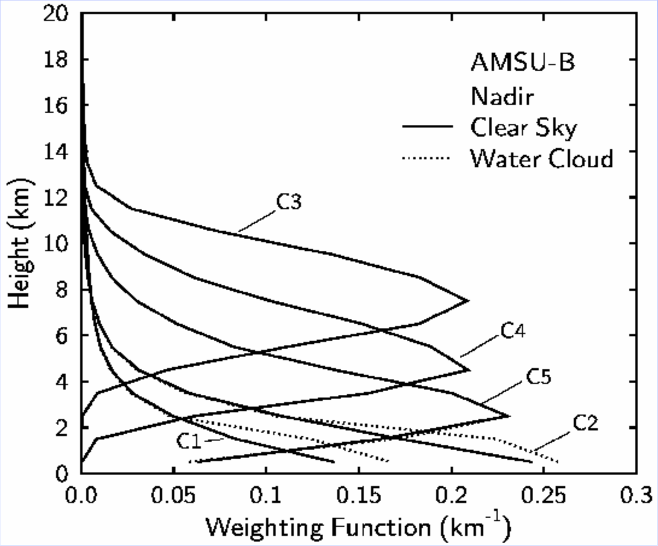

National Environmental Satellite, Data, and Information Service

# NOAA-16 AMSU-A Radiance Asymmetry (Channel 1,2,3,15)

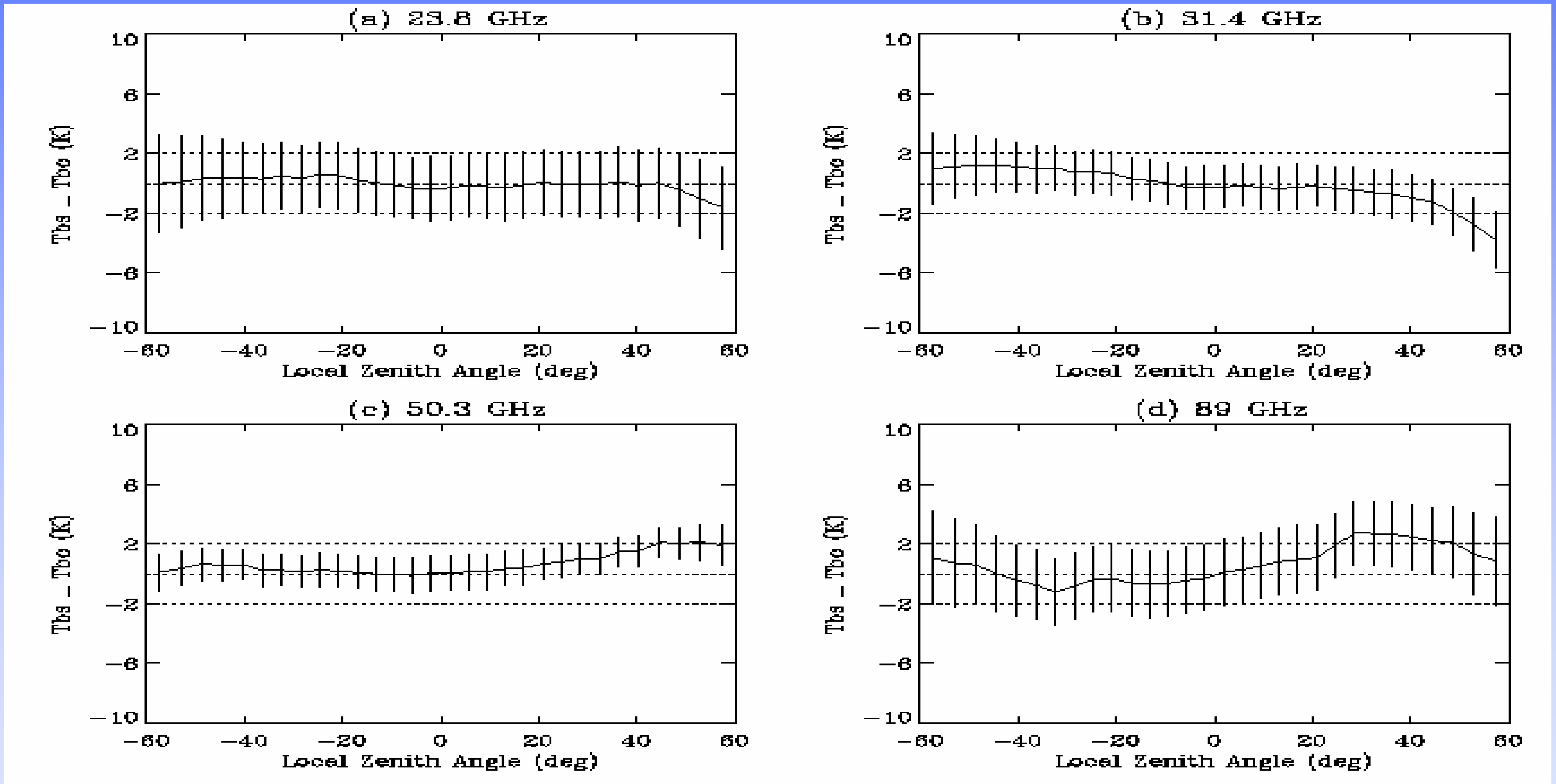


$$\Delta T = A_0 \exp\{ -0.5[(\theta - A_1) / A_2]^2 \} + A_3 + A_4 \theta + A_5 \theta^2$$

National Environmental Satellite, Data, and Information Service

# NOAA-15 AMSU-A Radiance Asymmetry (Channel 1,2,3,15)

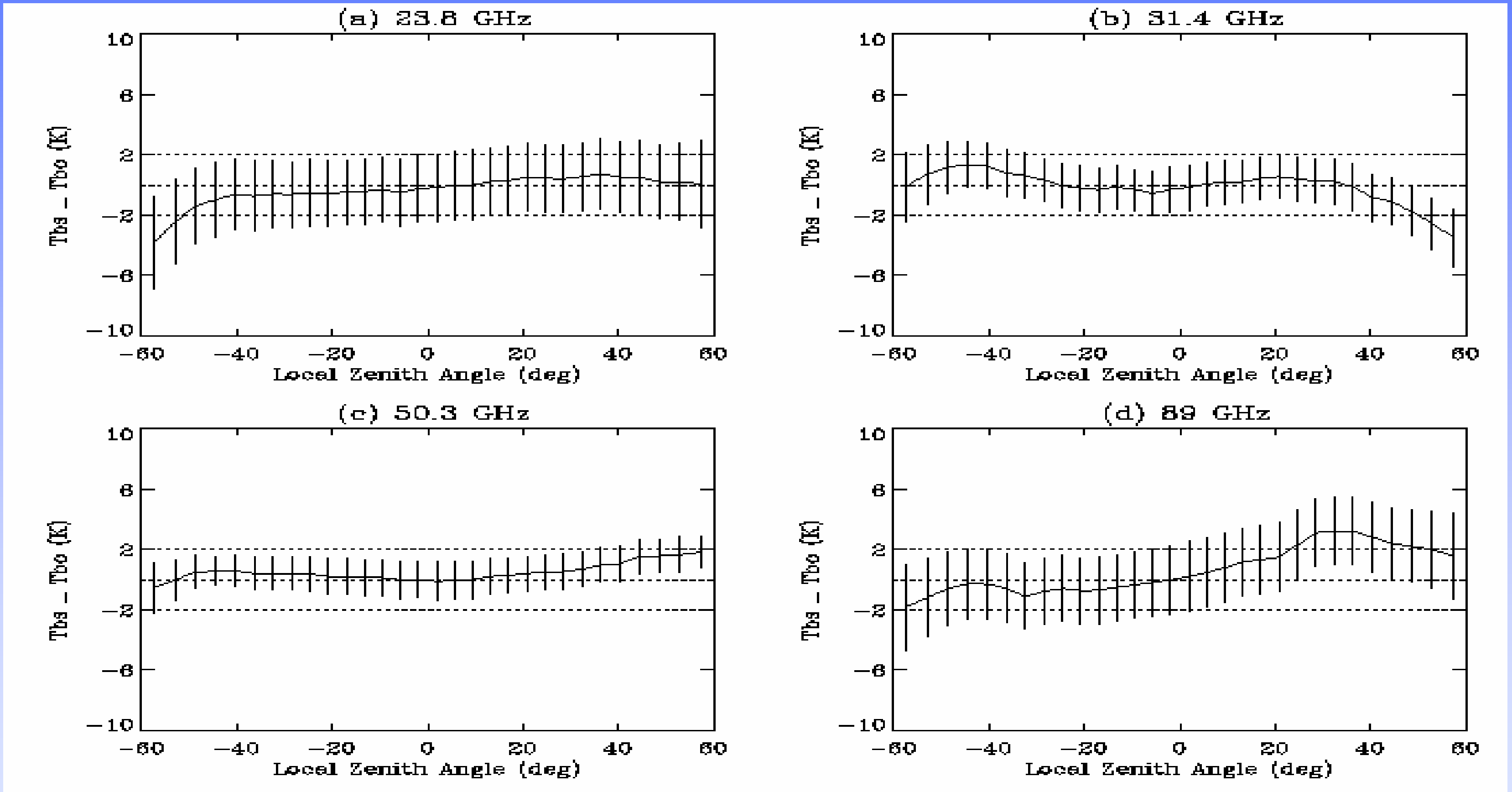


$$\Delta T = A_0 \exp\{ -0.5[(\theta - A_1) /A_2]^2 \} + A_3 + A_4 \theta + A_5 \theta^2$$

# AMSU Cloud Liquid Water Algorithm: Operational at NESDIS

- Algorithms are needed for correcting instrument asymmetry before the measurements are used in retrievals

- A physical retrieval was developed for cloud liquid water and total precipitable water

- Include cloud layer temperature effects and surface emissivity which is linked to surface temperature and sea wind speed

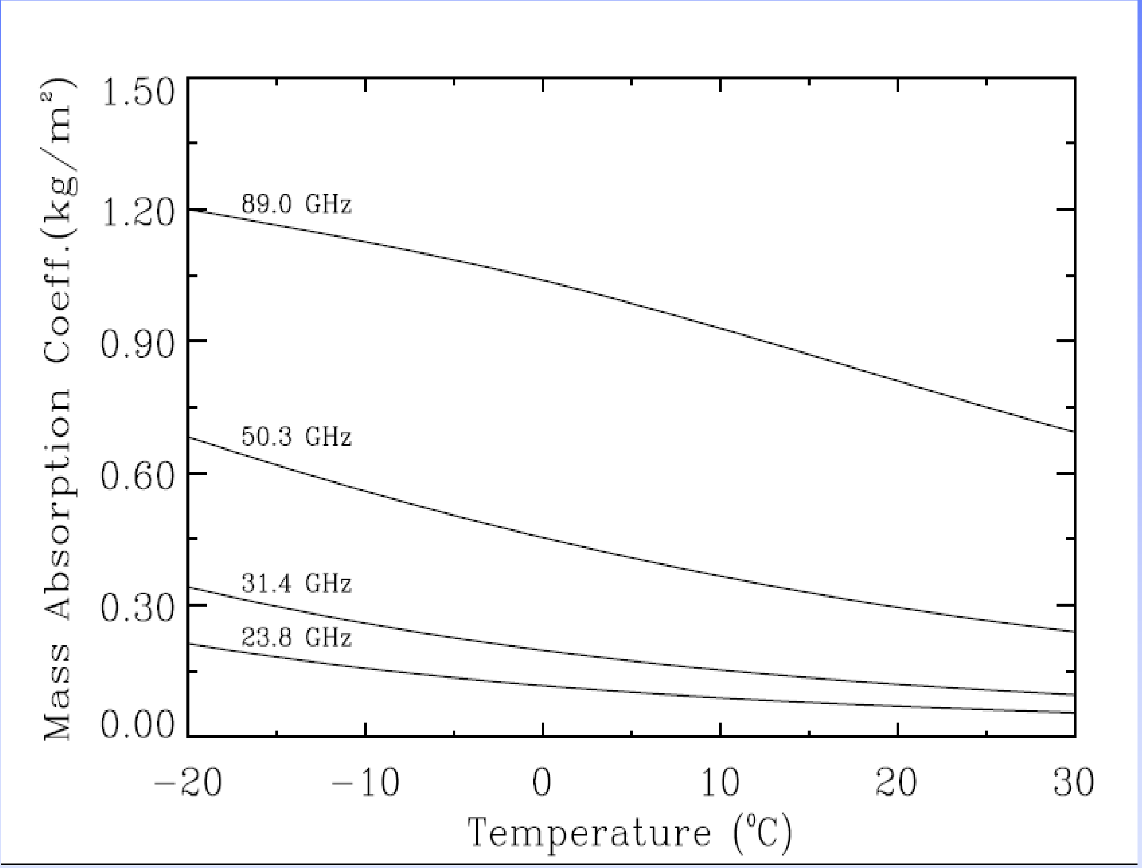

# AMSU Cloud Liquid Water

Before Asymmetry Correction

NOAA-15

After Asymmetry Correction

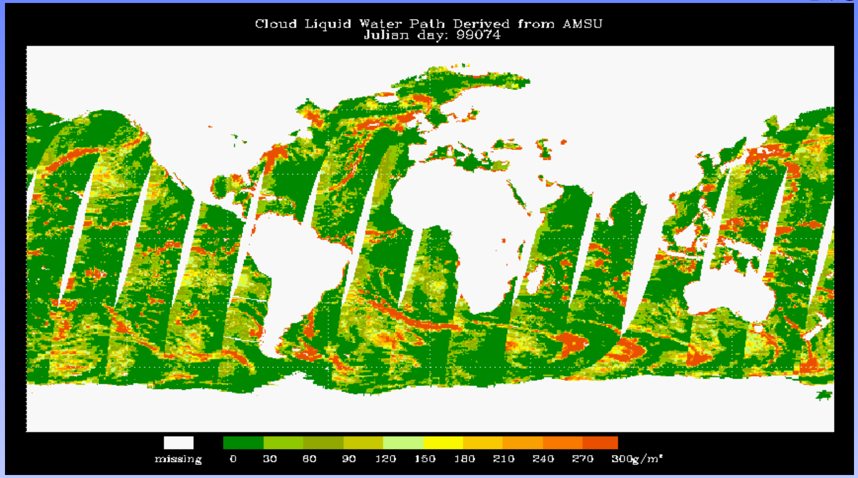


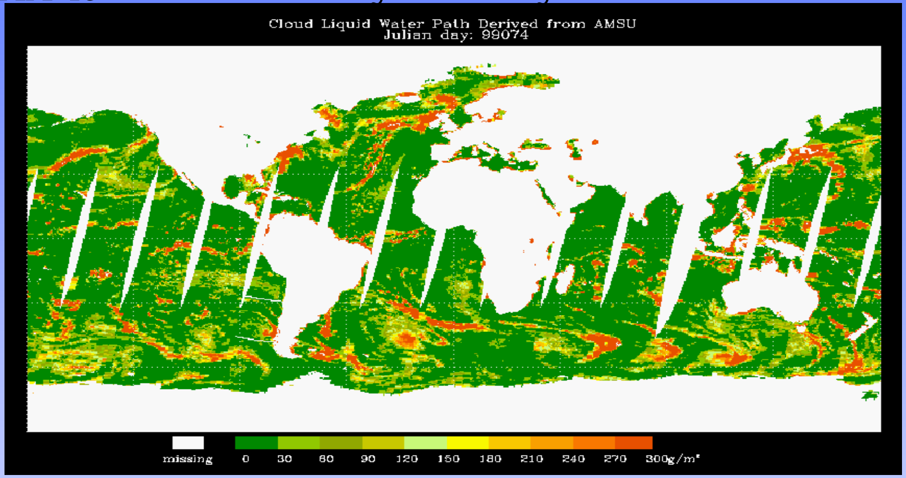


NOAA-16

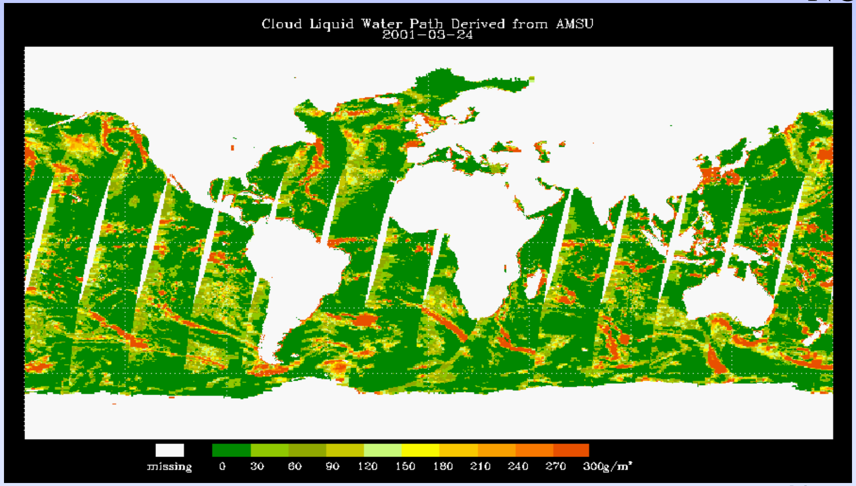


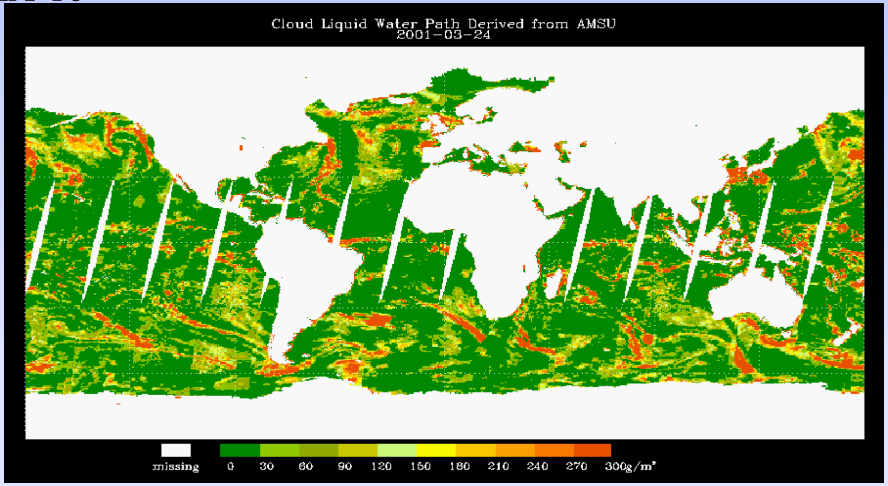

# Aqua AMSR-E Products

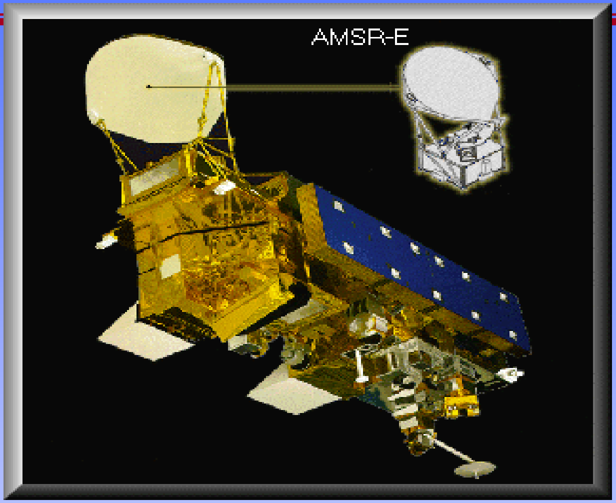


- Ocean products : RWP,CWP,SST,SSW,CIWP,TWP, Rain rate, Sea ice concentration
- Land products: LST, Soil moisture,Rain rate,Snow cover, Snow/Ice Types, Snow equivalent water

| Parameters | SMMR (Nimbus-7) | SSM/I (DMSP-F08,F10,F11,F13,F15) | AMSR (Aqua, ADEOS-II) |
|---|---|---|---|
| Time Period | 1978 to 1987 | 1987 to Present | Beginning 2001 |
| Frequency (GHz) | 6.6, 10.7, 18, 21, 37 | 19.3, 22.3, 36.5, 85.5 | 6.9, 10.7, 18.7, 23.8, 36.5, 89.0 |
| Sample Footprint Sizes (km) | 148 x 95 (6.6 GHz)<br>27 x 18 (37 GHz) | 37 x 28 (37 GHz)<br>15 x 13 (85.5 GHz) | 74 x 43 (6.9 GHz)<br>14 x 8 (36.5 GHz)<br>6 x 4 (89.0 GHz) |

# AMSR-E LWP&RWP Algorithms

The same physical retrieval with modification for AMSR-E channels

**23.8, 37 V-pol for LWP and WVP,**
**23.8, 18 V-pol for RWP**

**LWP = a0 [ln(Ts-TV37)- a1 ln(Ts-TV23)-a2]**
**WVP = b0 [ln(Ts-TV37)- b1 ln(Ts-TV23)-b2]**
**RWP = c0 [ln(Ts-TV18)- c1 ln(Ts-TV23)-c2]**

**LWP**

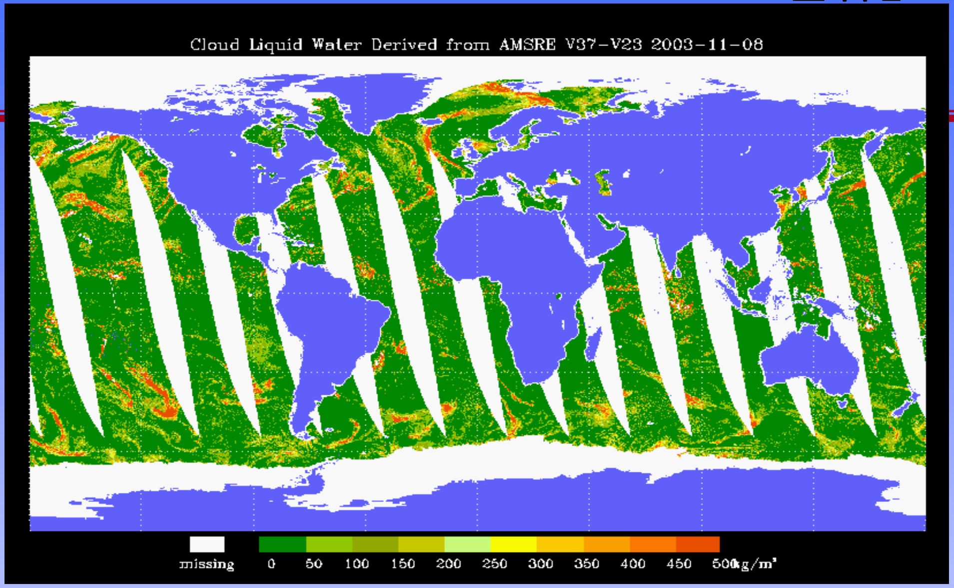


**RWP**

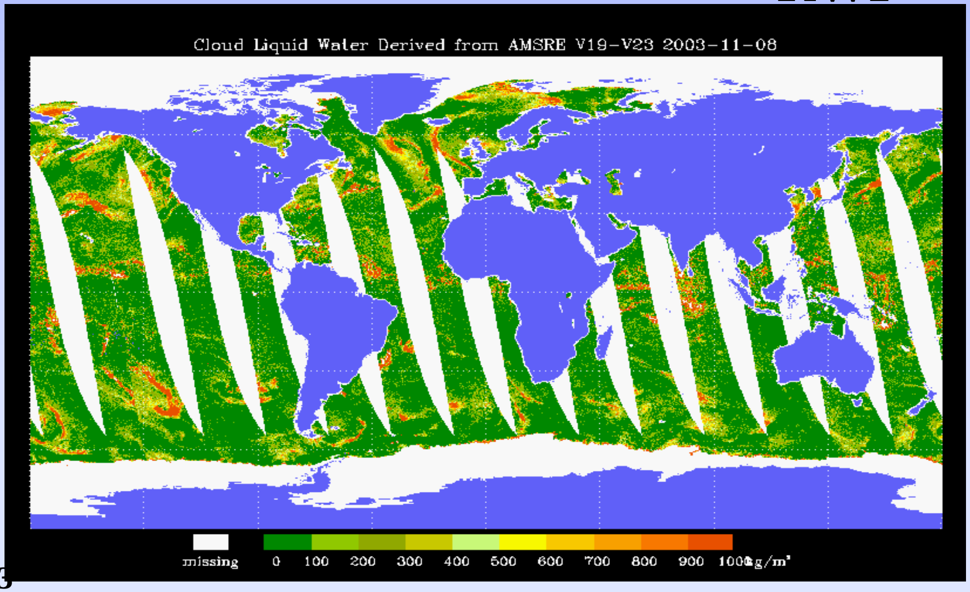

# Algorithms of Cloud Ice Water Path: Vertically Integrated Ice Water over Unit Area

# Cloud Ice Water Path Algorithm

$$I(\tau,\mu) = \frac{(I_0 - B)[\gamma_1 e^{-\kappa(\tau-\tau_1)} - \gamma_2 e^{\kappa(\tau-\tau_1)}] - (I_1 - B)[\beta^{-1} e^{\kappa(\tau-\tau_0)} - \beta e^{-\kappa(\tau-\tau_0)}]}{\gamma_4 e^{-\kappa(\tau_1-\tau_0)} - \gamma_3 e^{\kappa(\tau_1-\tau_0)}} + B$$

$I_0$ $\tau_0$

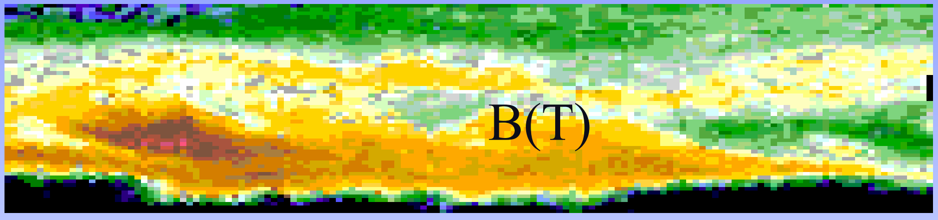


$I_1$ $\tau_1$

Weng and Grody (2000, JAS)
Zhao and Weng (2002, JAM)

**Asymptotic Limits:**

1. Emission Approach

$$I(\tau_1,\mu) = B[1-(1-\varepsilon)e^{-2\tau_1/\mu}] - [B(T_s) - B(T)](1-e^{-\tau_1/\mu})[1+(1-\varepsilon)e^{-\tau_1/\mu}]$$

2. Scattering Approach:

$$I(\tau_0,\mu) = \frac{I(\tau_1,\mu)}{1+\Omega(\mu)} \qquad \Omega(\mu) = \frac{IWP}{\mu\rho_i D_e}\Omega_N(x_e, m)$$

# Definitions of Cloud Ice Water Path

The influence of cloud microphysical parameters on microwave measurements may be quantitatively analyzed with the model developed in the previous section. The scattering parameter given in Eq. (3) is related to the cloud ice water path and particle size.

The optical thickness is

$$\tau = \int_{z_b}^{z_t} dz \int_0^\infty \frac{\pi}{4} D^2 Q_{\text{ext}}(x, m) N(D)\, dD, \qquad (6)$$

where $N(D)$ is the particle size distribution function, $Q_{\text{ext}}$ the extinction efficiency of ice particles, $x$ the particle size parameter, and $m$ the complex refractive index. For ice particles, $m$ is nearly constant at microwave frequencies. The cloud IWP is also related to the particle size distribution by

$$\text{IWP} = \int_{z_b}^{z_t} dz \int_0^\infty \frac{\pi}{6} \rho_i D^3 N(D)\, dD, \qquad (7)$$

where $\rho_i$ is the particle bulk density.

A monodispersed (uniform) type of $N(D)$ is considered first so that the scattering parameter can be directly related to the cloud microphysical parameters. For a cloud having a thickness, $\delta z$, the optical thickness is

$$\tau = \delta z N_t \frac{\pi D^2}{4} Q_{\text{ext}}(x, m) \quad \text{and} \qquad (8)$$

$$\text{IWP} = \delta z \frac{\pi}{6} \rho_i N_t D^3. \qquad (9)$$

Thus $\tau$ can be expressed in terms of the IWP and the extinction cross section, namely,

$$\tau = \frac{3}{2} \frac{\text{IWP}}{\rho_i D} Q_{\text{ext}}(x, m), \qquad (10)$$

and $\Omega$ is obtained by substituting Eq. (10) into Eq. (3):

$$\Omega(\mu) = \frac{\text{IWP}}{\mu \rho_i D} \Omega_N(x, m), \qquad (11)$$

where $x = (\pi D)/\lambda$ and $\Omega_N$ is the normalized scattering parameter, which is given by

$$\Omega_N(x, m) = \frac{3}{4}[Q_{\text{ext}}(x, m) - Q_{\text{sca}}(x, m) g(x, m)]. \qquad (12)$$

From Eq. (11), it is evident that the large scattering parameter is directly proportional to the IWP. However, the relationship between $\Omega$ and $D$ is nonlinear due to $\Omega_N$ and may also depend on the particular particle size distribution.

For polydispersed particles, $\Omega$ is calculated using Eq. (3). The optical parameters are derived through integrating over the entire range of particle diameters for a given size distribution. Using a gamma function that has an exponent of 2 (Ulbrich 1983) for the polydispersed particles, $\Omega$ is given as

$$\Omega(\mu) = \frac{\text{IWP}}{\mu \rho_i D_e} \Omega_N(x_e, m), \qquad (13)$$

where $x_e = (\pi D_e)/\lambda$ and $D_e$ is the particle effective diameter, which is defined as

$$D_e = \frac{\displaystyle\int_0^\infty N(D) D^3\, dD}{\displaystyle\int_0^\infty N(D) D^2\, dD}. \qquad (14)$$

# ER-2 MIR, DC-8 ARMAR, MODIS Simulator Measurements

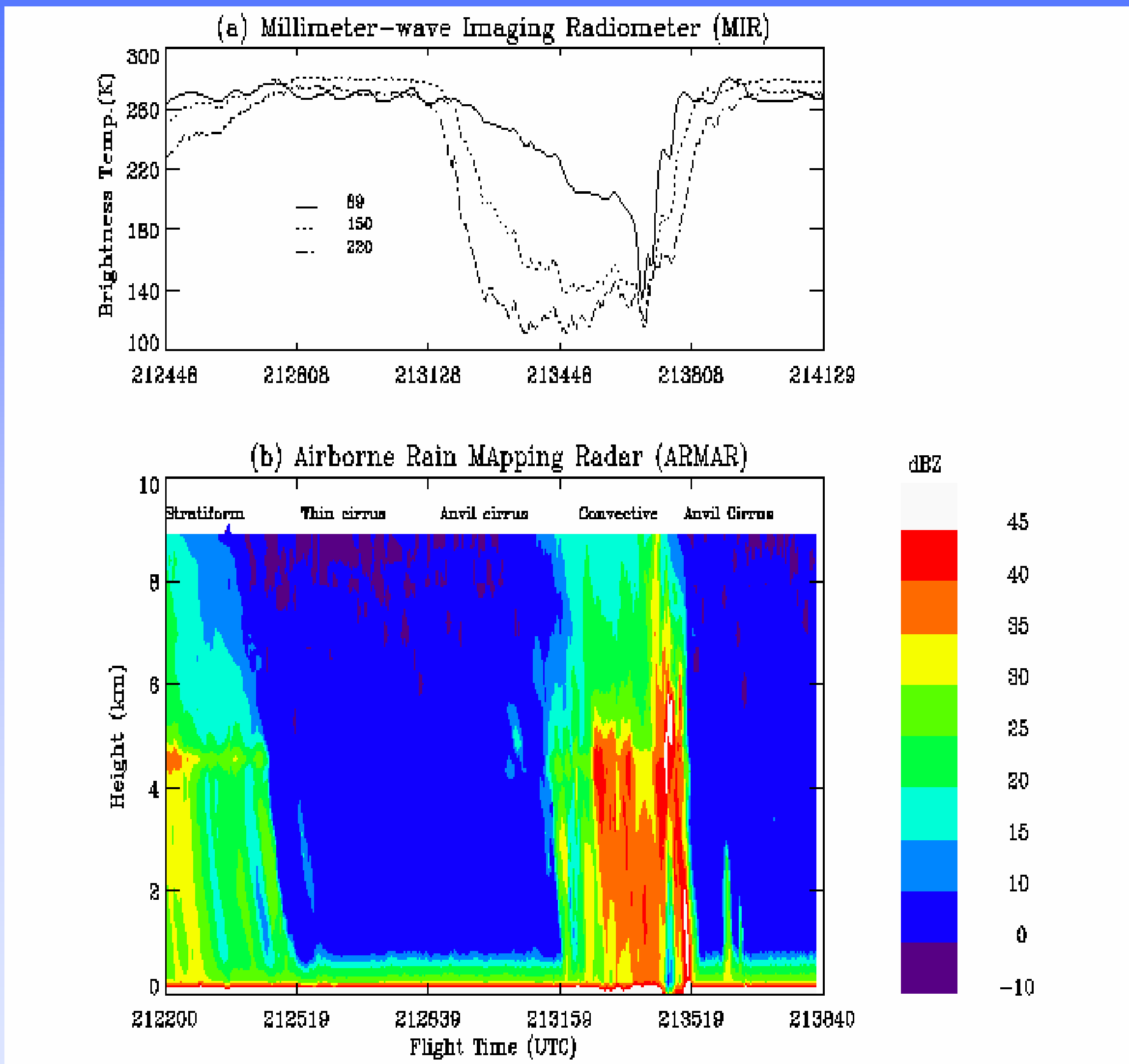


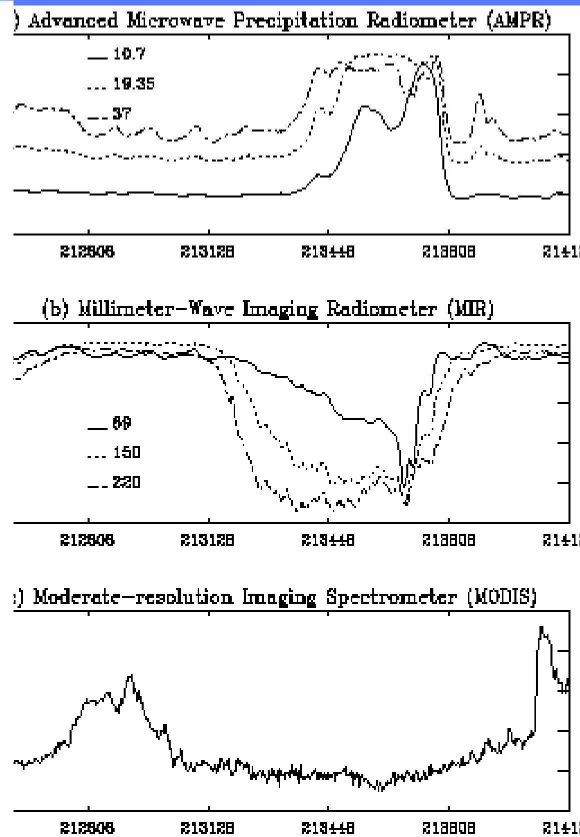


*llimeter wavelength channels provide the overa*
*ensitivity for cloud ice microphysics which can*
*ely used for precipitation mapping*

**Weng and Grody (2000, JAS)**

# MIR Window & Sounding Channel Observations

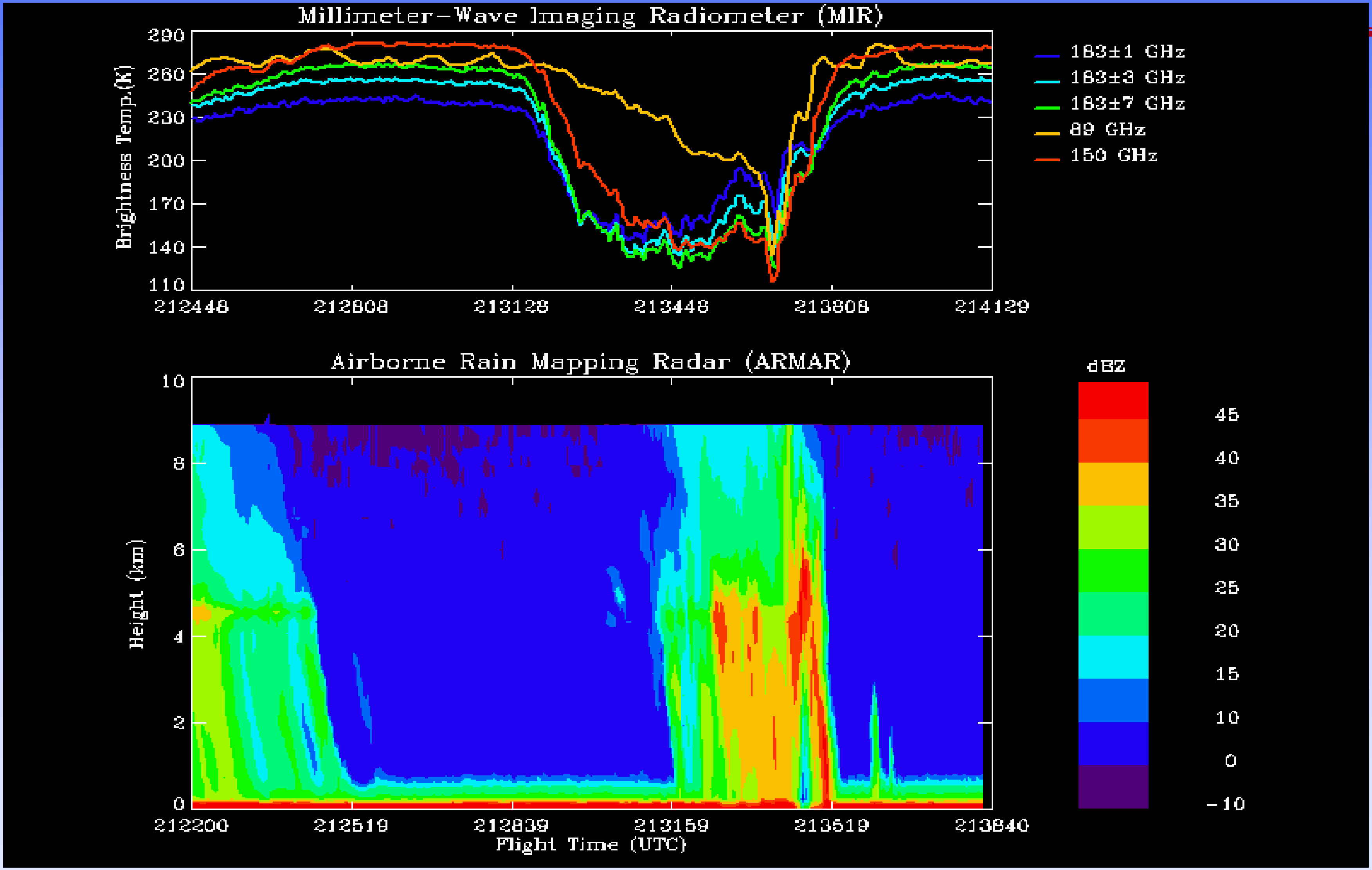

# Sensitivity of Sub-mm to Ice Cloud Parameters

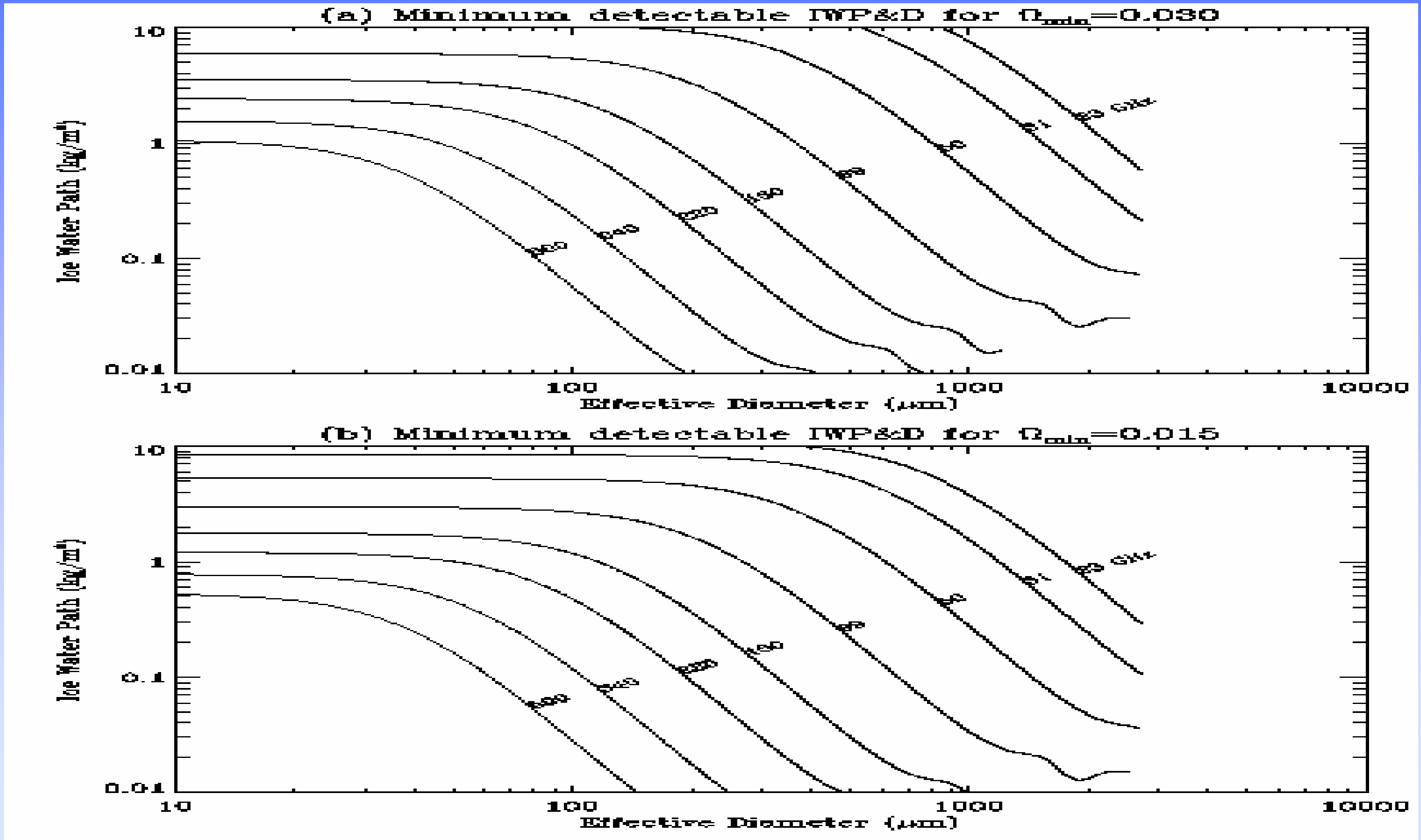

# Flowchart of Cloud Ice Algorithm

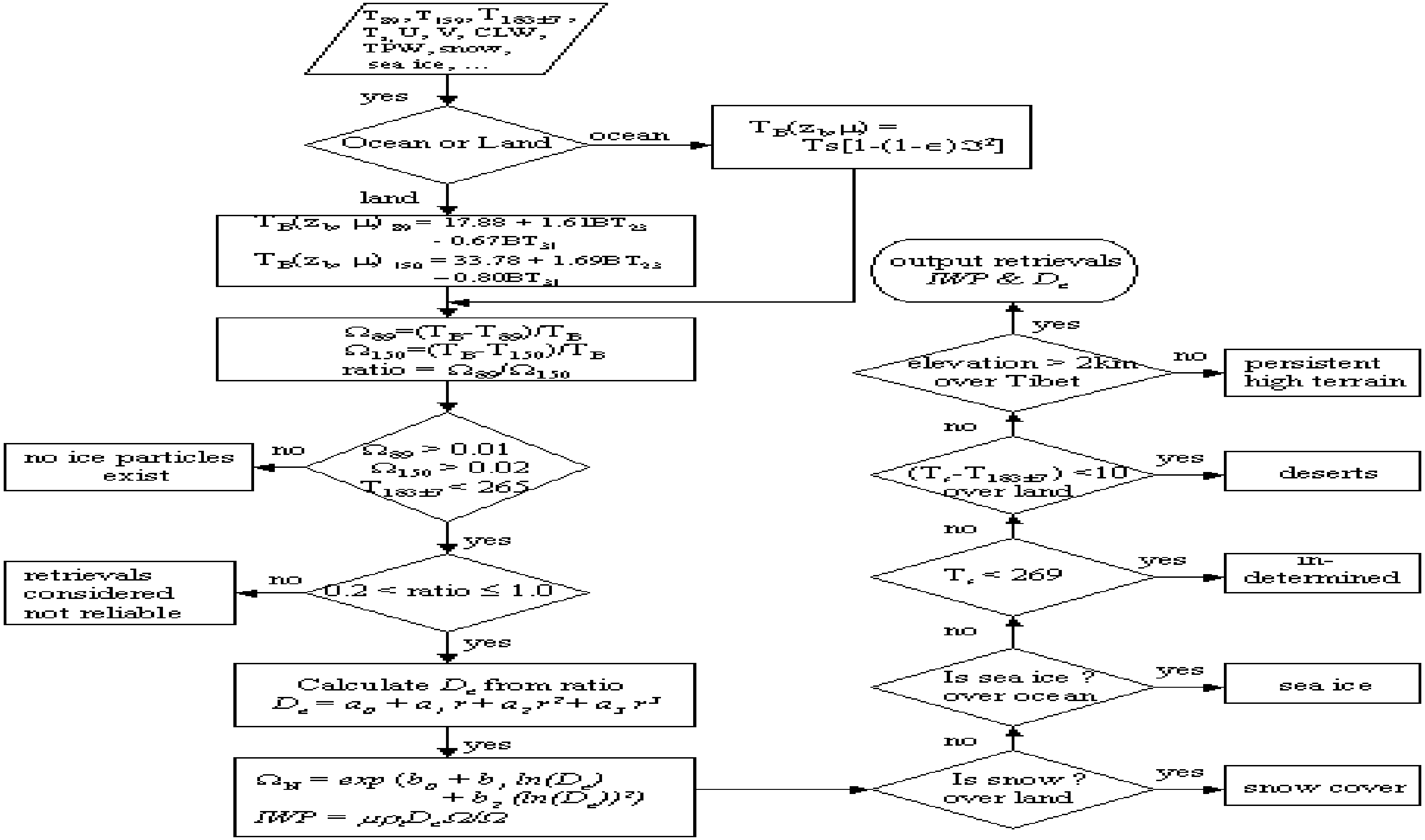


The flow chart of the global $IWP$ and $D_e$ retrieval algorithm

# Flowchart of Cloud Ice Algorithm

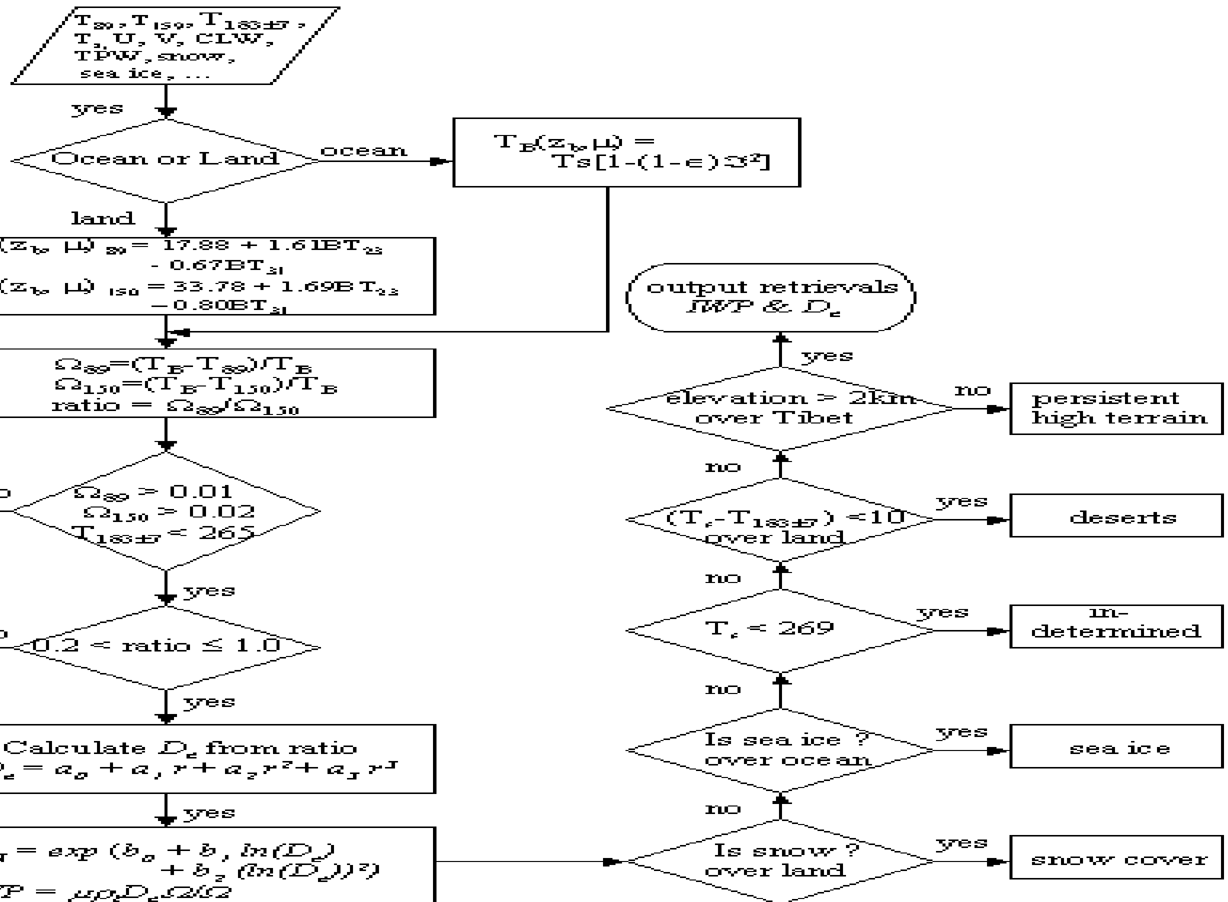


The flow chart of the global *IWP* and $D_e$ retrieval algorithm

# CIWP Error Budget

$$\Omega(\mu) = \frac{IWP}{\mu \rho_i D_e} \Omega_N(x_e, m)$$

The errors of CIWP are mainly due to

(1) uncertainty in the effective particle diameters

(2) uncertainty in the particle bulk volume density

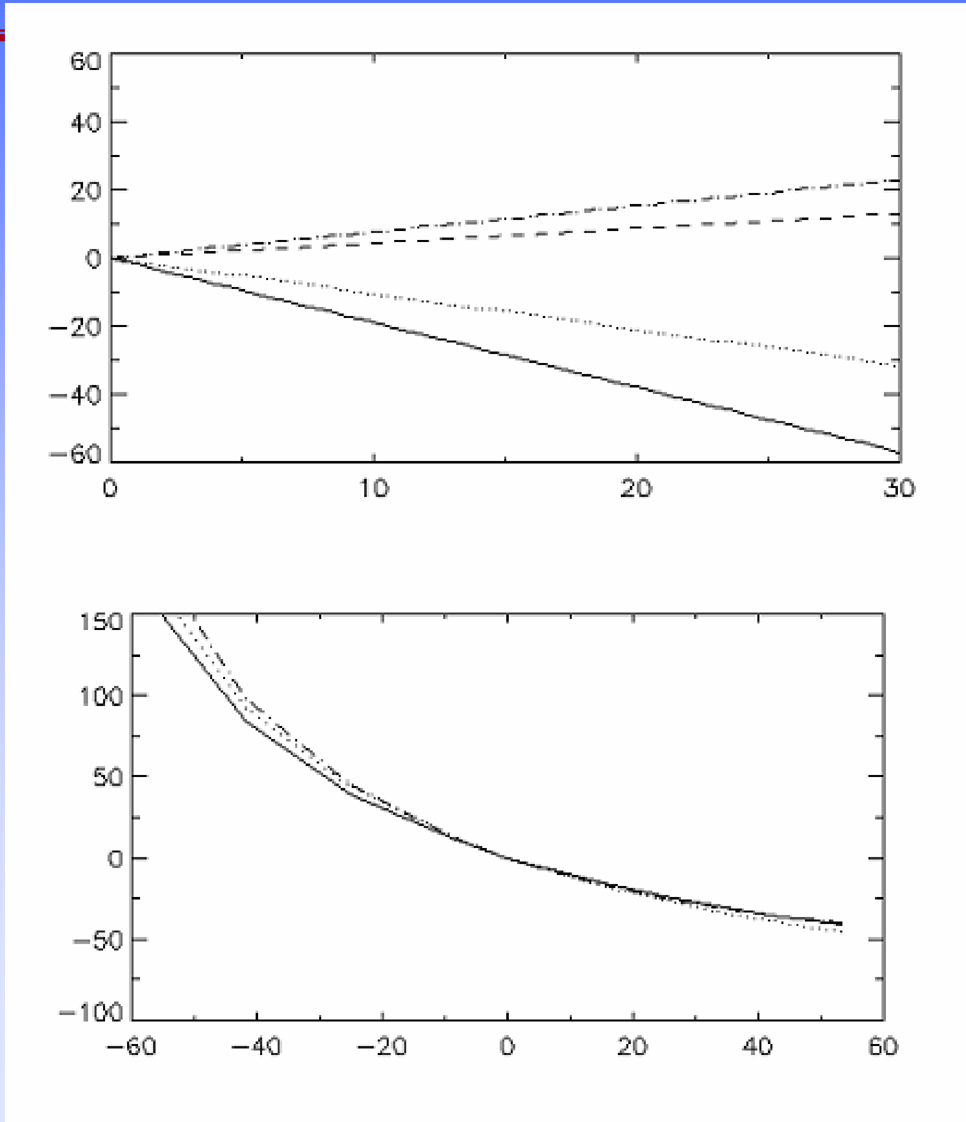

National Environmental Satellite, Data, and Information Service

# Cloud Ice Water Path

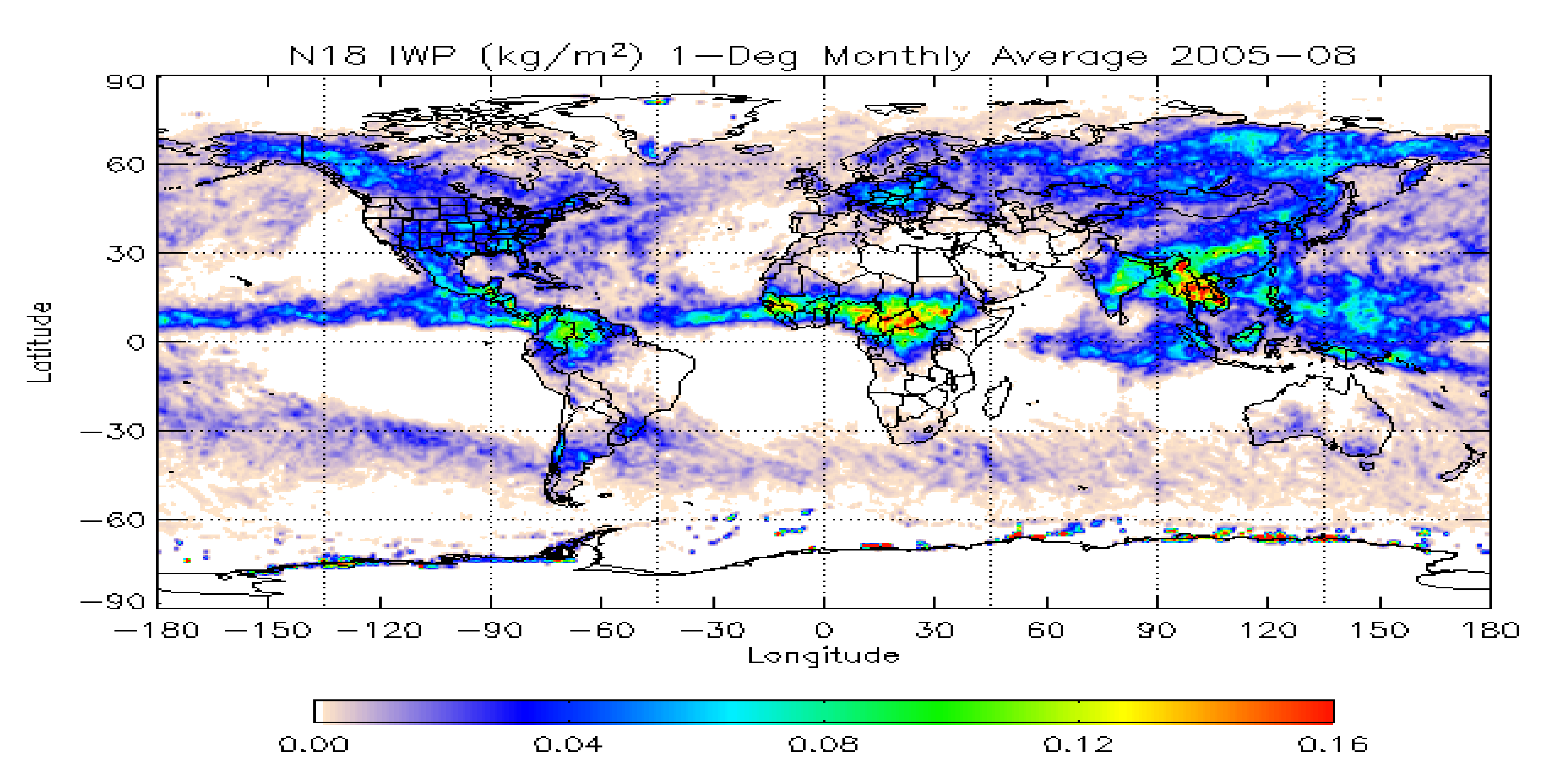


- Brightness temperatures from AMSU-B 89 and 150 GHz are two primary channels for IWP and De
- Retrieval algorithm was published in Journal of Atmos Sci (Weng and Gody, 2000) and J. Appli. Meteor (Zhao and Weng, 2002)
- AMSU-A window channels are used for surface screening.
- The algorithm works for opaque ice clouds having IWP greater than 0.05 kg/m2

# Algorithms for Atmospheric Temperature (T) and Water Vapor Sounding (Mixing Ratio)

# Microwave Sounding Principle

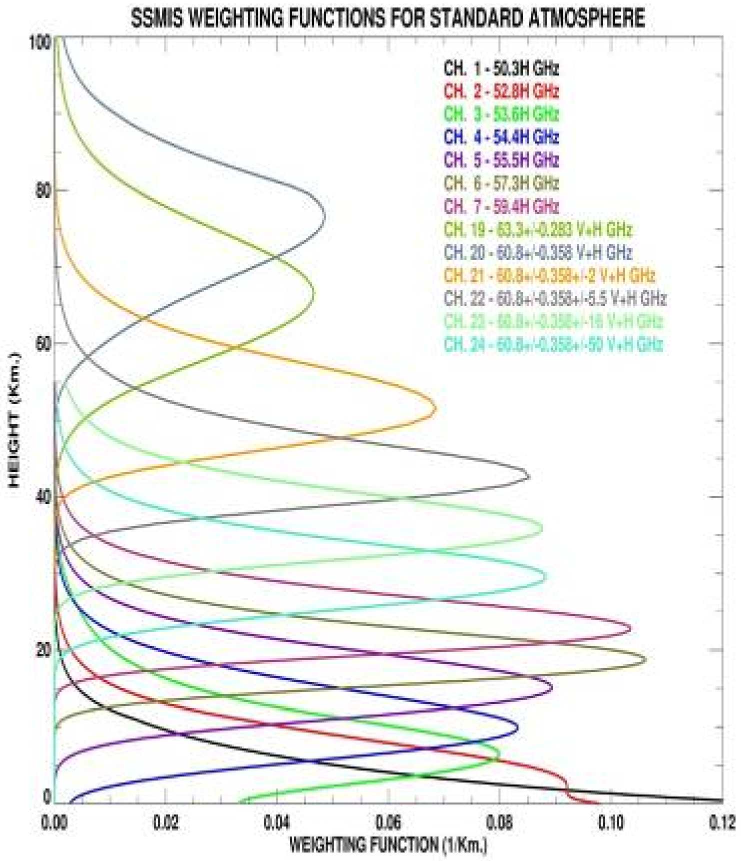


For an atmosphere having a transmittance of zero, the microwave channel will become surface and only sense atmospheric structure. From Eq. 5.1, we have

$$T_b = \int_{\Upsilon_s}^{1} B(T)\, d\Upsilon \qquad (7.1)$$

where

$$d\Upsilon = \exp\left(-\frac{(\tau_s - \tau)}{\mu}\right) d\tau / \mu \qquad (7.2)$$

Atmospheric weighting function is defined as

$$W = \frac{\partial \Upsilon}{\partial \ln p}, \qquad (7.3)$$

where a logarithmic function is used for the pressure coordinate.

Thus, the brightness temperature for a channel, $i$, can be written as

$$T_{b,i} = \int_{P_s}^{0} B(T) W_i \, d\ln p \qquad (7.4)$$

Since Planck function is a linear function of temperature at microwave region (e.g. Rayleigh-Jean's approximation), it is typical to replace $B$ with physical temperature and also discretize the integration with summation such that

$$T_{b,i} = \sum_{j=1}^{L} c_i T_j W_{i,j}, \qquad (7.5)$$

where $L$ is the number of layer for atmospheric vertical stratification and $c_i$ is the coefficient relating the temperature to Planck function, which is dependent on wavelength.

# Regression Algorithm

$$T(p) = C_0(p,\mu) + \sum_{j=1}^{L} C_j(p,\mu) T_{b,j}(\mu), \qquad (7.6)$$

where $C$ is derived using collocated Radiosonde and satellite data. For AMSU, $C$ is derived at each pressure level and viewing angles separately (Zhu et al., 2002). In the data collocation process, a pair of the AMSU and rawinsonde observations is selected when the two observations are made within 1 h and $1^0$ latitude–longitude. Since AMSU is a cross-track scanning instrument, the temperature retrieval at each pressure level is derived separately for each scanning angle. At least 115 observed soundings are used at each scanning angle and about 1800 soundings for the 15 angles are used to calculate the regression coefficients.

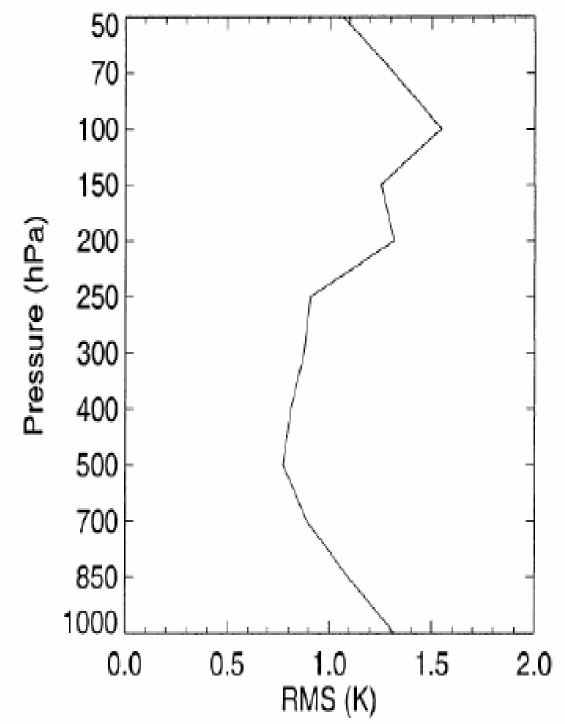

# One Dimensional Variational Retrieval (1dvar) (1 of 3)

### 7.4.1 Mathematical Approach

The mathematical basis of one dimension variation retrieval (1dvar) is a proven and widely used variational approach described in (Rodgers 1976). We will briefly review it here for the purpose of showing that it is valid in precipitating conditions as well. We will follow the probabilistic approach as it will highlight the only three important assumptions made for this type of retrievals; Namely, the local-linearity of the forward problem, the Gaussian nature of both the geophysical state vector and the errors associated with the forward model and the instrument noise, and finally that the measurements and the forward operator are non-biased to each other. It is important to keep in mind that the variational, Bayesian, optimal estimation theory, maximum probability are all the same solutions (if the same assumptions are made), although reached through different paths. The following will link the probabilistic approach to the variational solution which seeks to minimize a cost function. Intuitively, the retrieval problem amounts to finding the geophysical vector $x$ which maximizes the probability of being able to simulate the measurements vector $y$ using $x$ as an input and using $H$ as the forward operator. This translates mathematically into maximizing The Bayes theorem states that the joint probability $P(x/y)$ could be written as

$$P(x,y) = P(y/x)P(x) = P(x/y)P(y) \qquad (7.8)$$

# One Dimensional Variational Retrieval (1dvar) (2 of 3)

Therefore, the retrieval problem amount to maximizing

$$P(x/y) = \frac{P(y/x)P(x)}{P(y} \tag{7.9}$$

$x$ is assumed to follow a Gaussian distribution:

$$P(x) = \exp[-\frac{1}{2}(x - x_b)^T B^{-1}(x - x_b)] \tag{7.10}$$

where $x_b$ and $B$ are the mean vector (or background) and covariance matrix of $x$, respectively.

Ideally, the probability, $P(y/x)$ is a Dirac-Delta function with a value of zero except for $x$. Modeling errors and instrumental noises all influence this probability. For simplicity, it is assumed that the PDF of $P(y/x)$ is also a Gaussian function with $y(x)$ as the mean value (i.e. the errors of modeling and instrumental noise are non-biased), which could be written as:

$$P(y/x) = \exp[-\frac{1}{2}(y - H(x))^T R^{-1}(y - H(x))] \tag{7.11}$$

$R$ is the measurement and/or modeling error covariance matrix. Maximizing $P(x/y)$ is a minimization of $-\ln(P(x/y))$which could be computed from the equations above as:

$$J(x) = \frac{1}{2}(x - x_b)^T B^{-1}(x - x_b) + \frac{1}{2}[y - H(x)]^T R^{-1}[y - H(x)] \tag{7.12}$$

where $J(x)$ is called the cost function which we want to minimize. The first right term $J_b$ represents the penalty in departing from the background value (a-priori information) and the second right term $J_r$ represents the penalty in departing from the measurements. The solution that minimizes this two-terms cost function is sometimes referred to as a constrained solution. The minimization of this cost function is also the basis for the variational analysis retrieval. In theory one could also find another optimal cost function for a non-Gaussian distribution and non-linear problems. It is just not as a straightforward problem. The solution that minimizes this cost function is easily found by solving for

$$\frac{\partial J(x)}{\partial x} = 0, \tag{7.13}$$

and assuming local linearity around, $x$, which is generally a valid assumption if there is no discontinuity in the forward operator

$$H(x_b) = H(x) + K(x_b - x), \tag{7.14}$$

where $K$ in this case is the Jacobian or derivative of $y$ with respect to $x$. This results into the following departure-based solution:

$$\Delta x = x - x_b = \{(B^{-1}K^T R^{-1} K)^{-1} K^T R^{-1}\}[y - H(x_b)], \tag{7.15}$$

# One Dimensional Variational Retrieval (1dvar) (3 of 3)

If the above equations are ingested into an iterative loop, each time assuming that the forward operator is linear, we end up with the following solution to the cost function minimization process

$$x_{n+1} = \{(B^{-1}K^TR^{-1}K)^{-1}K^TR^{-1}\}[y - H(x_b)] + K_n\Delta x_n, \qquad (7.16)$$

where n is the iteration index. The previous solution could be rewritten in another form after matrix manipulations

$$x_{n+1} = \{BK_n^T(K_nBK_n^T + R)^{-1}\}\{[y^m - y(x_n)] + K_n\Delta x_n\}, \qquad (7.17)$$

The latter is more efficient as it requires the inversion of only one matrix. At each iteration $n$, we compute the new optimal departure from the background given the derivatives as well as the covariance matrices. This is an iterative-based numerical solution that accommodates moderately non-linear problems or/and parameters with moderately non-Gaussian distributions. This approach to the solution is generally labeled under the general term of physical retrieval and is also employed in NWP assimilation schemes along with horizontal and temporal constraints. The whole geophysical vector is retrieved as one entity including the temperature, moisture and hydrometeor profiles as well as skin surface temperature and emissivity vector, ensuring a consistent solution that fits the radiances.

# MIRS Concept

**Variational Assimilation Retrieval (1DVAR)**

- **Algorithm valid in all-weather conditions, over all-surface types**
  - CRTM as forward operator, validity-> clear, cloudy and precip conditions
  - Emissivity spectrum is part of the retrieved state vector
- **Cloud & Precip profiles retrieval (no cloud top, thickness, etc)**
  - EOF decomposition
- **Sensor-independent**
  - Highly Modular Design
- **Flexibility and Robustness**
  - Selection of Channels to use, parameters to retrieve
  - Modeling & Instrumental Errors are input to algorithm

# System Design & Architecture

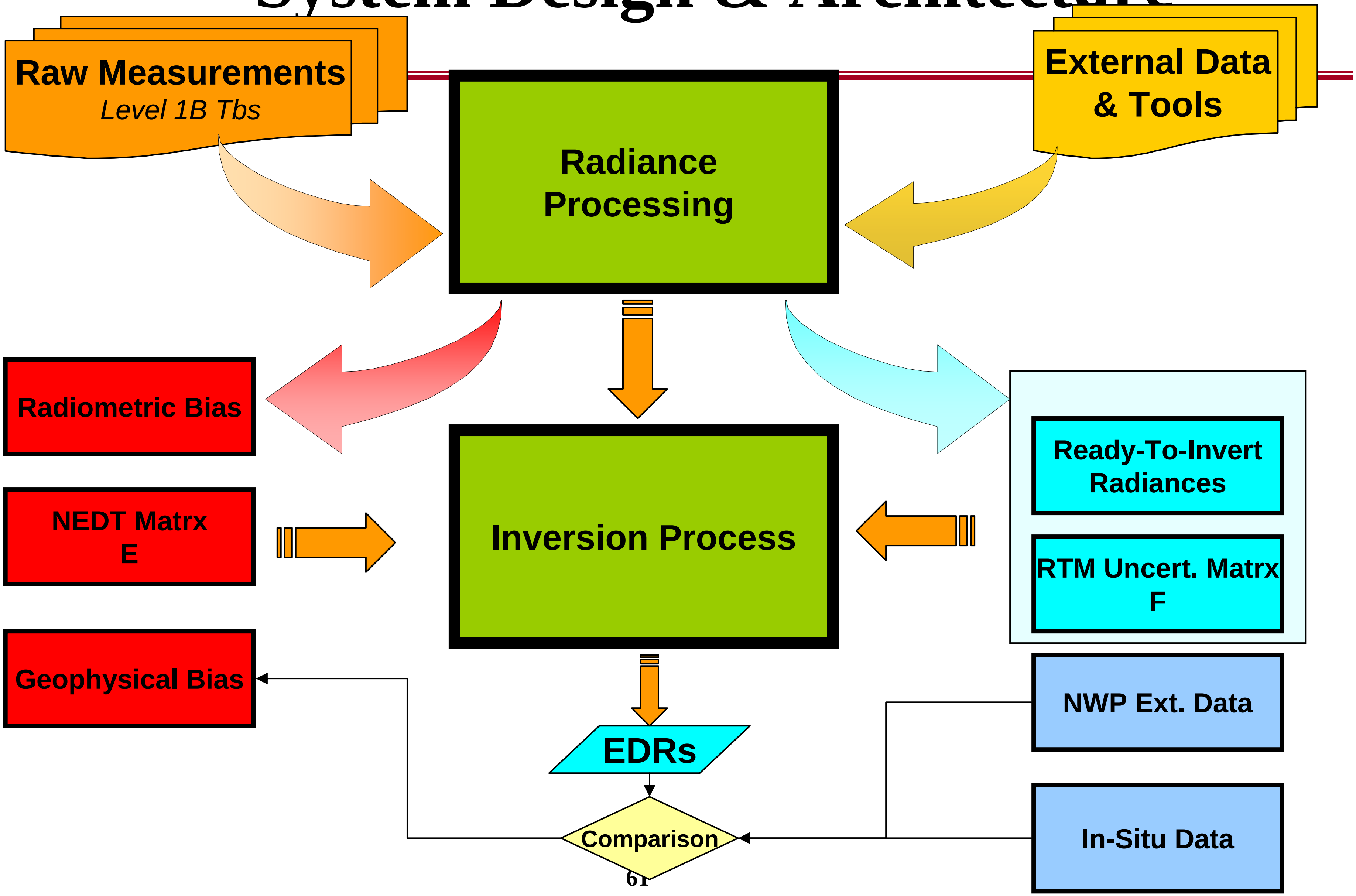

# MIRS Products Performance Monitoring

- **Cross-Sensor Intercomparison**
  - Comparison of advanced products from AMSU/MHS and SSMI/S (TPW images below)

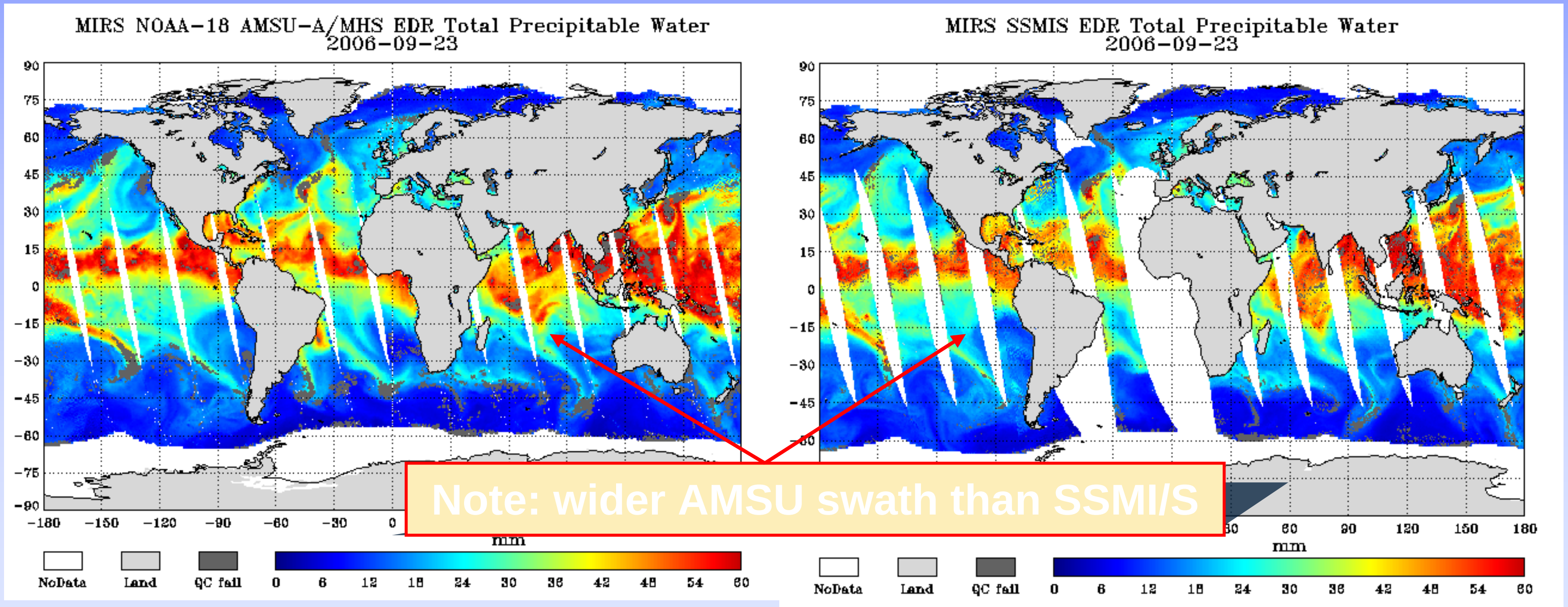

# Microwave TPW Extended over Land

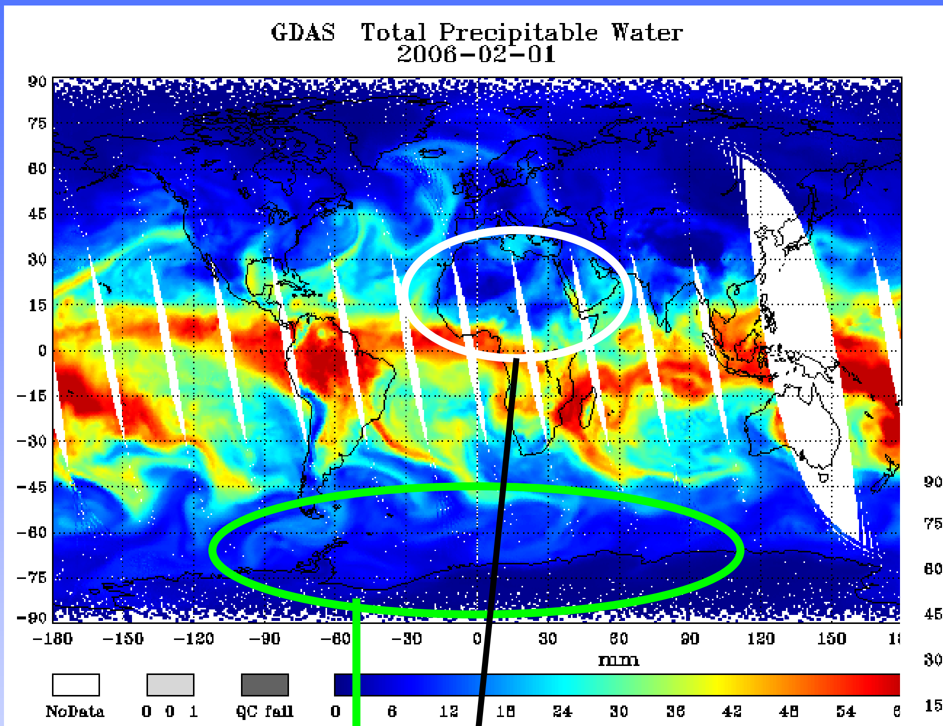


GDAS Analysis

**snow-covered surfaces need better handling**

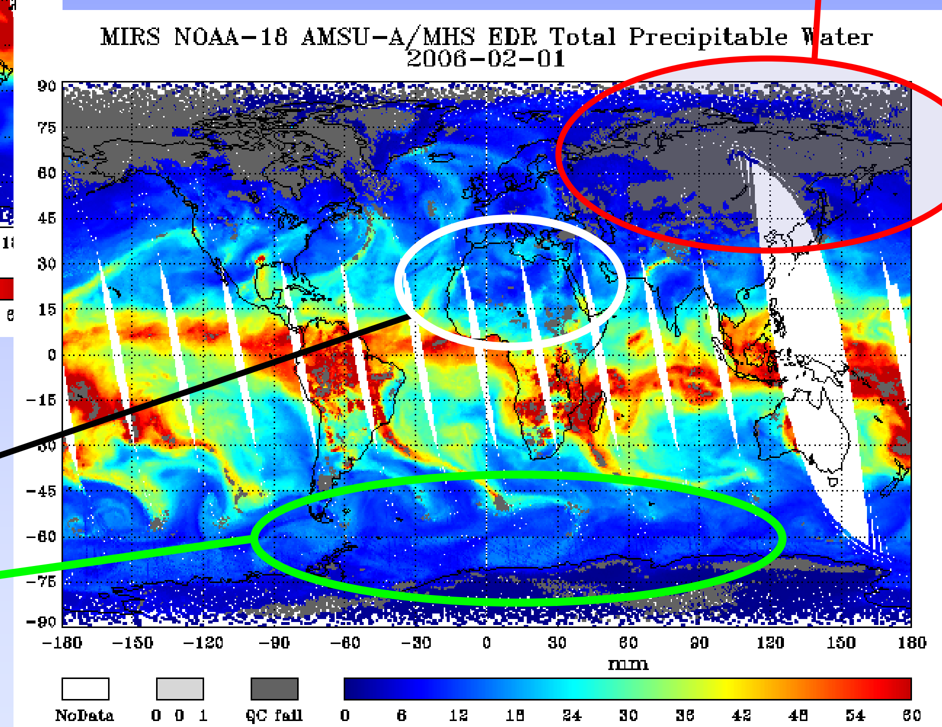


**Retrieval over sea-ice and most land areas capturing same features as GDAS**

MIRS Retrieval

National Environmental Satellite, Data, and Information Service

# Validation of TPW Retrieval over Land

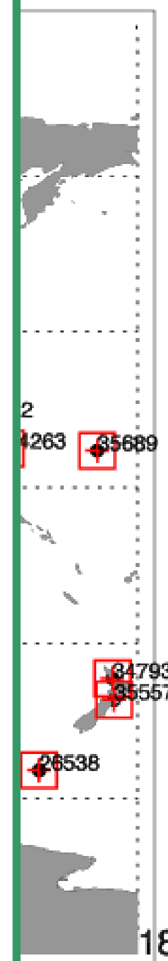


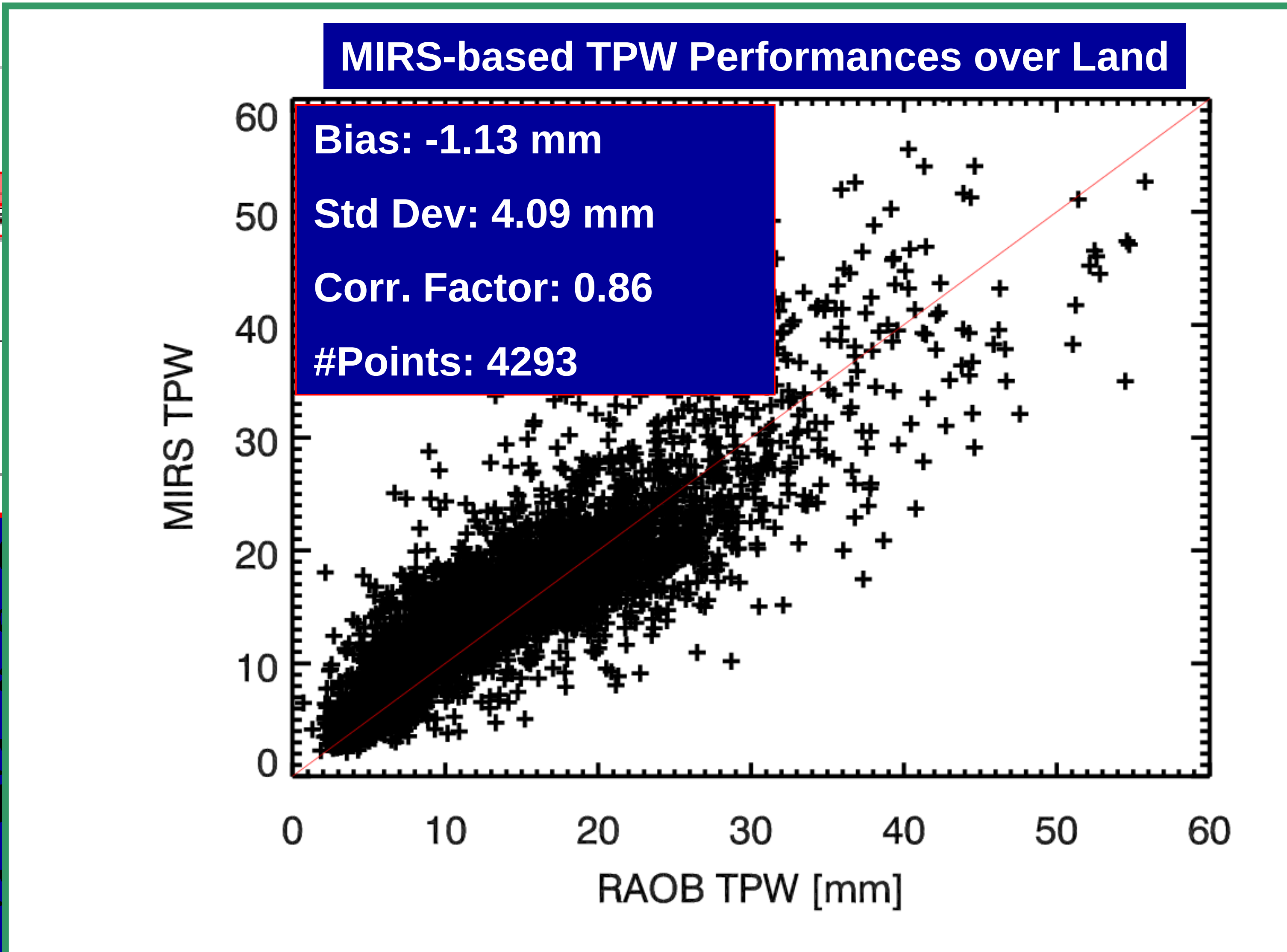


- ~40(
  coll
  radi
- Only
  land
- Only
  and
- Cloudy points included, up to

# Global Temperature Profiling

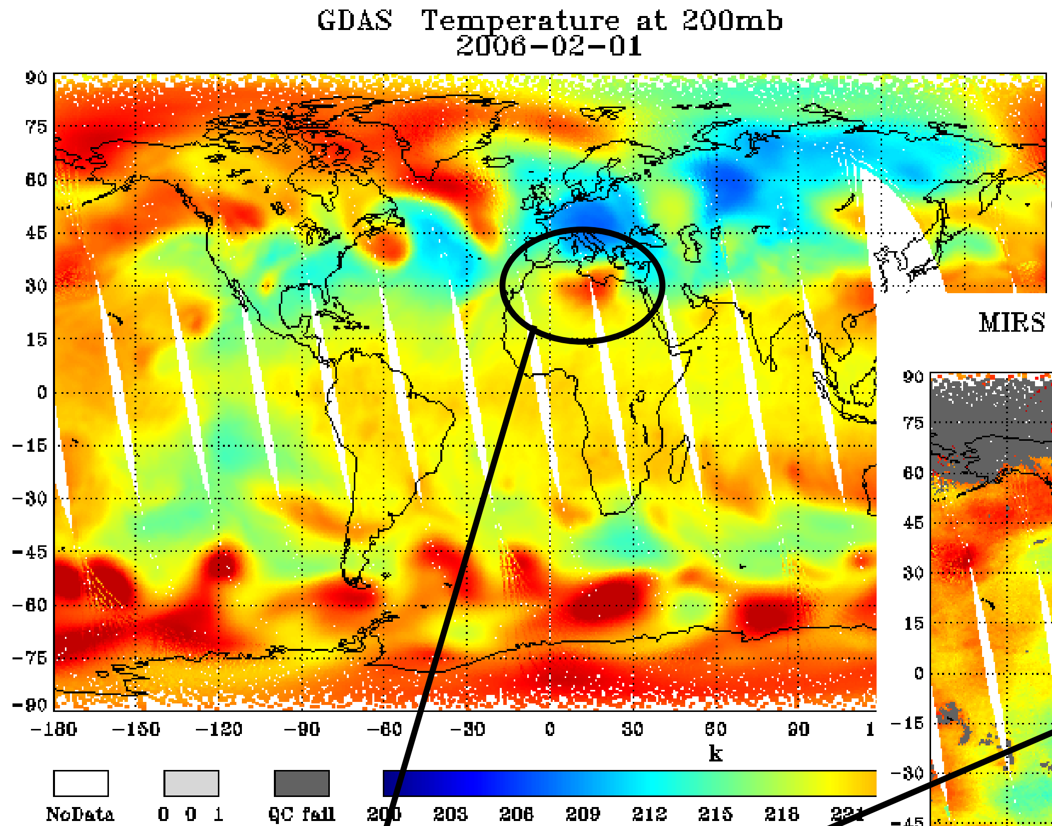


**No Scan-Dependence in retrieval**
**Smooth Transition Land/Ocean**

**QC-failure is based on convergence: Focus of on-going work**

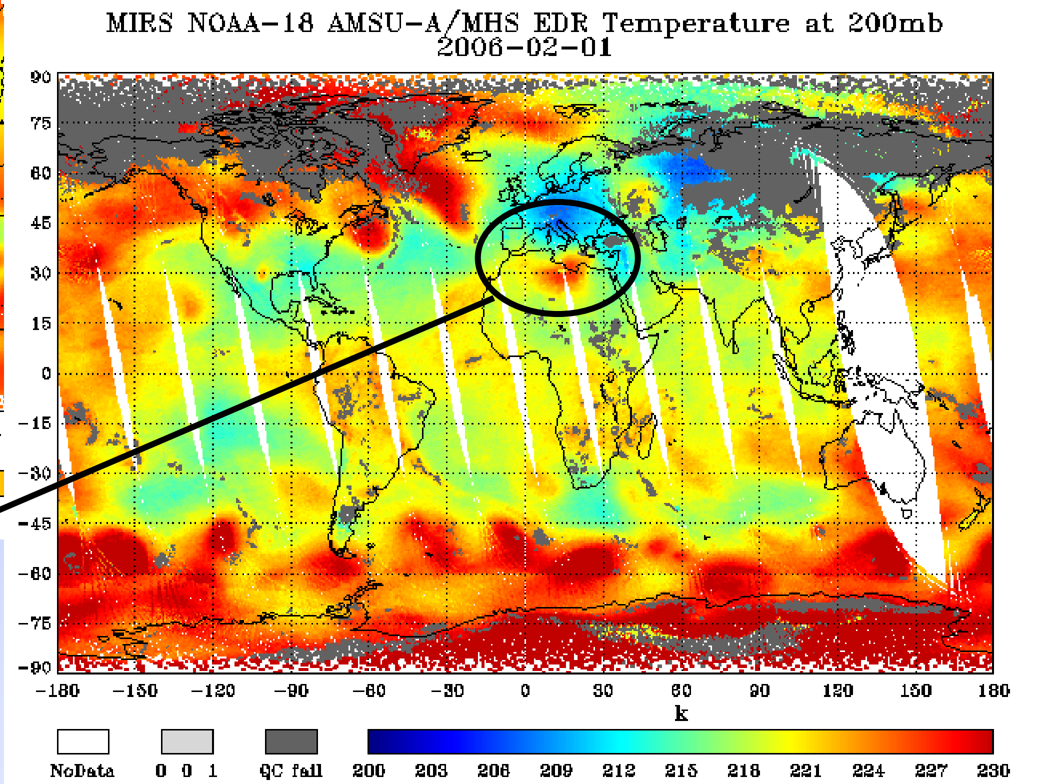


**Similar Features Captured**

# Global Humidity Profiling

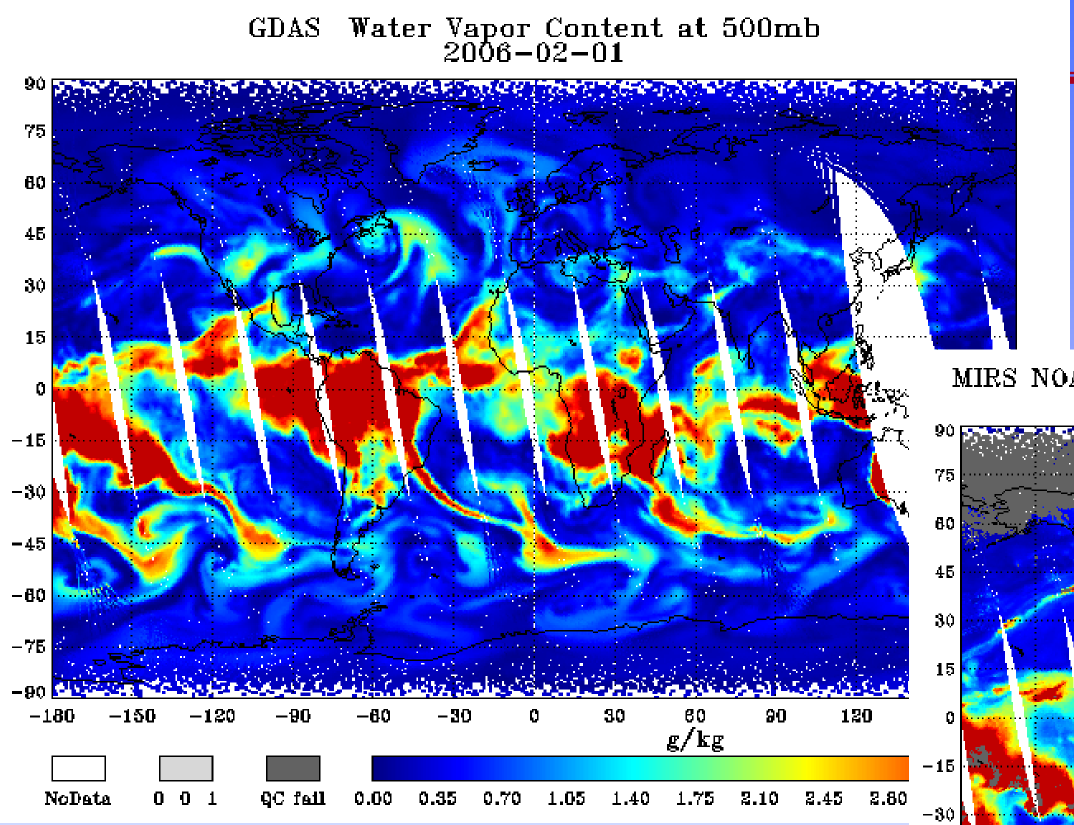


**No Scan-dependence noticed: Angle dependence properly accounted for**

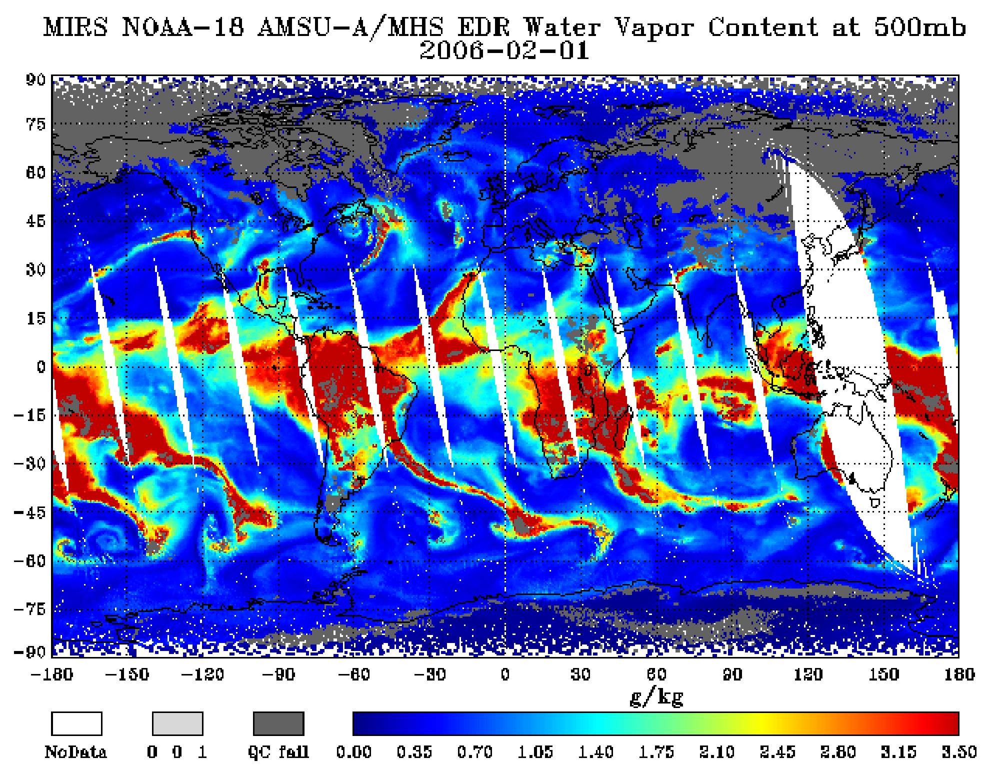

# Vertically Integrated Water Vapor

Match-up TPW from radiosondes and AMSU retrieval in 2002.

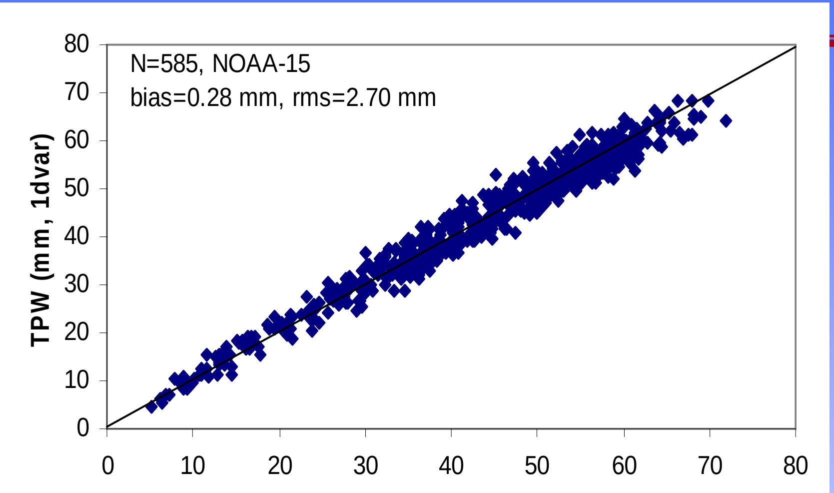


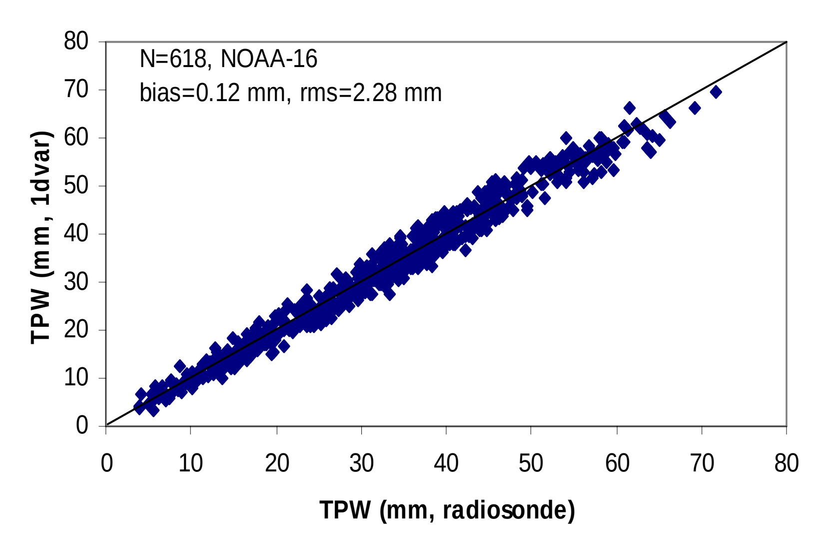


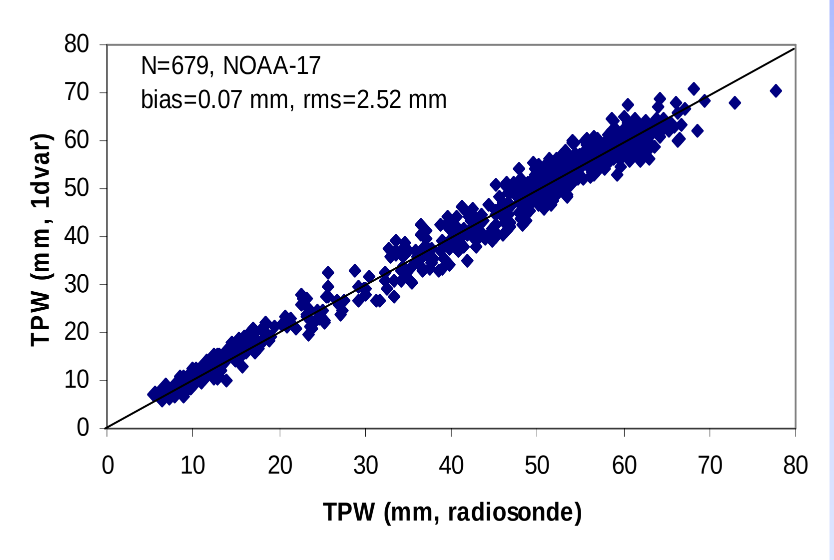

# Hurricane Bonnie Warm Core from AMSU

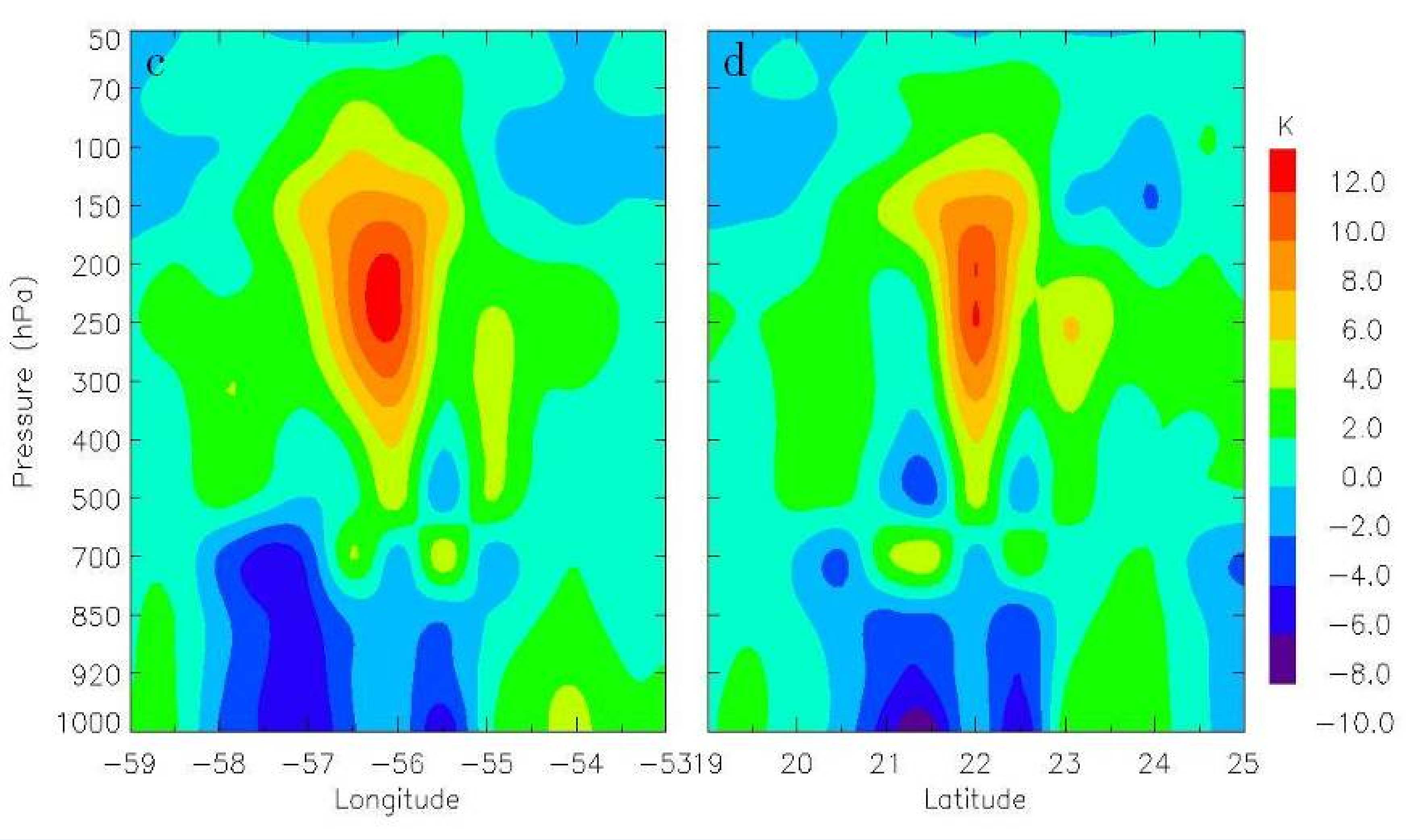

# Hurricane Isabel

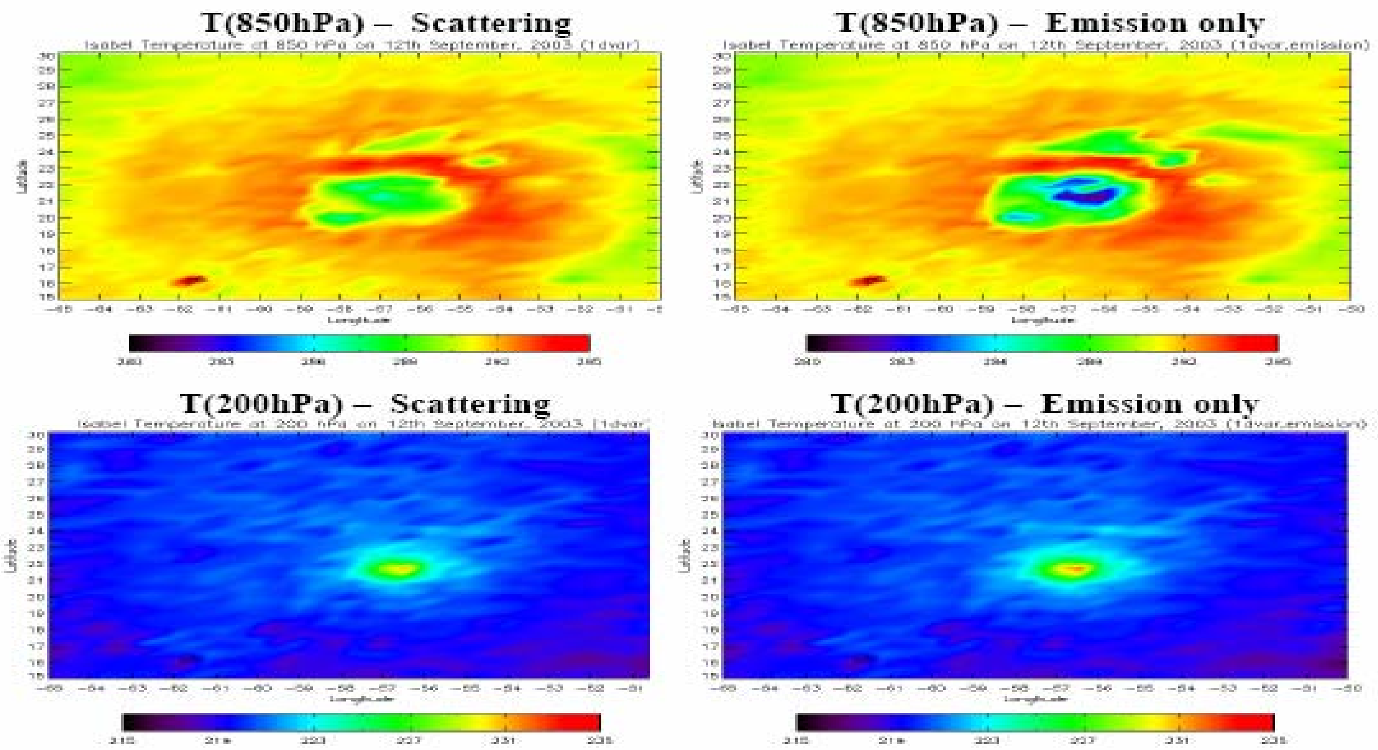


Figure 7.7: Retrieved atmospheric temperature at 850 hPa through a scattering radiative transfer model (a), and an emission radiative transfer model (b); and the retrieved atmospheric temperature at 200 hPa through the scattering radiative transfer model (c) and the emission radiative transfer model (d) for Hurricane Isabel on 12th September, 2003

# Content

- Introduction
  - Impact of satellite microwave data
  - MW gas spectrum
  - Sensor history
  - Radiometry system
  - Data format
- Radiative Transfer Approximation
  - Emission-based
  - Scattering based
- Retrieval Algorithms
  - Cloud liquid water
  - Cloud ice water
  - Atmospheric temperature and water vapor
- Product Applications
  - Intercomparison
  - NWP model validations
  - Climate monitoring

# Intercomparison between MODIS and AMSR-E LWP for Stratus Clouds

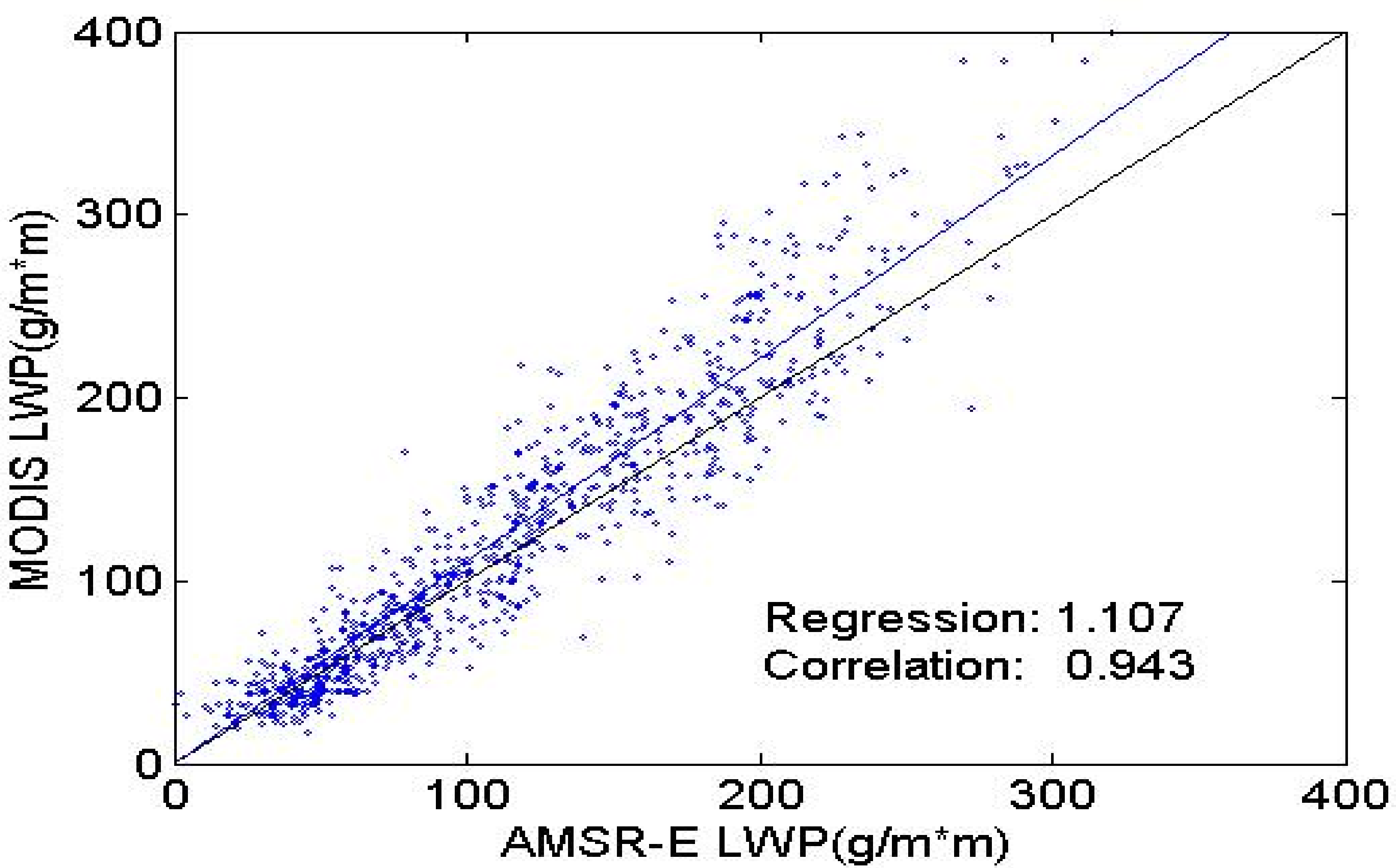

# Validation of General Circulation Model

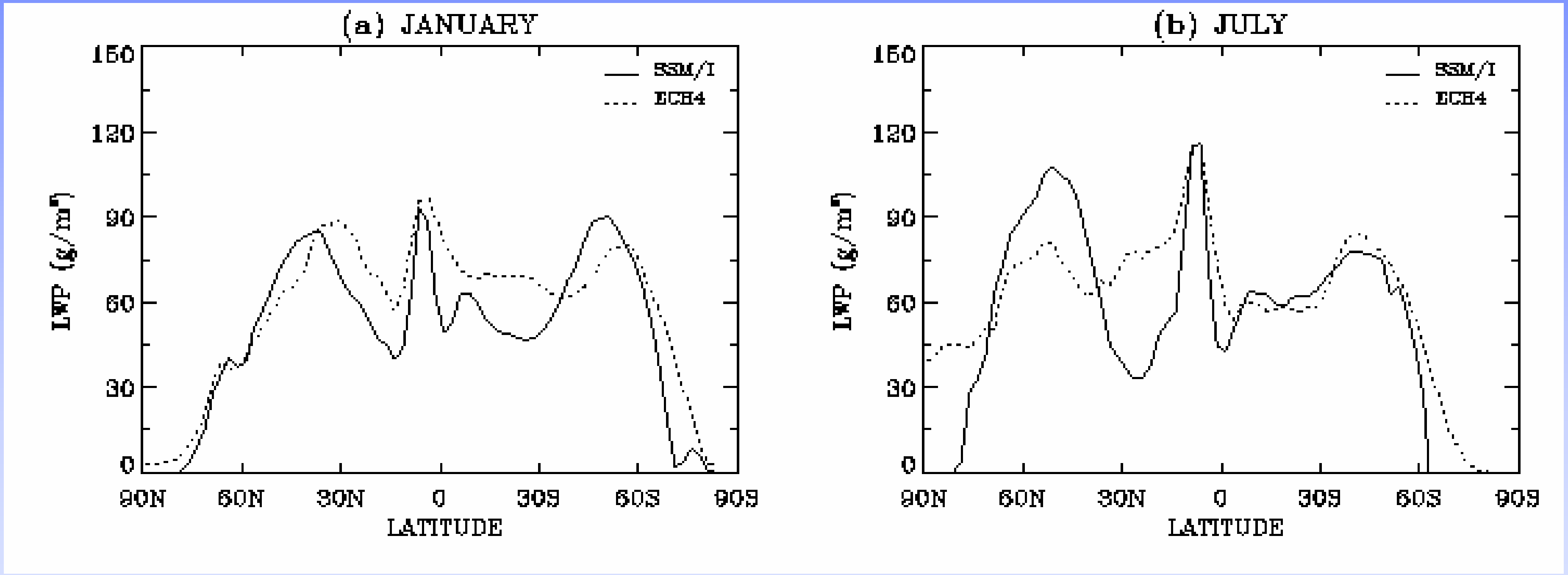

# Validation of Numerical Weather Prediction Models

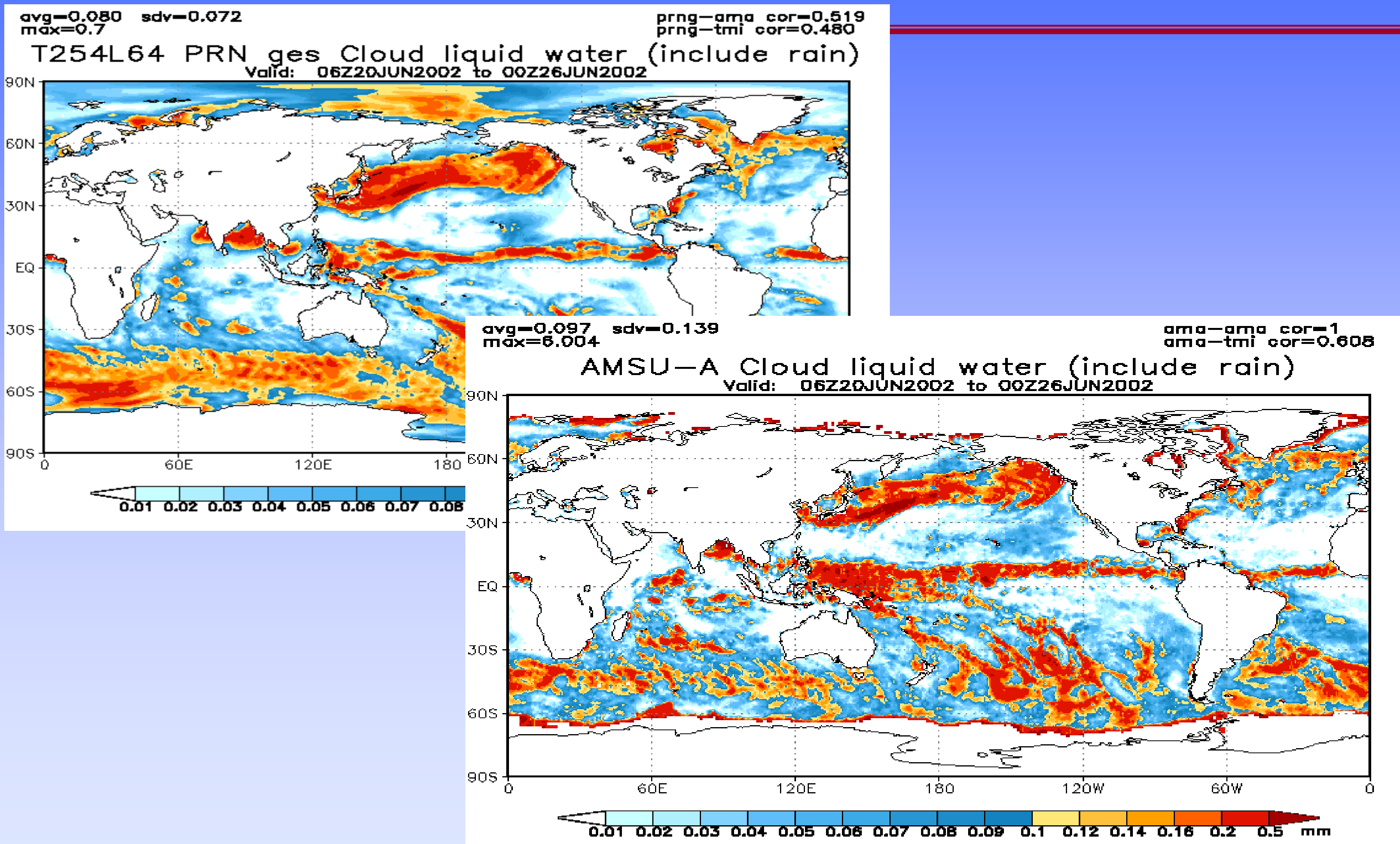

Zonal mean cloud liquid water (rain free ocean only)

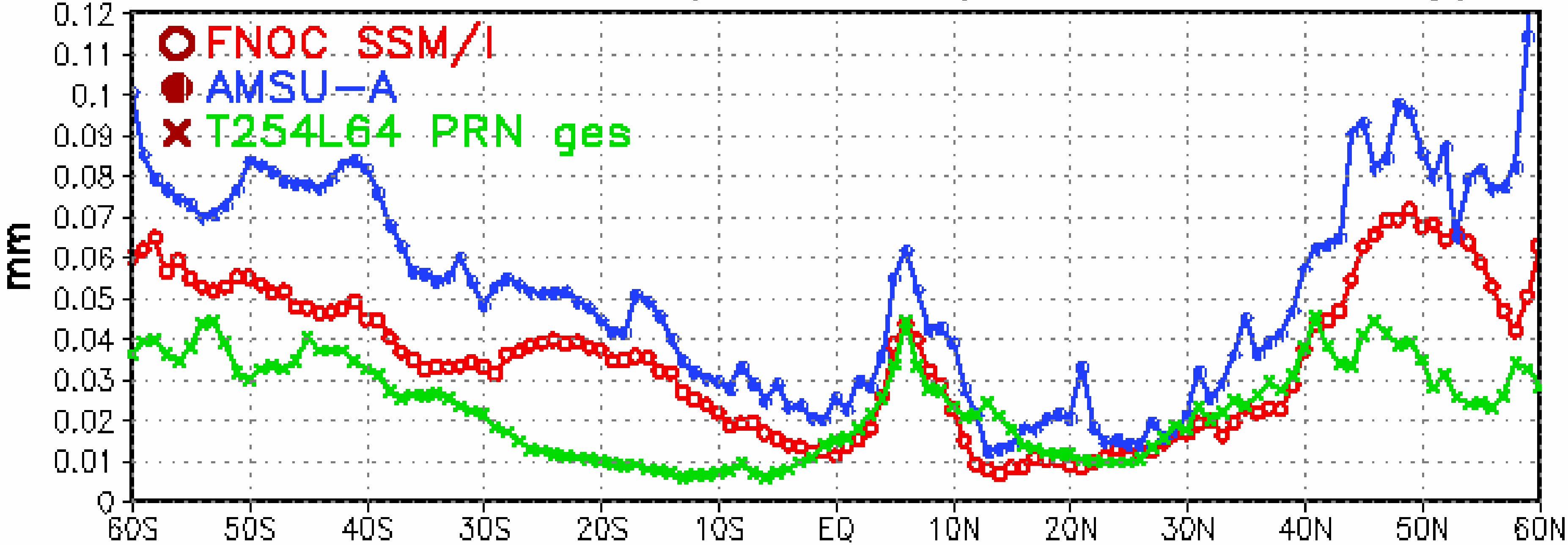


Zonal mean cloud liquid water (include rain, ocean only)

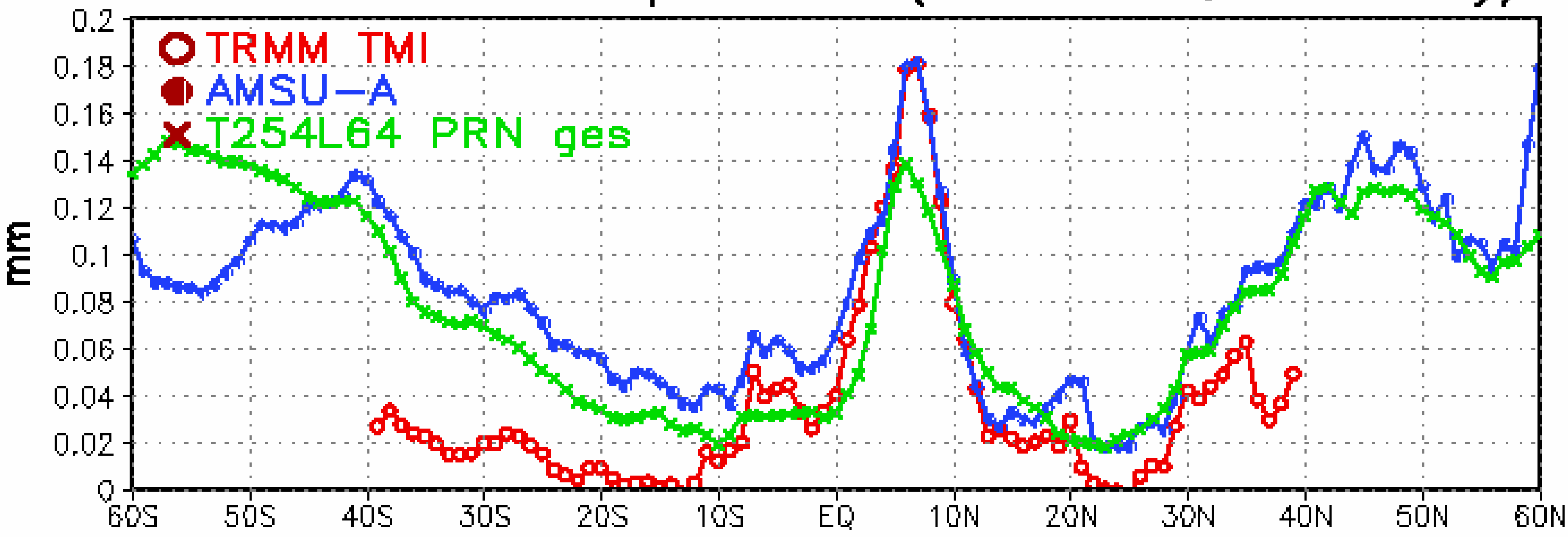

# GFS Prognostic Scheme vs. AMSU Cloud Water

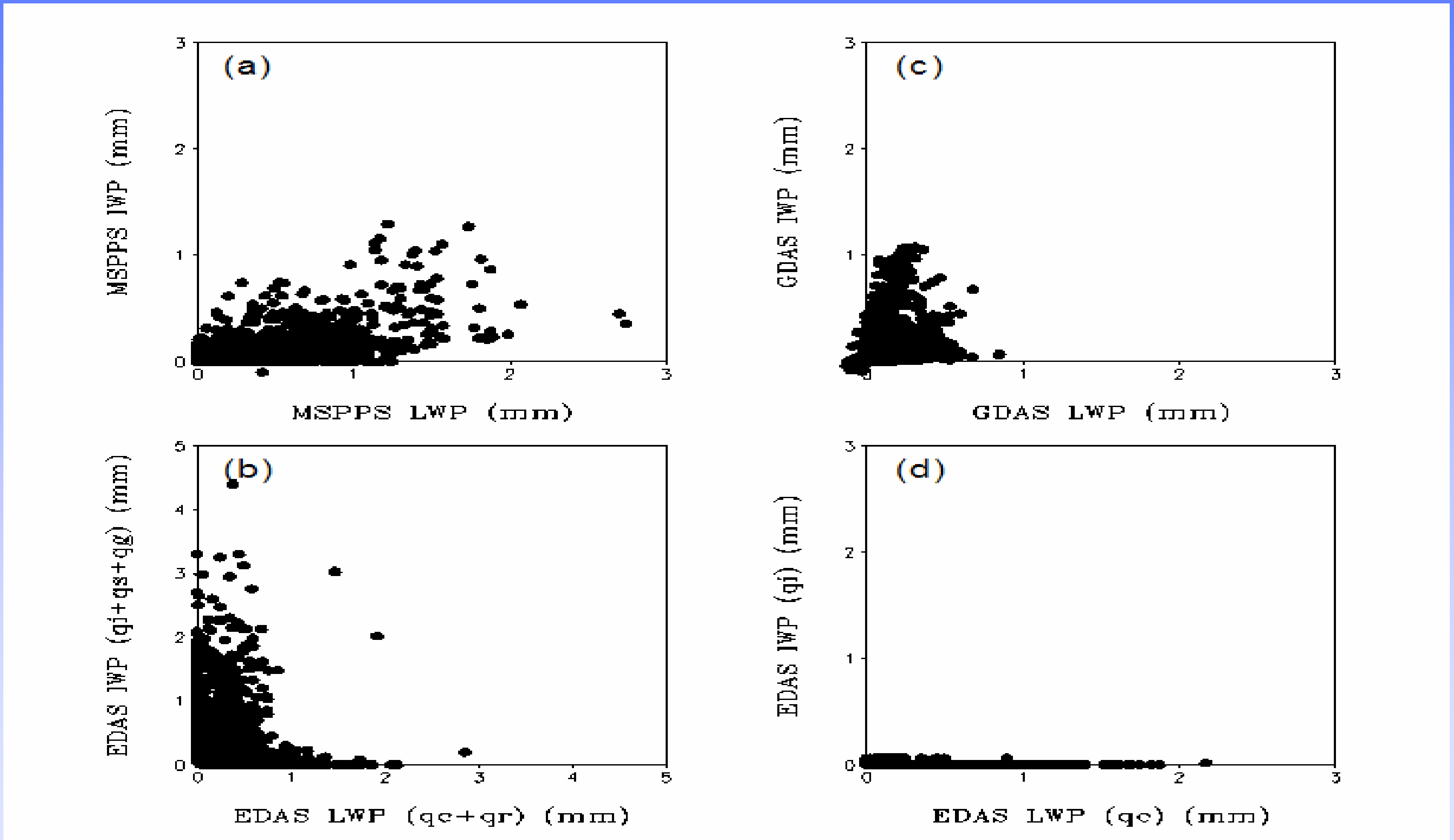


***It is obvious that global/regional models have "ice happy" physics***

# Climate Monitoring from NOAA Operational AMSU Product

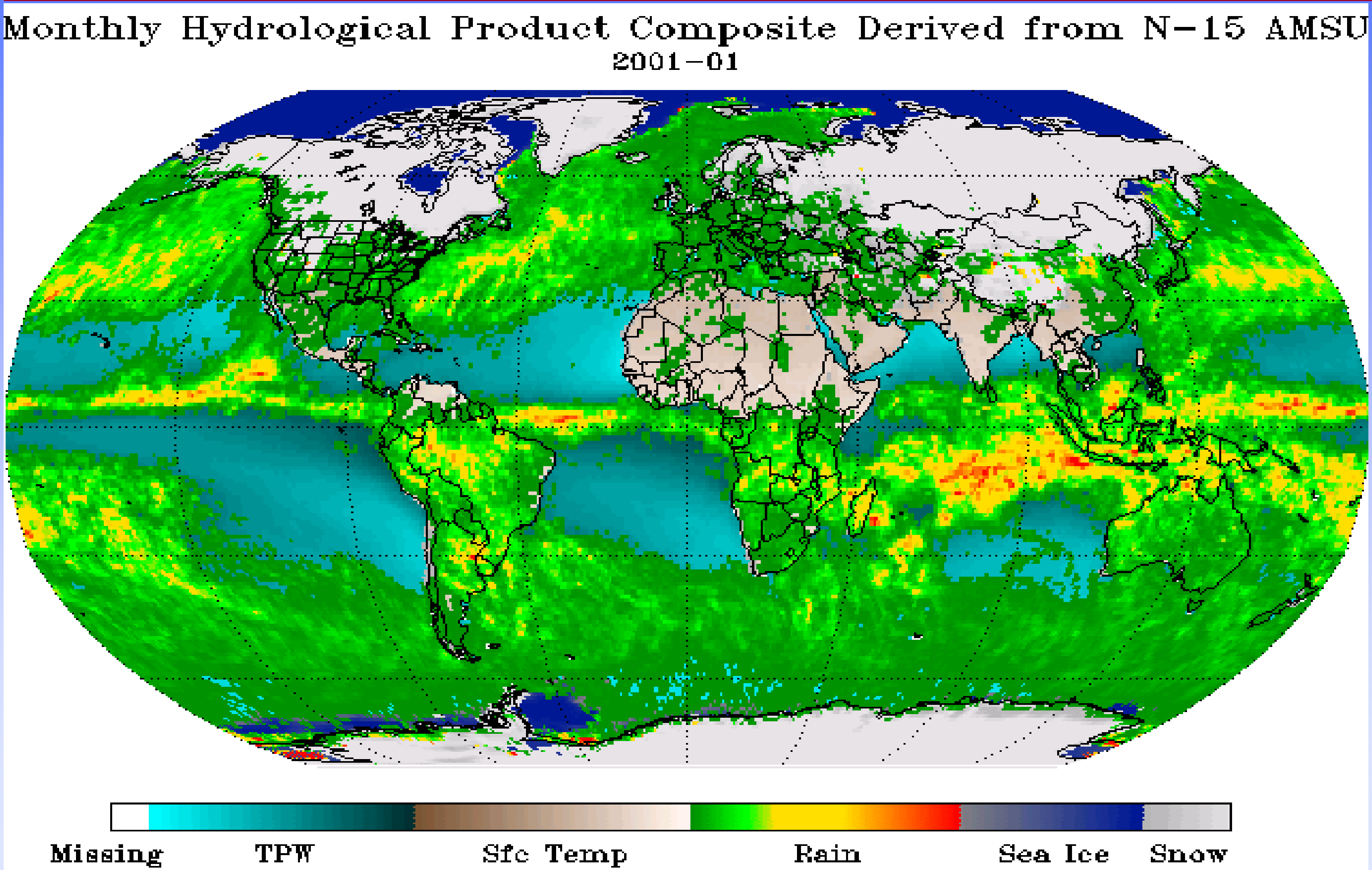

# Concluding Remarks

**NESDIS is offering a center of expertise, from research to operation, on microwave remote sensing. We are closely linked to customers in understanding their needs and we are also collaborating with universities in various research frontiers**

# Homework

1. For an isothermal atmosphere, brightness temperature at microwave wavelength can be expressed as

$$T_b = T_s[1-(1-\epsilon)\Upsilon^2] - \Delta T(1-\Upsilon)[1+(1-\epsilon)\Upsilon],$$

where $\Delta T = T_s - T_m$ and $T_s$ and $T_m$ are the surface temperature and atmospheric effective temperature, respectively; $\Upsilon$ is the atmospheric transmittance, and $\epsilon$ is surface emissivity. Explain the observed brightness temperature difference between land and ocean using this equation for a relatively transparent atmosphere (uses of plots are welcome).

2. Cloud absorption coefficient in microwave frequency decreases as cloud layer temperature increases. Discuss the impacts of this relationship on microwave brightness temperature for clouds over oceans (hints: using the emission approach and isothermal atmosphere)

3. For the cloud droplets in a liquid phase whose size is much smaller compared to wavelength, its absorption coefficient is

$$\sigma_a = 4xIm\left\{\frac{m^2-1}{m^2+2}\right\}$$

where $x = 2\pi r/\lambda$ and $m$ is the complex refractive index. Thus, the total extinction is predominated by cloud absorption. Prove the extinction coefficient for a size distribution of n(r) is independent of particle size and derive cloud optical thickness for a cloud layer of $\Delta Z$ is a function of vertically integrated liquid water content. Discuss the result implications for microwave remote sensing of clouds.

# References


Ferraro, R., F. Weng, N. Grody and L. Zhao, 2000: Precipitation characteristics over land from the NOAA-15 AMSU sensor, Geophys. Res. Let., 27, 2669-267.

Grody, N., J. Zhao, R. Ferraro, F. Weng, and R. Boers, 2001: Determination of precipitable water and cloud liquid water over ocean from the NOAA 15 Advanced microwave sounding unit, J. Geophys. Res. , 106, 2943-2953.

Weng, F., B. Yan, and N. C. Grody, 2001: A microwave land emissivity model, J. Geophys. Res. 106. 20,115-20,123.

Zhao, L. and F. Weng, 2002: Retrieval of ice cloud parameters using the Advanced Microwave Sounding Unit (AMSU). J. Appl. Meteorol. , 41, 384-395..

Weng, F. 2002: Microwave polarimetric signals from hurricane environments, J. Elec. & Appl. 16, 467-480.

Liu, Q. and F. Weng, 2002: A microwave polarimetric two-stream radiative transfer model. J. Atmos. Sci. , 59, 2396 -2402..

Weng, F., L. Zhao, R. Ferraro, G. Poe, X. Li, N. Grody, 2003: Advanced Microwave Sounding Unit Cloud and Precipitation Algorithms. Radio Sci., 38, 8,086-8,096.

Liu, Q. and F. Weng, 2003, Retrieval of Sea Surface Wind Vector from Simulated Satellite Microwave Polarimetric Measurements. Radio Sci., 38, 8078-8088.

Ferraro, R., F. Weng et al., 2002: NOAA Satellite-derived hydrological products prove their worth, EOS Transactions, 83, 42,436 c 42,437.

Weng, F. and Q. Liu, 2003: Satellite data assimilation in numerical weather prediction models, 1. Forward radiative transfer and Jacobian models under cloudy conditions, J. Atmos. Sci., 60, 2633 – 2646.

Liu, Q. and F. Weng, 2005: One-dimensional variation retrieval algorithm for temperature, water vapor and cloud profiles from Advanced Microwave Sounding Unit (AMSU). IEEE Trans. Geosci. & Remote Sensing. 43, 1078-1095.

Ferraro, R. R., F. Weng et al. 2005: NOAA operational hydrological products from AMSU IEEE Trans. Geosci. & Remote Sensing. ,43, 1036-1049.

Liu, Q. and F. Weng, 2005: Vicarious Calibration of the 3rd and 4th Stokes Parameters of Windsat Measurements, Appl. Opt., 44, 7403-7406.

Liu, Q. and F. Weng, 2006: Detecting Warm Core of Hurricane from the Special Sensor Microwave Imager Sounder, Geophys. Res. Letters, 33